Research Paper
Computational Methods for Differential Equations
http://cmde.tabrizu.ac.ir
Vol. *, No. *, *, pp. 1-64
DOI:10.22034/CMDE.2024.56288.2353

Mechanics of nanofluidic flow induced nonlinear vibrations of single and multi-walled branched nanotubes in a thermal-magnetic environment

Ahmed Amoo Yinusa[1,4,*], Musibau Gbeminiyi Sobamowo[1], Adekunle Omolade Adelaja[1], Sunday Joshua Ojolo[1], Mufutau Adekojo Waheed[2], Ridwan Ola-Gbadamosi[3], and Ridwan Adesesan Amokun[1]

[1]Department of Mechanical Engineering, University of Lagos, Nigeria.

[2]Department of Mechanical Engineering, Federal University of Agriculture, Abeokuta, Nigeria.

[3]Department of Mechanical Engineering, Lagos State University, Nigeria.

[4]Department of Mechanical Engineering, Massachusetts Institute of Technology, Cambridge, USA.

Abstract

The nonlinear vibration analysis of embedded multi-walled branching nanotubes with integrated nanofluids that are resting on a Winkler-Pasternak foundation in a thermal-magnetic environment is the main emphasis of this work. The coupled equations of motion controlling the transverse and longitudinal vibrations of the nanotube are derived using the Euler-Bernoulli theory, Hamilton's principle, and nonlocal elasticity theory. Additionally, the pressure variation in the tubes and the equation for the deformation of the nanotubes are derived. Furthermore, the vibration models are coupled with the Navier-Stokes equation and the energy equation for the fluid and nanotube. Since the dynamics of multi-walled carbon nanotubes differ from the typical assumption of plug flow, careful investigation is needed when combining them with Navier-Stokes and energy equations. Thus, the generated coupled systems of nonlinear partial differential equations in this work are solved using multi-dimensional differential transformation method. With the aid of the analytical solution, parametric studies are performed. The findings show that the system's stability reduces as the downstream angle increases. Furthermore, the system's dynamic behavior yielded results that show the magnetic effect has a 20% attenuating or damping effect. Additionally, there is a more than 11% discrepancy between the plug flow assumption and real functioning procedures. Existing analytical, numerical, and experimental results were used to verify and validate the analytical method. It is hoped that this study will provide further understanding of the design of nanotubes and act as a reference for further research in the field.

Keywords. Nanofluidic flow, Nonlinear vibrations, Nanotubes, Thermal-magnetic environment.

1991 Mathematics Subject Classification. 65L05, 34K06, 34K28.

1. Introduction

The engineering sciences and medical technology are undergoing a new revolution owing to the development of carbon nanotubes. For nanoelectromechanical systems (NEMS), nanoresonators, and nanosensors, among other nanodevices, carbon nanotubes (CNTs) play crucial roles in enhancing their functionality [22, 23]. On the synthesis and uses of branched single and multi-walled nanotubes, the fabrication of Y junctions has been achieved using branches and stems at acute angles to each other [32]. Y junctions have been described as novel structures with variable terminals and chirality [7]. An experimental study has been presented on the synthesis of Y-branching multi-walled carbon nanotubes with a bamboolike structure and it enumerated how this novel structure may offer promising applications for nanotube-based composites [19]. One of the applications of carbon nanotubes is using biological sensors to detect the mass of bacteria, cells, and viruses. Typically, two static and dynamic methods are used to detect added mass in nano-mass sensors. In the static method, the added mass is determined by measuring the deflection of a nanobeam resulting from the attached mass on the surface. In the dynamic method, measuring the frequency shift due to attached

Received: 22 April 2023 ; Accepted: 29 May 2024.

∗ Corresponding author. Email: aayinusa@unilag.edu.ng .

mass is considered [26]. A higher frequency shift indicates more sensitivity performance of mass sensor [35]. Consequently, a huge amount of research has been conducted to increase and evaluate the sensitivity of mass nanosensors. Carbon nanotube-based bio-sensors have also been studied[10]. They determined the suitable boundary conditions for the mass sensing. The transverse vibration of nanobeam with an attached mass, rotational, and transverse springs at its end has been studied [57]. The influence of various geometrics microbeams on mass sensors has been examined and it was realized that the sensitivity of the microsensor increases with the microbeam rigidity[3]. In comparing micro CNTs and beam mass sensors, it was found that a CNT-based sensor is more sensitive than microbeam ones [8]. Studies have been conducted on the position and mass identification in single-wall carbon nanotube (SWCNT) mass sensor[20]. Soltani et al. The nonlocal theory of elasticity has been used to carry out sensitivity analysis on a nanotube sensor resting on an elastic foundation[44]. DWCNT vibration has been analysed for sensing biological objects[37]. They considered six different types of DWCNTs and determined the best type for the mass sensors. The magnetic force effects have been considered in research regarding micro and nano mechanical elements' behaviour as an external parameter. It has been demonstrated that the frequencies of a DWCNT increase with increasing the magnetic field[30, 31]. Subsequently, the impacts of axial magnetic fields on the vibrations of magnetically sensitive systems were inspected. The influence of magnetic field strength on the stability of an elastic foundation embedded SWCNT was shown [60]. In another work, they considered SWCNTs under the influence of an axial magnetic field [59]. The vibration of a nanofluid-conveying CNT in a magnetic environment has been explored[39]. A Timoshenko beam has been considered and developed vibration models used for investigating the influences of axial magnetic field on nanotube responses [61]. Similarly, the axial magnetic field has been studied and transverse deflection of the DWCNT system has been analysed[1]. They found that an augmentation in the magnetic field's intensity decreases nanotube deflection. In the study, the sensitivity of the DWCNTs was investigated and the governing equations of motion were put forward. Influences of axial magnetic field on nanotube configurations have also been studied. In conclusion, they established how the work will be helpful for further development and design of mass sensors based on the DWCNT in a longitudinal magnetic field [27, 33, 47]. On classical and nonlocal flow-induced vibrations, the applications of nanotubes and junctions are vital and of tremendous importance especially in drug delivery systems. A presentation has been made on research that carbon nanotubes can serve as scaffoldings for treatments of broken bones [58]; and transport proteins for cancer treatments [24]. An experimental investigation was performed on the impacts of high-velocity fluid flow on the bending vibrations and static divergence of a simply supported pipe[11]. The experimental setup was used to determine the relationship between the critical velocity of flow through the pipe and the frequency for stable, unstable, and divergent regions. This experimental result was used to validate the developed analytical solution in this work by reducing the present study to the level of the experiment. Focusing on past works and the need for further studies on the dynamic analysis/vibration of nanotubes, some researchers have presented nonlinear flow-induced dynamic response analyses of DWCNTs resting on elastic foundations [15–17]. In another work linear continuum mechanics assumption and reduction of the derived equation of motion was applied for a SWCNT to only vertical displacement under thermally induced vibrations[4]. Associated Eigenvalues were also presented for CNT under clamped-clamped (C-C). The following year, the fundamental frequencies and mode shapes were obtained from the solution of the Eigen problem after using the static condensation method. The obtained resonant frequencies for SWCNT and DWCNT were then used for stability analysis and divergence control[28]. A transverse vibration model for an elastic nanotube model under compressive exciting forcing function has also been presented[34]. The work includes the van der Waal forces interactions that exist between the outer and inner nanotubes. They concluded with an obtained relationship between the excitation load and frequency ratio for the DWCNT investigated. An investigation on the stability of a flow-induced CNT has been conducted[56]. The research explores the impact of internal mean flow velocity on the structural instability of CNTs. The obtained relationship between the mean velocity and response frequency for the flow-induced SWCNT is then used to estimate the critical velocity of flow as well as the stability region of the CNT. A numerical technique was used to investigate the fundamental vibration frequencies and contraction behaviours of nanotubes under thermal loading[9]. In the work, the thermofluidic induced vibration models were obtained and the thermal profiles for stable and unstable SWCNT were presented. A mathematical relationship between the wall thickness and elastic properties of a nanotube (SWCNT) was presented[45]. Amplitude ratio and frequency ratio are vital variables used to monitor excitation frequency in order to prevent resonance and total damage of structures under vibration. As a result of the need for adequate monitoring of CNT under operation, this phenomenon has been analysed using the principle of forced vibration model and relationships between the variables have been obtained[25]. A longitudinal vibration model via nonlocal theory has been presented with a relationship for the SWCNT amplitude and length as well as frequency parameters and mode numbers obtained [14]. A nano-scale influence on the un-damped forced vibrations of connected DWCNT excited by mobile nanoparticles has also been considered[40]. The vibration in the elastically connected double-walled carbon nanotubes is induced by mobile nanoparticles. Also, thermal influences on SWCNT embedded in elastic foundations via a nonlocal theory approach have been presented [2]. They used arbitrary end conditions to obtain and envisage the CNT responses. To understand the impact of the small-scale term, a study on the vibration of carbon nanotubes conveying fluid embedded in a viscoelastic medium was considered [38]. The natural flow-induced vibrations SWCNT under the multi-physics field have been analyzed [46]. They scrutinized the impact of magnetic terms on the response of the SWCNT. Also, the influence of magnetic strength on the nanotube's stability was presented and discussed. Moreover, investigation on the vibrations and stability analyses of a fluid conveying nanotube under axial magnetic fields have been reported [21]. The magnetic term was observed to be an important parameter for shifting instability modes to stability. Other interesting works through modelling have also been presented to justify the widespread application of CNTs [41] and [42]. Flow-induced vibrations of TWCNTs has been explored and the stability curve for the first three modes of vibration was obtained[36]. Meanwhile, [12] carried out free vibration analysis and obtained nondimensional critical loads for three modes and varying end conditions. Recently, [54], [55],[53], [51], [43], and [50], carried out comprehensive studies on the dynamic analyses and stability responses SWCNT and MWCNT using numerical, analytical and experimental methods. It is known that equations of motion that describe flow-induced vibrations in nanotubes are usually presented in dimensionless PDE or ODE forms, attentions need to be shown to how these equations are analysed. The common option is to use numerical techniques which have their residue. To beat this challenge, approximate analytical schemes have been put forward. These schemes include PADE-approximants, Parameter Variations method (VPM), Perturbation method with Homotopy (HPM), Iteration Variational method (VIM), Temini and Ansari's method (TA'M), Differential transformation method (DTM) etc., in classical forms work immaculately for small convergence domains. However, PADE -approximants is challenged with right PADE-numbers before convergence, VIM and VPM necessitate arbitrary coefficients coupled with arduous integrations before use, HPM just decomposes the equations and needs additional methods before getting complete solutions while DTM is stable and converges regardless of the value of the independent variables. The main merit of DTM is its ability to be used directly on nonlinear and linear equations without discretization and linearization. Hence, discretization error does not affect the method of solution. Therefore, a scrutiny of previous researches shows that no work has been reported concerning the nonlinear thermal-mechanical vibration analyses of embedded branched nanotube conveying fluid under magnetic influence with Navier Stokes coupled with the vibration model. On the other hand, the different end shapes considered in this work such as I, Y, and T shaped-CNTs can find applications in many nanoelectromechanical systems (NEMS). Motivated by the aforementioned considerations, this novel research work explores nonlinear thermal-mechanical vibration Analysis of embedded branched carbon nanotube conveying nanofluid under the influence of magnetic fields with Navier stokes coupled with vibration using multi-dimensional differential transformation method (MDTM).

2. Description of problem and equations of motion.

The mathematical modelling of the vibration of mechanical systems such as nanotubes, pipes and engineering structures generates nonlinear differential equations. These equations are called the equations of motion of the system. The terms in the obtained equations of motion have their effects on the dynamic behaviour of the structure. The economic background knowledge of these mechanical systems under vibration has been extensively discussed by [18].

2.1. **Nanotubes with varying downstream or junction angles.** Figure 1 illustrates the branched-nanofluid-conveying carbon nanotube resting on elastic foundations in a thermal-magnetic environment. The possible shapes due to variations in junction angle are depicted in Table 1.

2.2. **Derivation of the Equations of Motion.** The principle of variation used to obtain equations of motion for dynamics of rigid bodies and systems of particles is named Hamilton's principle. Here, the functional derivatives are

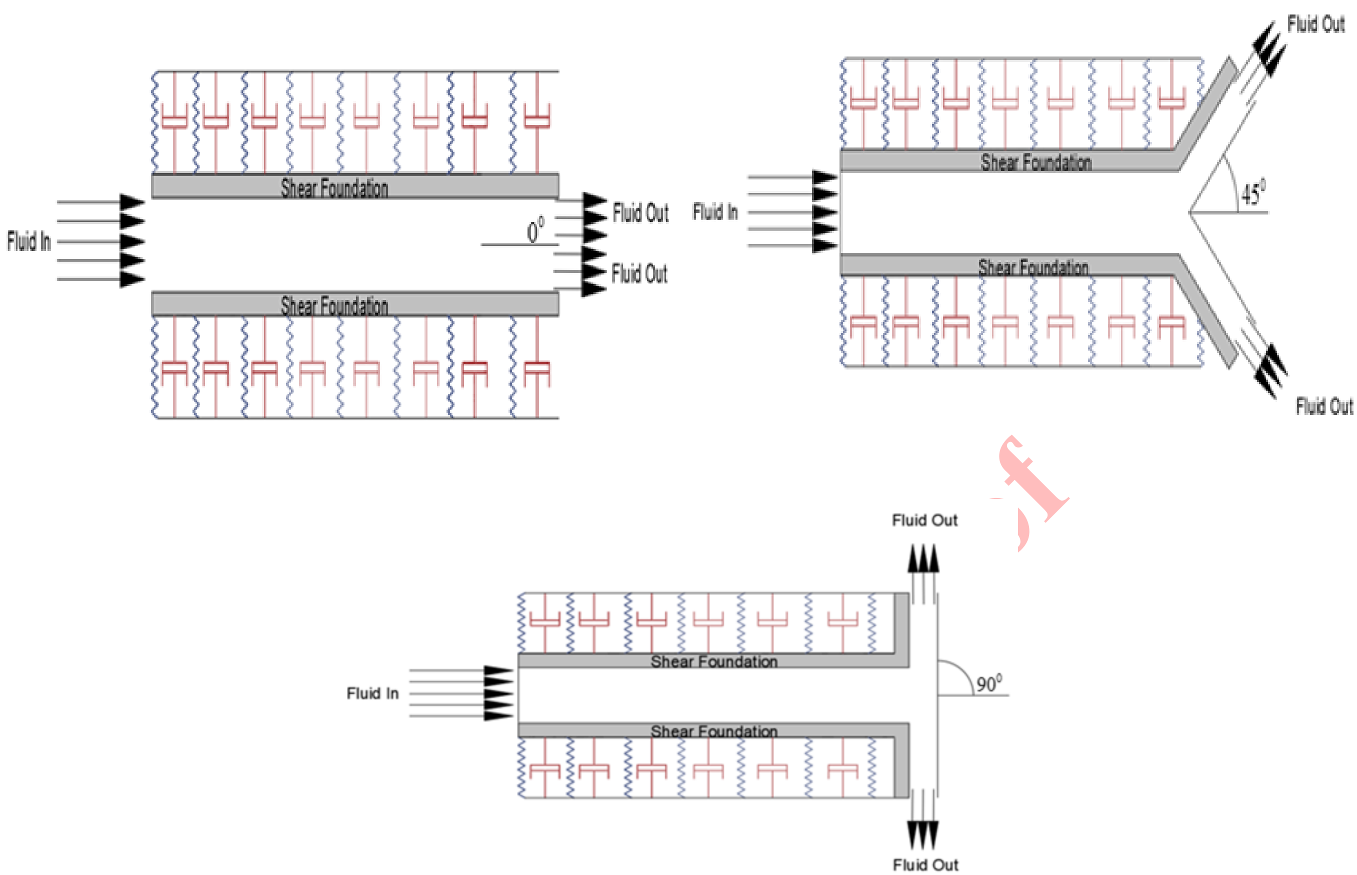

FIGURE 1. Schematic of nanotubes with varying downstream angles.

TABLE 1. Different nanotube shapes due to varying junction angle.

Junction Angle	**Nanotube Shape**
0^o	I Shaped NT
15^o	Sharp Y Shaped NT
30^o	Sharp Y Shaped NT
45^o	Y Shaped NT
60^o	Slack Shaped NT
75^o	Slack Shaped NT
90^o	T Shaped NT

taken with respect to time [5, 13]. Now, considering the system under investigation and beginning with Hamilton's principle given in Equation (2.1):

$$\int_0^t (\delta u_T - \delta k_T - \delta v_T) dt = 0. \tag{2.1}$$

The variation in strain or potential energy is;

$$\delta u_T = \frac{1}{2}\iiint\limits_{V_t} \sigma_{xx}\delta\varepsilon_{xx} dV_t = \frac{1}{2}\int\limits_0^L \int\limits_{A_t} \sigma_{xx}\delta\varepsilon_{xx} dx dA_t \tag{2.2}$$

since $\varepsilon_{xx} = -zw''$, put in Equation (2.1)and make it simpler to get:

$$\delta u_T = \frac{1}{2}\int\limits_0^L \left[M_{xx}\nabla^2\left(\delta w\right)\right] dx. \tag{2.3}$$

Correspondingly, that kinetic energy and virtual work done become:

$$\delta k_T = \left(\begin{array}{l} \frac{1}{2}\int\limits_0^L \int\limits_{A_t} \rho_t \left[\left(\frac{\partial(\delta\tilde{u})}{\partial t}\right)^2 + \left(\frac{\partial(\delta\tilde{w})}{\partial t}\right)^2\right] dx dA_t \\ +\frac{1}{2}\int\limits_0^L \int\limits_{A_t^f} \rho_t^f \delta\left[(\Gamma U)^2 + \left(\frac{\partial w}{\partial t} + \Gamma U\frac{\partial w}{\partial x}\right)^2\right] dx dA_t^f \\ +\frac{1}{2}\int\limits_0^L m_j\delta\left(\delta\left(x-L\right)\left[\left(\frac{\partial\tilde{u}}{\partial t}\right)^2 + \left(\frac{\partial\tilde{w}}{\partial t}\right)^2\right]\right) dx \\ \frac{1}{2}\int\limits_0^L m_j^f\delta\left[(\Gamma U)^2 + \left(\frac{\partial w}{\partial t} + \Gamma U\frac{\partial w}{\partial x}\right)^2\right]\delta\left(x-L\right) dx \end{array}\right), \tag{2.4}$$

and

$$\delta v_T = \int\limits_0^L \left(\begin{array}{l} \mu_{eff}A_t^{vf}\nabla^2\left(\frac{\partial w}{\partial t} + \Gamma U\frac{\partial w}{\partial x}\right) + \left(\begin{array}{c} M_f(\Gamma U)^2\left[1-\cos\phi\right] \\ +PA - T - K_P - \frac{EA\alpha\Delta\theta}{1-2v} \end{array}\right)\frac{\partial^2 w}{\partial x^2} \\ +\left[\frac{B_o^2\cos^2\alpha A_t}{\mu_p}\right]\nabla^2 w - \left[\frac{B_o^2\sin^2\alpha I^{CNT}}{\mu_p}\right]\nabla^4 w \\ -\sigma B_o^2\cos^2\alpha A_f\left(\frac{\partial w}{\partial t} + \Gamma U\frac{\partial w}{\partial x}\right) + k_w w + k_3 w^3 - G\frac{\partial^2 w}{\partial x^2} + c\frac{\partial w}{\partial t} \end{array}\right)\delta w dx. \tag{2.5}$$

Substitute Equations (2.3),(2.4) and (2.5) into Equation (2.1) and integrate by part to convert from weak form to strong form and subsequently nullifying the arbitrary function, give the equations of motion for longitudinal and transverse vibrations as:

For multi-walled CNT, the transverse vibration model for the first tube (N = 1) is developed to be:

$$
\begin{aligned}
&m\ddot{w}_1 + \left(c + A_f\sigma B_o^2 cos^2\varphi\right)\dot{w}_1 + 2m_f\Gamma U\dot{w}'_1 + m_f\Gamma\dot{U}w'_1 + m_f\Gamma^2 UU'w'_1 \\
&-\left[T_0 - P\left(1-2v\delta\right)A - G - k_p - m_f\Gamma^2U^2cos\phi - \tfrac{B_o^2cos^2\varphi}{\mu_p}\right]w''_1 + \\
&\left[T_0 - P\left(1-2v\delta\right)A - G - EA\right]\left[w'_1u''_1 + w''_1u'_1 + \tfrac{3}{2}{w'_1}^2w''_1\right] \\
&+P\left(1-2v\delta\right)Aw'_1\left(1 - u'_1 - \tfrac{1}{2}{w'_1}^2\right) - EA\left[w'_1u'_1 + \tfrac{1}{2}{w'_1}^3\right] + \\
&E\alpha A\Delta Tw'_1\left(1 - u'_1 - \tfrac{1}{2}{w'_1}^2\right) + E\alpha A\Delta T'\left(1 - u'_1 - \tfrac{1}{2}{w'_1}^2\right) + \\
&E\alpha A'\Delta Tw'_1\left(1 - u'_1 - \tfrac{1}{2}{w'_1}^2\right) - E\alpha A\Delta Tw'_1\left(u''_1 + w'_1w''_1\right) + \left(EI + \tfrac{IB_o^2sin^2\varphi}{\mu_p}\right)w_1^{iv} \\
&-EI\left(3u'''_1w''_1 + 4u''_1w'''_1 + 2u'_1w_1^{iv} + w'_1u_1^{iv} + 2{w'_1}^2w_1^{iv} + 8w'_1w''_1w'''_1 + 2{w''_1}^3\right) \\
&-\tfrac{EA}{L}\int_0^L\left(z'_0w'_1 + \tfrac{1}{2}{w'_1}^2\right)dx\left[w''_1 + z''_0\right] + k_1w_1 + k_2w_1^3 + \left(e_oa\right)^2 \\
&\left\{\begin{array}{l}
m\ddot{w}''_1 + \left(c + A_f\sigma B_o^2cos^2\varphi\right)\dot{w}''_1 + 2\Gamma m_f\left(U''\dot{w}'_1 + 2U'\dot{w}''_1 + U\dot{w}'''_1\right) + \\
\Gamma m_f\left(\dot{U}''w'_1 + 2\dot{U}'w''_1 + \dot{U}w'''_1\right) + \\
\Gamma^2m_f\left(3U''U'w'_1 + 2{U'}^2w''_1 + UU'''w'_1 + 2UU''w''_1 + UU'w'''_1\right) \\
-\left(\begin{array}{c} T_0 - G - k_p \\ -\frac{B_o^2cos^2\varphi}{\mu_p}\end{array}\right)w_1^{iv} + \left(1-2v\delta\right)\left(\begin{array}{l} P''Aw''_1 \\ +2P'A'w''_1 \\ +2P'Aw''_1 \\ +PA''w''_1 \\ +2PA'w'''_1 \\ +PAw_1^{iv}\end{array}\right) + m_f\Gamma^2cos\phi\left(\begin{array}{l} 2{U'}^2w''_1 \\ +4Uw'''_1U' \\ +2Uw''_1U'' \\ +U^2w_1^{iv}\end{array}\right) \\
+\left(\begin{array}{l}
-\left(\frac{3}{2}w''_1{w'_1}^2 + U'w''_1 + U''w'_1\right)\left(\begin{array}{l} \left(-2v\delta P + E + P\right)A'' \\ -\left(2v\delta - 1\right)\left(P''A + 2P'A'\right)\end{array}\right) \\
-2\left(-2v\delta P + E + P\right)A' + 4P'A\left(v\delta - \frac{1}{2}\right)\left(\frac{3}{2}{w'_1}^2 + U'\right)w'''_1 + \\
3w'_1{w''_1}^2 + w'_1U''' \\
+2w''_1U'' + \left(\left(\begin{array}{c} 2v\delta P- \\ E - P\end{array}\right)A - G + T_o\right)\left(\frac{3}{2}{w'_1}^2 + U'\right)w_1^{iv} + w'_1U^{iv} \\
+\left(9w'_1w''_1 + 3U''\right)w'''_1 + 3w_1''^3 + 3w''_1U'''
\end{array}\right) \\
+\left(2v\delta - 1\right) \\
\left(\begin{array}{l}
AP\left(\frac{3}{2}{w'_1}^2 + U' - 1\right)w'''_1 + APw'_1U''' + 3APw'_1w_1''^2 + \\
\left(2APU'' + 2\left(P'A + PA'\right)\left(\frac{3}{2}{w'_1}^2 + U' - 1\right)\right)w''_1 \\
+w'P\left(\frac{1}{2}w'^2 + U' - 1\right)A'' + A\left(\frac{3}{2}w'^2 + U' - 1\right)P'' + \\
\left(2P'A + 2PA'\right)U'' + 2A'\left(\frac{1}{2}w'^2 + U' - 1\right)P'
\end{array}\right) \\
-E\left(\begin{array}{l}
Aw'''_1U' + 2Aw''_1U'' + 2A'w''_1U' \\
+Aw'_1U + 2A'w'_1U'' + A''w'_1U' + \\
\frac{1}{2}A''{w'_1}^3 + 3A'{w'_1}^2w'' + 3Aw'_1w_1''^2 \\
+\frac{3}{2}A{w'_1}^2w'''_1
\end{array}\right) \\
+E\alpha\left(\begin{array}{l}
A''\Delta T\left(1 - u'_1 - 1/2{w'_1}^2\right)w'_1 + 2A'\Delta T'\left(1 - u'_1 - 1/2w'^2\right)w'_1 \\
+2A'\Delta T\left(-u''_1 - w'_1w''_1\right)w'_1 + 2A'\Delta T\left(1 - u'_1 - 1/2{w'_1}^2\right)w''_1 \\
+A\Delta T''\left(1 - u'_1 - 1/2{w'_1}^2\right)w'_1 + 2A\Delta T'\left(-u''_1 - w'_1w''_1\right)w'_1 \\
+2A\Delta T'\left(1 - u'_1 - 1/2{w'_1}^2\right)w''_1 + A\Delta T\left(-u''_1 - w_1''^2 - w'_1w'''_1\right)w'_1 \\
+2A\Delta T\left(-u''_1 - w'_1w''_1\right)w''_1 + A\Delta T\left(1 - u'_1 - 1/2{w'_1}^2\right)w'''_1
\end{array}\right) \\
+J_1
\end{array}\right\} \\
&= F_1(x,t) + \left(e_oa\right)^2\frac{\partial^2F_1(x,t)}{\partial x^2},
\end{aligned}
\tag{2.6}
$$

Where:

$$
\begin{aligned}
&J_1 = \\
&\left(\begin{array}{l}
\left(\begin{array}{l} -P''\left(-2\,\delta\,v+1\right)A-2\,P'\left(-2\,\delta\,v+1\right)A' \\ -P\left(-2\,\delta\,v+1\right)A''-EA'' \end{array} \right) \left(\begin{array}{l} w'{}_1u''{}_1+w''{}_1u'{}_1 \\ +3/2\,w'{}_1{}^2w''{}_1 \end{array} \right) \\
+2\left(\begin{array}{l} -P'\left(-2\,\delta\,v+1\right)A- \\ P\left(-2\,\delta\,v+1\right)A'-EA' \end{array} \right) \left(\begin{array}{l} 2\,w''{}_1u''{}_1+w'{}_1u''' \\ {}_1+w'''{}_1\,u'{}_1 \\ +3\,w'{}_1w''{}_1{}^2+ \\ 3/2\,w'{}_1{}^2w'''{}_1 \end{array} \right) \\
+\left(\begin{array}{l} T_o-P\left(-2\,\delta\,v+1\right) \\ A-G-EA \end{array} \right) \left(\begin{array}{l} 3\,w'''{}_1\,u''{}_1+3\,w''{}_1u'''{}_1+ \\ w'{}_1u_1^{iv}+w_1^{iv}u'{}_1 \\ +3\,w_1''^3+9w'{}_1w''{}_1w'''{}_1+ \\ 3/2\,w'{}_1{}^2w_1^{iv} \end{array} \right)
\end{array} \right) + \left(\begin{array}{l} EI+ \\ \frac{IB_o^2 sin^2\varphi}{\mu_p} \end{array} \right) w^{vi} \\
&+E\alpha \\
&\left(\begin{array}{l}
\left(\begin{array}{l}
A''\,\Delta T'\left(1-u'{}_1-1/2\,w'{}_1{}^2\right) \\
+2\,A'\Delta T''\left(1-u'{}_1-1/2\,w'{}_1{}^2\right) \\
+2\,A'\Delta T'\left(-u''{}_1-w'{}_1w''{}_1\right) \\
+2\,A'\Delta T'\left(1-u'{}_1-1/2\,w'{}_1{}^2\right) \\
+A\Delta T'''\left(1-u'{}_1-1/2\,w'{}_1{}^2\right) \\
+2\,A\Delta T''\left(-u''{}_1-w'{}_1w''{}_1\right) \\
+2\,A\Delta T''\left(1-u'{}_1-1/2\,w'{}_1{}^2\right) \\
+A\Delta T'\left(-u''{}_1-w''{}_1{}^2-w'{}_1w'''{}_1\right) \\
+2\,A\Delta T'\left(-u''{}_1-w'{}_1w''{}_1\right) \\
+A\Delta T'\left(1-u'{}_1-1/2w'{}_1{}^2\right)
\end{array} \right) \\
+\left(\begin{array}{l}
A'''\,\Delta T\left(1-u'{}_1-1/2\,w'{}_1{}^2\right)w'{}_1 \\
+2\,A''\Delta T'\left(1-u'{}_1-1/2\,w'{}_1{}^2\right)w'{}_1 \\
+2\,A''\Delta T\left(-u''{}_1-w'{}_1w''{}_1\right)w'{}_1 \\
+2\,A''\Delta T\left(1-u'{}_1-1/2\,w'{}_1{}^2\right)w''{}_1 \\
+A'\Delta T''\left(1-u'{}_1-1/2\,w'{}_1{}^2\right)w'{}_1 \\
+2\,A'\Delta T'\left(-u''{}_1-w'{}_1w''{}_1\right)w'{}_1 \\
+2\,A'\Delta T'\left(1-u'{}_1-1/2\,w'{}_1{}^2\right)w''{}_1 \\
+A'\Delta T\left(-u''{}_1-w''{}_1{}^2-w'{}_1w'''{}_1\right)w'{}_1 \\
+2\,A'\Delta T\left(-u''{}_1-w'{}_1w''{}_1\right)w''{}_1 \\
+A'\Delta T\left(1-u'{}_1-1/2w'{}_1{}^2\right)w'''{}_1
\end{array} \right)
+\left(\begin{array}{l}
A''\Delta T\left(u''{}_1+w'{}_1w''{}_1\right)w'{}_1 \\
+2\,A'\Delta T'\left(u''{}_1+w'{}_1w''{}_1\right)w'{}_1 \\
+2\,A'\Delta T\left(u'''{}_1+w''{}_1{}^2+w'{}_1w'''{}_1\right)w'{}_1 \\
+2\,A'\Delta T\left(u''{}_1+w'{}_1w''{}_1\right)w''{}_1 \\
+A\Delta T''\left(u''{}_1+w'{}_1w''{}_1\right)w'{}_1 \\
+2\,A\Delta T'\left(u'''{}_1+w''{}_1{}^2+w'{}_1w'''{}_1\right)w'{}_1 \\
+2\,A\Delta T'\left(u''{}_1+w'{}_1w''{}_1\right)w''{}_1 \\
+A\Delta T\left(u_1^{iv}+3\,w''{}_1w'''{}_1+w'{}_1w_1^{iv}\right)w'{}_1 \\
+2\,A\Delta T\left(u'''{}_1+w''{}_1{}^2+w'{}_1w'''{}_1\right)w''{}_1 \\
+A\Delta T\left(u''{}_1+w'{}_1w''{}_1\right)w'''{}_1
\end{array} \right)
\end{array} \right) \\
&+ \\
&EI\left(\begin{array}{l} 5\,u_1^{v}w''{}_1+11\,u_1^{iv}w'''{}_1+13\,u''{}_1w_1^{iv}+8\,u''{}_1w_1^{v} \\ +2\,u'{}_1w_1^{vi}+w'{}_1u_1^{vi}+26\,w_1''^2w_1^{iv}+16\,w'{}_1w_1^{v}w''{}_1 \\ +28\,w'{}_1w_1^{iv}w'''{}_1+2\,w'{}_1{}^2w_1^{vi}+36\,w''{}_1w_1'''^2 \end{array} \right) \\
&+\tfrac{EA}{L}\int_0^L\left(z'w'{}_1+\left(\tfrac{1}{2}w'{}_1\right)^2\right)dx\left(w_1^{iv}+z_0^{iv}\right)+2\tfrac{EA'}{L}\int_0^L\left(z'w'{}_1+\left(\tfrac{1}{2}w'{}_1\right)^2\right)dx\left(w'''{}_1+z'''{}_0\right) \\
&+\tfrac{EA''}{L}\int_0^L\left(z'w'{}_1+\left(\tfrac{1}{2}w'{}_1\right)^2\right)dx\left(w''{}_1+z''{}_0\right)+k_1w''{}_1+k_2\left(3w''{}_1w_1^2+6w_1w_1'{}^2\right),
\end{aligned}
$$

(2.7)

While the longitudinal vibration for the first tube (N = 1) becomes:

$$
\begin{array}{l}
m\ddot{u}_1 + 2m_f\Gamma U\dot{u}_1'' + m_f\Gamma\dot{U}u'''_1 + m_f\Gamma\ddot{U} + m_f\Gamma^2UU'\left(1+u'_1\right) + \left[T_0 - G - EA_t\right]w'_1w''_1 - \\
\left(EA_t - m_f\Gamma^2U^2\right)u''_1 + (PA)'\left(1-2v\delta\right) - PA\left(1-2v\delta\right)w'_1w''_1 \\
-EA'_t\left(u'_1 + \frac{1}{2}{w'_1}^2\right) - \frac{(PA)'}{2}\left(1-2v\delta\right){w'_1}^2 + E\alpha\left(A\Delta T' + A'\Delta T\right) - \\
\frac{E\alpha}{2}{w'_1}^2\left(A\Delta T' + A'\Delta T\right) - E\alpha A\Delta T w'_1w''_1 - EI\left({w_1}^{iv}w'_1 + w''_1w'''_1\right) \\
+(e_oa)^2\left[\begin{array}{l}
m\ddot{u}_1'' + 2\Gamma m_f\left(\begin{array}{l} U''\dot{u}_1'' + \\ 2U'\dot{u}_1''' + U\dot{u}_1^{iv}\end{array}\right) + \Gamma m_f\left(\dot{U}''u'''_1 + 2\dot{U}'\dot{u}_1^{iv} + \dot{U}\dot{u}_1^{v}\right) + \\
\Gamma m_f\ddot{U}'' + \Gamma^2 m_f\left(\begin{array}{l} 3U'U''\left(1+u'\right) + 2{U'}^2u''_1 + UU'''\left(1+u'_1\right) \\ +2UU''u''_1 + UU'u'''_1\end{array}\right) \\
+\left(\begin{array}{l} \left(T_0 - G - EA_t\right)w'_1{w_1}^{iv} + 3\left(T_0 - G - EA_t\right)w''_1w'''_1 \\ -2EA'_tw'_1w'''_1 - 2EA'_t{w''_1}^2 - EA''_tw'_1w''_1\end{array}\right) + \\
\left(\left(\begin{array}{l} {EA_t}'' - 2\Gamma^2m_f{U'}^2 \\ -2\Gamma^2m_fUU''\end{array}\right)u''_1 + 2\left(\begin{array}{l} EA'_t - \\ 2m_f\Gamma^2UU'\end{array}\right)u'''_1 + \left(\begin{array}{l} EA_t - \\ m_f\Gamma^2U^2\end{array}\right){u_1}^{iv}\right) \\
+\left(1-2v\delta\right)\left(P'''A + 3P''A' + 3P'A'' + PA'''\right) + \left(1-2v\delta\right) \\
\left(\begin{array}{l} P''Aw'_1w''_1 + 2P'A'w'_1w''_1 + 2P'A{w''_1}^2 + \\ 2P'Aw'_1w'''_1 + PA''w'_1w''_1 + 2PA'{w''_1}^2 \\ +2PA'w'_1w'''_1 + 3PAw''_1w'''_1 + PAw'_1{w_1}^{iv}\end{array}\right) \\
+E\left({A_t}'''\left(u'_1 + \frac{1}{2}{w'_1}^2\right) + 2{A_t}''\left(u''_1 + w'_1w''_1\right) + {A_t}'\left(\begin{array}{l} u'''_1 + {w''_1}^2 + \\ w'_1w'''_1\end{array}\right)\right) \\
+\frac{1}{2}\left(1-2v\delta\right)\left(\begin{array}{l} \left(P'''A + 3P''A' + 3P'A''w''_1w''_1 + PA'''w'_1w'''_1\right){w'_1}^2 \\ +\left(4P''A + 2P'A' + PA''\right)w''_1w'_1 \\ +2\left(P'A + PA'\right){w''_1}^2 + \left(P'A + PA'\right)w'''_1\end{array}\right) \\
+E\alpha\left(3A''\Delta T' + 3A'\Delta T'' + A\Delta T''' + A'''\Delta T\right) + \\
\frac{E\alpha}{2}\left(\begin{array}{l} \left(\begin{array}{l} 3A''\Delta T' + 3A'\Delta T'' \\ +A\Delta T''' + A'''\Delta T\end{array}\right){w'_1}^2 + 4\left(\begin{array}{l} 2A'\Delta T' + A\Delta T'' + \\ A''\Delta T\end{array}\right)w'_1w''_1 \\ +2\left(A\Delta T' + A'\Delta T\right){w''_1}^2 + 2\left(A\Delta T' + A'\Delta T\right)w'_1w'''_1\end{array}\right) \\
+E\left(\begin{array}{l} \alpha\left(\begin{array}{l} A''\Delta Tw'_1w''_1 + 2A'\Delta T'w'_1w''_1 + 2A'\Delta T{w''_1}^2 \\ +2A'\Delta Tw'_1w'''_1 + A\Delta T''w'_1w''_1 + 2A\Delta T'{w''_1}^2 \\ +2A\Delta T'w'_1w'''_1 + 3A\Delta Tw''_1w'''_1 + A\Delta Tw'_1{w_1}^{iv}\end{array}\right) + \\ EI\left({w_1}^{vi}w'_1 + 3{w_1}^{v}w''_1 + 4{w_1}^{iv}w'''_1\right)\end{array}\right)
\end{array}\right] \\
= F_1(x,t) + (e_oa)^2\frac{\partial^2F_1(x,t)}{\partial x^2},
\end{array}
\tag{2.8}
$$

For tubes not in direct contact with fluid (i.e., for the second, third, fourth up to the last tube), the velocity components in the vibration models become nullified. For multi-walled CNT, the transverse vibration for the second tube (N = 2) is:

$$
\begin{array}{l}
m\ddot{w}_2 + \left(c + A_f\sigma B_o^2 cos^2\varphi\right)\dot{w}_2 + \left[T_0 - G - k_p - \frac{B_o^2 cos^2\varphi}{\mu_p}\right] w''_2 + [T_0 - G - EA]\left[w'_2u''_2 + w''_2u'_2 + \frac{3}{2}{w'_2}^2 w''_2\right] \\
-EA\left[w'_2u'_2 + \frac{1}{2}{w'_2}^3\right] + E\alpha A\Delta T w'_2\left(1 - u'_2 - \frac{1}{2}{w'_2}^2\right) + E\alpha A\Delta T'\left(1 - u'_2 - \frac{1}{2}{w'_2}^2\right) + \\
E\alpha A'\Delta T w'_2\left(1 - u'_2 - \frac{1}{2}{w'_2}^2\right) - E\alpha A\Delta T w'_2\left(u''_2 + w'_2w''_2\right) + \left(EI + \frac{IB_o^2 sin^2\varphi}{\mu_p}\right) {w_2}^{iv} \\
-EI\left(3u'''_2w''_2 + 4u''_2w'''_2 + 2u'_2{w_2}^{iv} + w'_2{u_2}^{iv} + 2{w'_2}^2{w_2}^{iv} + 8w'_2w''_2w'''_2 + 2{w''_2}^3\right) \\
-\frac{EA}{L}\int\limits_0^L\left(z'_0w'_2 + \frac{1}{2}{w'_2}^2\right)dx\,[w''_2 + z''_0] + k_1w_2 + k_2{w_2}^3 + (e_oa)^2 \\
\left\{
\begin{array}{l}
m\ddot{w}''_2 + \left(c + A_f\sigma B_o^2cos^2\varphi\right)\dot{w}''_2 + \begin{pmatrix} T_0 - G - k_p \\ -\frac{B_o^2cos^2\varphi}{\mu_p} \end{pmatrix} {w_2}^{iv} + \\
\begin{pmatrix} -\left(\frac{3}{2}w''_2{w'}^2\right)(EA'') \\ -2EA' + 3w'_2{w''_2}^2 \\ +(EA - G + T_o)\left(\frac{3}{2}{w'_2}^2\right){w_2}^{iv} \\ +(9w'_2w''_2)w'''_2 + 3{w''_2}^3 \end{pmatrix} - E\begin{pmatrix} \frac{1}{2}A''{w'_2}^3 + 3A'{w'_2}^2w''_2 + 3Aw'_2{w''_2}^2 \\ +\frac{3}{2}A{w'_2}^2w'''_2 \end{pmatrix} \\
+E\alpha\begin{pmatrix}
A''\Delta T\left(1 - u'_2 - 1/2{w'_2}^2\right)w'_2 + 2A'\Delta T'\left(1 - u'_2 - 1/2{w'_2}^2\right)w'_2 \\
+2A'\Delta T\left(-u''_2 - w'_2w''_2\right)w'_2 + 2A'\Delta T\left(1 - u'_2 - 1/2{w'_2}^2\right)w''_2 \\
+A\Delta T''\left(1 - u'_2 - 1/2{w'_2}^2\right)w' + 2A\Delta T'\left(-u'' - w'w''\right)w' \\
+2A\Delta T'\left(1 - u' - 1/2{w'}^2\right)w''_2 + A\Delta T\left(-u''_2 - {w''_2}^2 - w'_2w'''_2\right)w'_2 \\
+2A\Delta T\left(-u''_2 - w'_2w''_2\right)w''_2 + A\Delta T\left(1 - u'_2 - 1/2{w'_2}^2\right)w'''_2
\end{pmatrix} + \\
\begin{pmatrix}
(-EA'')\left(w'_2u''_2 + w''_2u'_2 + 3/2{w'_2}^2w''_2\right) \\
+2(-EA')\begin{pmatrix} 2w''_2u''_2 + w'_2u'''_2 + w'''_2u'_2 \\ +3w'_2{w''_2}^2 + 3/2{w'_2}^2w'''_2 \end{pmatrix} \\
+(T_o - G - EA)\begin{pmatrix} 3w'''_2u''_2 + 3w''_2u'''_2 + w'_2{u_2}^{iv} + {w_2}^{iv}u'_2 \\ +3{w''_2}^3 + 9w'_2w''_2w'''_2 + 3/2{w'_2}^2{w_2}^{iv} \end{pmatrix}
\end{pmatrix} + \begin{pmatrix} EI+ \\ \frac{IB_o^2sin^2\varphi}{\mu_p} \end{pmatrix} {w_2}^{vi} \\
+E\alpha\left(\begin{array}{c}
\begin{pmatrix}
A''\Delta T'\left(1 - u'_2 - 1/2{w'_2}^2\right) \\
+2A'\Delta T''\left(1 - u'_2 - 1/2{w'_2}^2\right) \\
+2A'\Delta T'\left(-u''_2 - w'_2w''_2\right) \\
+2A'\Delta T'\left(1 - u'_2 - 1/2{w'_2}^2\right) \\
+A\Delta T'''\left(1 - u'_2 - 1/2{w'_2}^2\right) \\
+2A\Delta T''\left(-u''_2 - w'_2w''_2\right) \\
+2A\Delta T''\left(1 - u'_2 - 1/2{w'_2}^2\right) \\
+A\Delta T'\left(-u''_2 - {w''_2}^2 - w'_2w'''_2\right) \\
+2A\Delta T'\left(-u''_2 - w'_2w''_2\right) \\
+A\Delta T'\left(1 - u'_2 - 1/2{w'_2}^2\right)
\end{pmatrix} + \begin{pmatrix}
A'''\Delta T\left(1 - u'_2 - 1/2{w'_2}^2\right)w'_2 \\
+2A''\Delta T'\left(1 - u'_2 - 1/2{w'_2}^2\right)w'_2 \\
+2A''\Delta T\left(-u''_2 - w'_2w''_2\right)w'_2 \\
+2A''\Delta T\left(1 - u'_2 - 1/2{w'_2}^2\right)w''_2 \\
+A'\Delta T''\left(1 - u'_2 - 1/2{w'_2}^2\right)w'_2 \\
+2A'\Delta T'\left(-u''_2 - w'_2w''_2\right)w'_2 \\
+2A'\Delta T'\left(1 - u'_2 - 1/2{w'_2}^2\right)w''_2 \\
+A'\Delta T\left(-u''_2 - {w''_2}^2 - w'_2w'''_2\right)w'_2 \\
+2A'\Delta T\left(-u''_2 - w'_2w''_2\right)w''_2 \\
+A'\Delta T\left(1 - u'_2 - 1/2{w'_2}^2\right)w'''_2
\end{pmatrix} \\
+\begin{pmatrix}
A''\Delta T\left(u''_2 + w'_2w''_2\right)w'_2 + 2A'\Delta T'\left(u''_2 + w'_2w''_2\right)w'_2 \\
+2A'\Delta T\left(u'''_2 + {w''_2}^2 + w'_2w'''_2\right)w'_2 + 2A'\Delta T\left(u''_2 + w'_2w''_2\right)w''_2 \\
+A\Delta T''\left(u''_2 + w'w''_2\right)w'_2 + 2A\Delta T'\left(u''' + {w''}^2 + w'w'''\right)w' \\
+2A\Delta T'\left(u''_2 + w'_2w''_2\right)w''_2 + A\Delta T\left(u^{iv} + 3w''_2w'''_2 + w'_2{w_2}^{iv}\right)w'_2 \\
+2A\Delta T\left(u'''_2 + {w''_2}^2 + w'_2w'''_2\right)w''_2 + A\Delta T\left(u''_2 + w'_2w''_2\right)w'''_2
\end{pmatrix}
\end{array}\right) + \\
J_2
\end{array}
\right\} \\
= F_2(x,t) + (e_oa)^2\frac{\partial^2 F_2(x,t)}{\partial x^2},
\end{array}
$$

$$\tag{2.9}$$

Where:

$$
\begin{aligned}
&J_2 = \\
&EI\left(\begin{array}{l} 5u_2{}^{v}w''_2 + 11u_2{}^{iv}w'''_2 + 13u''_2w_2{}^{iv} + 8u''_2w_2{}^{v} \\ +2u'_2w_2{}^{vi} + w'_2u_2{}^{vi} + 26w''_2{}^2w_2{}^{iv} + 16w'_2w_2{}^{v}w''_2 \\ +28w'_2w_2{}^{iv}w'''_2 + 2w'_2{}^2w_2{}^{vi} + 36w''_2w'''_2{}^2 \end{array}\right) \\
&+\tfrac{EA}{L}\int_0^L \left(z'w'_2 + \left(\tfrac{1}{2}w'_2\right)^2\right)dx\left(w_2{}^{iv} + z_0^{iv}\right) + \\
&2\tfrac{EA'}{L}\int_0^L \left(z'w'_2 + \left(\tfrac{1}{2}w'_2\right)^2\right)dx\left(w'''_2 + z'''_0\right) \\
&+\tfrac{EA''}{L}\int_0^L \left(z'w'_2 + \left(\tfrac{1}{2}w'_2\right)^2\right)dx\left(w''_2 + z''_0\right) + \\
&k_1w''_2 + k_2\left(3w''_2w_2{}^2 + 6w_2w'_2{}^2\right),
\end{aligned}
\tag{2.10}
$$

The longitudinal vibration for the second tube (N = 2) becomes:

$$
\begin{aligned}
&m\ddot{u}_2 + [T_0 - G - EA_t]\,w'_2w''_2 - (EA_t)\,u''_2 \\
&-EA'_t\left(u'_2 + \tfrac{1}{2}w'_2{}^2\right) + E\alpha\left(A\Delta T' + A'\Delta T\right) - \\
&\tfrac{E\alpha}{2}w'_2{}^2\left(A\Delta T' + A'\Delta T\right) - E\alpha A\Delta T w'_2w''_2 \\
&-EI\left(w_2{}^{iv}w'_2 + w''_2w'''_2\right) + (e_oa)^2 \\
&\left[\begin{array}{l}
m\ddot{u}''_2 + \left(\begin{array}{l} (T_0 - G - EA_t)\,w'_2w_2{}^{iv} + 3\,(T_0 - G - EA_t)\,w''_2w'''_2 \\ -2EA'_tw'_2w'''_2 - 2EA'_tw''_2{}^2 - EA''_tw'_2w''_2 \end{array}\right) \\
+\left(\left(EA_t{}''\right)u''_2 + 2\left(EA'_t\right)u'''_2 + (EA_t)\,u_2{}^{iv}\right) \\
+E\left(\begin{array}{l} A_t{}'''\left(u'_2 + \tfrac{1}{2}w'_2{}^2\right) \\ +2A_t{}''\left(u''_2 + w'_2w''_2\right) + A_t{}'\left(u'''_2 + w''_2{}^2 + w'_2w'''_2\right) \end{array}\right) \\
+E\alpha\left(3A''\Delta T' + 3A'\Delta T'' + A\Delta T''' + A'''\Delta T\right) + \\
\tfrac{E\alpha}{2}\left(\begin{array}{l} \left(\begin{array}{l} 3A''\Delta T' + 3A'\Delta T'' \\ +A\Delta T''' + A'''\Delta T \end{array}\right)w'_2{}^2 + 4\left(\begin{array}{l} 2A'\Delta T' + \\ A\Delta T'' + A''\Delta T \end{array}\right)w'_2w''_2 \\ +2\left(A\Delta T' + A'\Delta T\right)w''_2{}^2 + 2\left(A\Delta T' + A'\Delta T\right)w'_2w'''_2 \end{array}\right) \\
+E\left(\begin{array}{l} \alpha\left(\begin{array}{l} A''\Delta T w'_2w''_2 + 2A'\Delta T'w'_2w''_2 + \\ 2A'\Delta T w''_2{}^2 + 2A'\Delta T w'_2w'''_2 + \\ A\Delta T''w'_2w''_2 + 2A\Delta T'w''_2{}^2 \\ +2A\Delta T'w'_2w'''_2 + 3A\Delta T w''_2w'''_2 + \\ A\Delta T w'_2w_2{}^{iv} \end{array}\right) + \\ I\left(w_2{}^{vi}w'_2 + 3w_2{}^{v}w''_2 + 4w_2{}^{iv}w'''_2\right) \end{array}\right)
\end{array}\right] \\
&= F_2(x,t) + (e_oa)^2\frac{\partial^2 F_2(x,t)}{\partial x^2},
\end{aligned}
\tag{2.11}
$$

For multi-walled CNT, the transverse vibration for the third tube (N = 3) is:

$$
\begin{aligned}
& m\ddot{w}_3 + \left(c + A_f\sigma B_o^2 cos^2\varphi\right)\dot{w}_3 + \left[T_0 - G - k_p - \tfrac{B_o^2 cos^2\varphi}{\mu_p}\right] w''_3 + \\
& [T_0 - G - EA]\left[w'_3u''_3 + w''_3u'_3 + \tfrac{3}{2}{w'_3}^2 w''_3\right] - EA\left[w'_3u'_3 + \tfrac{1}{2}{w'_3}^3\right] + \\
& E\alpha A\Delta T w'_3\left(1 - u'_3 - \tfrac{1}{2}{w'_3}^2\right) + E\alpha A\Delta T'\left(1 - u'_3 - \tfrac{1}{2}{w'_3}^2\right) + \\
& E\alpha A'\Delta T w'_3\left(1 - u'_3 - \tfrac{1}{2}{w'_3}^2\right) - E\alpha A\Delta T w'_3\left(u''_3 + w'_3w''_3\right) + \\
& \left(EI + \tfrac{IB_o^2 sin^2\varphi}{\mu_p}\right) {w_3}^{iv} - EI\begin{pmatrix} 3u'''_3w''_3 + 4u''_3w'''_3 + \\ 2u'_3{w_3}^{iv} + w'_3{u_3}^{iv} + \\ 2{w'_3}^2{w_3}^{iv} + 8w'_3w''_3w'''_3 + \\ 2{w''_3}^3 \end{pmatrix} \\
& -\tfrac{EA}{L}\int_0^L\left(z'_0w'_3 + \tfrac{1}{2}{w'_3}^2\right)dx\,[w''_3 + z''_0] + k_1w_3 + k_2{w_3}^3 + (e_oa)^2 \\
& \left\{\begin{array}{l}
m\ddot{w}''_3 + \left(c + A_f\sigma B_o^2cos^2\varphi\right)\dot{w}''_3 + \begin{pmatrix} T_0 - G - k_p \\ -\frac{B_o^2cos^2\varphi}{\mu_p}\end{pmatrix}{w_3}^{iv} + \\
\begin{pmatrix} -\left(\frac{3}{2}w''_3{w'}^2_3\right)(EA'') \\ -2EA' + 3w'_3{w''_3}^2 \\ +(EA - G + T_o)\left(\frac{3}{2}{w'_3}^2\right){w_3}^{iv} \\ +(9w'_3w''_3)w'''_3 + 3{w''_3}^3 \end{pmatrix} - E\begin{pmatrix} \frac{1}{2}A''{w'_3}^3 + 3A'{w'_3}^2w''_3 + 3Aw'_3{w''_3}^2 \\ +\frac{3}{2}A{w'_3}^2w'''_3 \end{pmatrix} \\
+E\alpha\begin{pmatrix} A''\Delta T\left(1 - u'_3 - 1/2{w'_3}^2\right)w'_3 + 2A'\Delta T'\left(1 - u'_3 - 1/2{w'_3}^2\right)w'_3 \\ +2A'\Delta T\left(-u''_3 - w'_3w''_3\right)w'_3 + 2A'\Delta T\left(1 - u'_3 - 1/2{w'_3}^2\right)w''_3 \\ +A\Delta T''\left(1 - u'_3 - 1/2{w'_3}^2\right)w'_3 + 2A\Delta T'\left(-u''_3 - w'_3w''_3\right)w'_3 \\ +2A\Delta T'\left(1 - u'_3 - 1/2{w'}^2_3\right)w''_3 + A\Delta T\left(-u''_3 - {w''_3}^2 - w'_3w'''_3\right)w'_3 \\ +2A\Delta T\left(-u''_3 - w'_3w''_3\right)w''_3 + A\Delta T\left(1 - u'_3 - 1/2{w'_3}^2\right)w'''_3 \end{pmatrix} \\
+\begin{pmatrix} (-EA'')\left(w'_3u''_3 + w''_3u'_3 + 3/2{w'_3}^2w''_3\right) \\ +2(-EA')\begin{pmatrix} 2w''_3u''_3 + w'_3u'''_3 + w'''_3u'_3 \\ +3w'_3{w''_3}^2 + 3/2{w'_3}^2w'''_3 \end{pmatrix} \\ +(T_o - G - EA)\begin{pmatrix} 3w'''_3u''_3 + 3w''_3u'''_3 + w'_3{u_3}^{iv} + {w_3}^{iv}u'_3 \\ +3{w''_3}^3 + 9w'_3w''_3w'''_3 + 3/2{w'_3}^2{w_3}^{iv} \end{pmatrix} \end{pmatrix} + \begin{pmatrix} EI + \\ \frac{IB_o^2sin^2\varphi}{\mu_p} \end{pmatrix}{w_3}^{vi} \\
+J_3
\end{array}\right\} \\
& = F_3(x,t) + (e_oa)^2\tfrac{\partial^2 F_3(x,t)}{\partial x^2},
\end{aligned}
\tag{2.12}
$$

$$
\begin{aligned}
J_3 = {} & E\alpha\left(\left(\begin{array}{l}
A''\,\Delta T'\left(1-u'_3-1/2\,{w'_3}^2\right)\\
+2\,A'\Delta T''\left(1-u'_3-1/2\,{w'_3}^2\right)\\
+2\,A'\Delta T'\left(-u''_3-w'_3w''_3\right)\\
+2\,A'\Delta T'\left(1-u'_3-1/2\,{w'_3}^2\right)\\
+A\Delta T'''\left(1-u'_3-1/2\,{w'_3}^2\right)\\
+2\,A\Delta T''\left(-u''_3-w'_3w''_3\right)\\
+2\,A\Delta T''\left(1-u'_3-1/2\,{w'_3}^2\right)\\
+A\Delta T'\left(-u''_3-{w''_3}^2-w'_3w'''_3\right)\\
+2\,A\Delta T'\left(-u''_3-w'_3w''_3\right)\\
+A\Delta T'\left(1-u'_3-1/2w'_3{}^2\right)
\end{array}\right)+\left(\begin{array}{l}
A'''\,\Delta T\left(1-u'_3-1/2\,{w'_3}^2\right)w'_3\\
+2\,A''\Delta T'\left(1-u'_3-1/2\,{w'_3}^2\right)w'_3\\
+2\,A''\Delta T\left(-u''_3-w'_3w''_3\right)w'_3\\
+2\,A''\Delta T\left(1-u'_3-1/2\,{w'_3}^2\right)w''_3\\
+A'\Delta T''\left(1-u'_3-1/2\,{w'_3}^2\right)w'_3\\
+2\,A'\Delta T'\left(-u''_3-w'_3w''_3\right)w'_3\\
+2\,A'\Delta T'\left(1-u'_3-1/2\,{w'_3}^2\right)w''_3\\
+A'\Delta T\left(-u''_3-{w''_3}^2-w'_3w'''_3\right)w'_3\\
+2\,A'\Delta T\left(-u''_3-w'_3w''_3\right)w''_3\\
+A'\Delta T\left(1-u'_3-1/2w'_3{}^2\right)w'''_3
\end{array}\right)\right.\\
& \left.+\left(\begin{array}{l}
A''\Delta T\left(u''_3+w'_3w''_3\right)w'_3+2\,A'\Delta T'\left(u''_3+w'_3w''_3\right)w'_3\\
+2\,A'\Delta T\left(u'''_3+{w''_3}^2+w'_3w'''_3\right)w'_3+2\,A'\Delta T\left(u''_3+w'_3w''_3\right)w''_3\\
+A\Delta T''\left(u''_3+w'_3w''_3\right)w'_3+2\,A\Delta T'\left(u'''_3+w''^2_3+w'_3w'''_3\right)w'_3\\
+2\,A\Delta T'\left(u''_3+w'_3w''_3\right)w''_3+A\Delta T\left({u_3}^{iv}+3\,w''_3w'''_3+w'_3{w_3}^{iv}\right)w'_3\\
+2\,A\Delta T\left(u'''_3+{w''_3}^2+w'_3w'''_3\right)w''_3+A\Delta T\left(u''_3+w'_3w''_3\right)w'''_3
\end{array}\right)\right)\\
& +EI\left(\begin{array}{l}
5\,{u_3}^{v}w''_3+11\,{u_3}^{iv}w'''_3+13\,u''_3{w_3}^{iv}+8\,u''_3{w_3}^{v}\\
+2\,u'_3{w_3}^{vi}+w'_3{u_3}^{vi}+26\,{w''_3}^2{w_3}^{iv}+16\,w'_3{w_3}^{v}w''_3\\
+28\,w'_3{w_3}^{iv}w'''_3+2\,{w'_3}^2{w_3}^{vi}+36\,w''_3{w'''_3}^2
\end{array}\right)\\
& +\frac{EA}{L}\int_0^L\left(z'w'_3+\left(\tfrac{1}{2}w'_3\right)^2\right)dx\left({w_3}^{iv}+z_0^{iv}\right)+2\frac{EA'}{L}\int_0^L\left(z'w'_3+\left(\tfrac{1}{2}w'_3\right)^2\right)dx\left(w'''_3+z'''_0\right)+\\
& \frac{EA''}{L}\int_0^L\left(z'w'_3+\left(\tfrac{1}{2}w'_3\right)^2\right)dx\left(w''_3+z''_0\right)+k_1w''_3+k_2\left(3w''_3{w_3}^2+6w_3{w'_3}^2\right)
\end{aligned}
\tag{2.13}
$$

The longitudinal vibration for the third tube (N = 3) becomes:

$$
\begin{array}{l}
m\ddot{u}_3 + \left[T_0 - G - EA_t\right] w'_3 w''_3 - \left(EA_t\right) u''_3 \\
-EA'_t \left(u'_3 + \frac{1}{2}{w'_3}^2\right) + E\alpha\left(A\Delta T' + A'\Delta T\right) \\
-\frac{E\alpha}{2}{w'_3}^2\left(A\Delta T' + A'\Delta T\right) \\
-E\alpha A\Delta T w'_3 w''_3 - EI\left({w_3}^{iv} w'_3 + w''_3 w'''_3\right) + \left(e_o a\right)^2 \\
\left[\begin{array}{l}
m\ddot{u}''_3 + \left(\begin{array}{l}
\left(T_0 - G - EA_t\right) w'_3 {w_3}^{iv} + \\
3\left(T_0 - G - EA_t\right) w''_3 w'''_3 \\
-2EA'_t w'_3 w'''_3 - 2EA'_t {w''_3}^2 \\
-EA''_t w'_3 w''_3
\end{array}\right) + \\
\left(\left(E{A_t}''\right) u''_3 + 2\left(EA'_t\right) u'''_3 + \left(EA_t\right) {u_3}^{iv}\right) \\
+E\left(\begin{array}{l}
{A_t}'''\left(u'_3 + \frac{1}{2}{w'_3}^2\right) + \\
2{A_t}''\left(u''_3 + w'_3 w''_3\right) + \\
{A_t}'\left(u'''_3 + {w''_3}^2 + w'_3 w'''_3\right)
\end{array}\right) + \\
E\alpha\left(\begin{array}{l}
3A''\Delta T' + 3A'\Delta T'' \\
+A\Delta T''' + A'''\Delta T
\end{array}\right) \\
+\frac{E\alpha}{2}\left(\begin{array}{l}
\left(\begin{array}{l}
3A''\Delta T' + \\
3A'\Delta T'' \\
+A\Delta T''' + \\
A'''\Delta T
\end{array}\right){w'_3}^2 + 4\left(\begin{array}{l}
2A'\Delta T' \\
+A\Delta T'' + \\
A''\Delta T
\end{array}\right) w'_3 w''_3 \\
+2\left(\begin{array}{l}
A\Delta T' + \\
A'\Delta T
\end{array}\right){w''_3}^2 + 2\left(\begin{array}{l}
A\Delta T' + \\
A'\Delta T
\end{array}\right) w'_3 w'''_3
\end{array}\right) \\
+E\left(\begin{array}{l}
\alpha\left(\begin{array}{l}
A''\Delta T w'_3 w''_3 + 2A'\Delta T' w'_3 w''_3 + \\
2A'\Delta T {w''_3}^2 + 2A'\Delta T w'_3 w'''_3 + \\
A\Delta T'' w'_3 w''_3 + 2A\Delta T' {w''_3}^2 \\
+2A\Delta T' w'_3 w'''_3 + 3A\Delta T w''_3 w'''_3 + \\
A\Delta T w'_3 {w_3}^{iv}
\end{array}\right) \\
+I\left(\begin{array}{l}
{w_3}^{vi} w'_3 \\
+3{w_3}^{v} w''_3 \\
+4{w_3}^{iv} w'''_3
\end{array}\right)
\end{array}\right)
\end{array}\right] \\
= F_3(x,t) + \left(e_o a\right)^2 \frac{\partial^2 F_3(x,t)}{\partial x^2}
\end{array}
\tag{2.14}
$$

The generalized transverse vibration for the MWCNT is

$$
\begin{aligned}
& m\ddot{w}_N + \left(c + A_f \sigma B_o^2 cos^2\varphi\right) \dot{w}_N + \left[T_0 - G - k_p - \frac{B_o^2 cos^2\varphi}{\mu_p}\right] w''_N \\
& + [T_0 - G - EA]\left[w'_N u''_N + w''_N u'_N + \tfrac{3}{2} {w'_N}^2 w''_N\right] \\
& - EA\left[w'_N u'_N + \tfrac{1}{2} {w'_N}^3\right] + E\alpha A\Delta T w'_N\left(1 - u'_N - \tfrac{1}{2}{w'_N}^2\right) + \\
& E\alpha A\Delta T'\left(1 - u'_N - \tfrac{1}{2}{w'_N}^2\right) + E\alpha A'\Delta T w'_N\left(1 - u'_N - \tfrac{1}{2}{w'_N}^2\right) \\
& - E\alpha A\Delta T w'_N\left(u''_N + w'_N w''_N\right) + \left(EI + \frac{IB_o^2 sin^2\varphi}{\mu_p}\right) {w_N}^{iv} \\
& - EI\left(3u'''_N w''_N + 4u''_N w'''_N + 2u'_N {w_N}^{iv} + w'_N {u_N}^{iv} + 2{w'_N}^2 {w_N}^{iv} + 8w'_N w''_N w'''_N + 2{w''_N}^3\right) \\
& - \frac{EA}{L}\int_0^L \left(z'_0 w'_N + \tfrac{1}{2}{w'_N}^2\right) dx \left[w''_N + z''_0\right] + k_1 w_N + k_2 {w_N}^3 + (e_o a)^2 \\
& \left\{
\begin{array}{l}
m\ddot{w}''_N + \begin{pmatrix} c+ \\ A_f\sigma B_o^2 cos^2\varphi \end{pmatrix} \dot{w}''_N + \begin{pmatrix} T_0 - G - k_p \\ -\frac{B_o^2 cos^2\varphi}{\mu_p} \end{pmatrix} {w_N}^{iv} + \begin{pmatrix} -\left(\tfrac{3}{2} w''_N {w'_N}^2\right)(EA'') \\ -2EA' + 3w'_N {w''_N}^2 \\ + (EA - G + T_o)\left(\tfrac{3}{2}{w'_N}^2\right) {w_N}^{iv} \\ + \left(9w'_N w''_N\right) w'''_N + 3{w''_N}^3 \end{pmatrix} \\
-E\begin{pmatrix} \tfrac{1}{2}A'' {w'_N}^3 + 3A'{w'_N}^2 w''_N + 3Aw'_N {w''_N}^2 \\ +\tfrac{3}{2}A{w'_N}^2 w'''_N \end{pmatrix} \\
+E\alpha\begin{pmatrix} A''\Delta T\left(1 - u'_N - 1/2{w'_N}^2\right) w'_N + 2A'\Delta T'\left(1 - u'_N - 1/2{w'_N}^2\right) w'_N \\ +2A'\Delta T\left(-u''_N - w'_N w''_N\right) w'_N + 2A'\Delta T\left(1 - u'_N - 1/2{w'_N}^2\right) w''_N \\ +A\Delta T''\left(1 - u'_N - 1/2{w'_N}^2\right) w'_N + 2A\Delta T'\left(-u''_N - w'_N w''_N\right) w'_N \\ +2A\Delta T'\left(1 - u'_N - 1/2{w'_N}^2\right) w''_N + A\Delta T\left(-u''_N - {w''_N}^2 - w'_N w'''_N\right) w'_N \\ +2A\Delta T\left(-u''_N - w'_N w''_N\right) w''_N + A\Delta T\left(1 - u'_N - 1/2{w'_N}^2\right) w'''_N \end{pmatrix} \\
+\begin{pmatrix} (-EA'')\left(w'_N u''_N + w''_N u'_N + 3/2{w'_N}^2 w''_N\right) \\ +2(-EA')\begin{pmatrix} 2w''_N u''_N + w'_N u'''_N + w'''_N u'_N \\ +3w'_N {w''_N}^2 + 3/2{w'_N}^2 w'''_N \end{pmatrix} \\ +(T_o - G - EA)\begin{pmatrix} 3w'''_N u''_N + 3w''_N u'''_N + w'_N {u_N}^{iv} + {w_N}^{iv} u'_N \\ +3{w''_N}^3 + 9w'_N w''_N w'''_N + 3/2{w'_N}^2 {w_N}^{iv} \end{pmatrix} \end{pmatrix} + \begin{pmatrix} EI+ \\ \frac{IB_o^2 sin^2\varphi}{\mu_p} \end{pmatrix} {w_N}^{vi} \\
+J_4
\end{array}
\right\} \\
& = F_N(x,t) + (e_o a)^2 \frac{\partial^2 F_N(x,t)}{\partial x^2},
\end{aligned}
\tag{2.15}
$$

$$
\begin{aligned}
& m\ddot{w}_N + \left(c + A_f \sigma B_o^2 cos^2\varphi\right)\dot{w}_N + \left[T_0 - G - k_p - \tfrac{B_o^2 cos^2\varphi}{\mu_p}\right] w''_N \\
& + \left[T_0 - G - EA\right]\left[w'_N u''_N + w''_N u'_N + \tfrac{3}{2} {w'_N}^2 w''_N\right] \\
& -EA\left[w'_N u'_N + \tfrac{1}{2}{w'_N}^3\right] + E\alpha A \Delta T w'_N \left(1 - u'_N - \tfrac{1}{2}{w'_N}^2\right) + \\
& E\alpha A \Delta T' \left(1 - u'_N - \tfrac{1}{2}{w'_N}^2\right) + E\alpha A' \Delta T w'_N \left(1 - u'_N - \tfrac{1}{2}{w'_N}^2\right) \\
& -E\alpha A \Delta T w'_N \left(u''_N + w'_N w''_N\right) + \left(EI + \tfrac{IB_o^2 sin^2\varphi}{\mu_p}\right) {w_N}^{iv} \\
& -EI\left(3u'''_N w''_N + 4u''_N w'''_N + 2u'_N {w_N}^{iv} + w'_N {u_N}^{iv} + 2{w'_N}^2 {w_N}^{iv} + 8w'_N w''_N w'''_N + 2{w''_N}^3\right) \\
& -\tfrac{EA}{L}\int_0^L \left(z'_0 w'_N + \tfrac{1}{2}{w'_N}^2\right)dx\left[w''_N + z''_0\right] + k_1 w_N + k_2 {w_N}^3 + (e_o a)^2 \\
& \left\{
\begin{array}{l}
m\ddot{w}''_N + \begin{pmatrix} c+ \\ A_f \sigma B_o^2 cos^2\varphi \end{pmatrix} \dot{w}''_N + \begin{pmatrix} T_0 - G - k_p \\ -\frac{B_o^2 cos^2\varphi}{\mu_p} \end{pmatrix} {w_N}^{iv} \\
+ \begin{pmatrix} -\left(\frac{3}{2} w''_N {w'_N}^2\right)(EA'') \\ -2EA' + 3w'_N {w''_N}^2 \\ + (EA - G + T_o)\left(\frac{3}{2}{w'_N}^2\right){w_N}^{iv} \\ + (9w'_N w''_N)\, w'''_N + 3{w''_N}^3 \end{pmatrix} \\
-E\begin{pmatrix} \frac{1}{2}A'' {w'_N}^3 + 3A' {w'_N}^2 w''_N + 3A w'_N {w''_N}^2 \\ + \frac{3}{2} A {w'_N}^2 w'''_N \end{pmatrix} \\
+E\alpha \begin{pmatrix} A''\Delta T\left(1 - u'_N - 1/2{w'_N}^2\right) w'_N + 2A'\Delta T'\left(1 - u'_N - 1/2{w'_N}^2\right) w'_N \\ +2A'\Delta T\left(-u''_N - w'_N w''_N\right) w'_N + 2A'\Delta T\left(1 - u'_N - 1/2{w'_N}^2\right) w''_N \\ +A\Delta T''\left(1 - u'_N - 1/2{w'_N}^2\right) w'_N + 2A\Delta T'\left(-u''_N - w'_N w''_N\right) w'_N \\ +2A\Delta T'\left(1 - u'_N - 1/2{w'_N}^2\right) w''_N + A\Delta T\left(-u''_N - {w''_N}^2 - w'_N w'''_N\right) w'_N \\ +2A\Delta T\left(-u''_N - w'_N w''_N\right) w''_N + A\Delta T\left(1 - u'_N - 1/2{w'_N}^2\right) w'''_N \end{pmatrix} \\
+ \begin{pmatrix} (-EA'')\left(w'_N u''_N + w''_N u'_N + 3/2{w'_N}^2 w''_N\right) \\ +2(-EA')\begin{pmatrix} 2w''_N u''_N + w'_N u'''_N + w'''_N u'_N \\ +3w'_N {w''_N}^2 + 3/2{w'_N}^2 w'''_N \end{pmatrix} \\ + (T_o - G - EA)\begin{pmatrix} 3w'''_N u''_N + 3w''_N u'''_N + w'_N {u_N}^{iv} + {w_N}^{iv} u'_N \\ +3{w''_N}^3 + 9w'_N w''_N w'''_N + 3/2{w'_N}^2 {w_N}^{iv} \end{pmatrix} \end{pmatrix} + \begin{pmatrix} EI+ \\ \frac{IB_o^2 sin^2\varphi}{\mu_p} \end{pmatrix} {w_N}^{vi} \\
+J_4
\end{array}
\right\} \\
& = F_N(x,t) + (e_o a)^2 \frac{\partial^2 F_N(x,t)}{\partial x^2}
\end{aligned}
\tag{2.16}
$$

Where,

$$
\begin{aligned}
J_4 &= \\
& E\alpha \left(\begin{array}{l}
\left(\begin{array}{l}
A'' \Delta T' \left(1 - u'_N - 1/2\, {w'_N}^2\right) \\
+2\, A' \Delta T'' \left(1 - u'_N - 1/2\, {w'_N}^2\right) \\
+2\, A' \Delta T' \left(-u''_N - w'_N w''_N\right) \\
+2\, A' \Delta T' \left(1 - u'_N - 1/2\, {w'_N}^2\right) \\
+ A \Delta T''' \left(1 - u'_N - 1/2\, {w'_N}^2\right) \\
+2\, A \Delta T'' \left(-u''_N - w'_N w''_N\right) \\
+2\, A \Delta T'' \left(1 - u'_N - 1/2\, {w'_N}^2\right) \\
+ A \Delta T' \left(-u''_N - {w''_N}^2 - w'_N w'''_N\right) \\
+2\, A \Delta T' \left(-u''_N - w'_N w''_N\right) \\
+ A \Delta T' \left(1 - u'_N - 1/2 {w'_N}^2\right)
\end{array} \right)
+
\left(\begin{array}{l}
A''' \Delta T \left(1 - u'_N - 1/2\, {w'_N}^2\right) w'_N \\
+2\, A'' \Delta T' \left(1 - u'_N - 1/2\, {w'_N}^2\right) w'_N \\
+2\, A'' \Delta T \left(-u''_N - w'_N w''_N\right) w'_N \\
+2\, A'' \Delta T \left(1 - u'_N - 1/2\, {w'_N}^2\right) w''_N \\
+ A' \Delta T'' \left(1 - u'_N - 1/2\, {w'_N}^2\right) w'_N \\
+2\, A' \Delta T' \left(-u''_N - w'_N w''_N\right) w'_N \\
+2\, A' \Delta T' \left(1 - u'_N - 1/2\, {w'_N}^2\right) w''_N \\
+ A' \Delta T \left(-u''_N - {w''_N}^2 - w'_N w'''_N\right) w'_N \\
+2\, A' \Delta T \left(-u''_N - w'_N w''_N\right) w''_N \\
+ A' \Delta T \left(1 - u'_N - 1/2 {w'_N}^2\right) w'''_N
\end{array} \right) \\
+ \left(\begin{array}{l}
A'' \Delta T \left(u''_N + w'_N w''_N\right) w'_N + 2\, A' \Delta T' \left(u''_N + w'_N w''_N\right) w'_N \\
+2\, A' \Delta T \left(u'''_N + {w''_N}^2 + w'_N w'''_N\right) w'_N + 2\, A' \Delta T \left(u''_N + w'_N w''_N\right) w''_N \\
+ A \Delta T'' \left(u''_N + w'_N w''_N\right) w'_N + 2\, A \Delta T' \left(u'''_N + {w''_N}^2 + w'_N w'''_N\right) w'_N \\
+2\, A \Delta T' \left(u''_N + w'_N w''_N\right) w''_N + A \Delta T \left({u_N}^{iv} + 3\, w''_N w'''_N + w'_N {w_N}^{iv}\right) w'_N \\
+2\, A \Delta T \left(u'''_N + {w''_N}^2 + w'_N w'''_N\right) w''_N + A \Delta T \left(u''_N + w'_N w''_N\right) w'''_N
\end{array} \right)
\end{array} \right) \\
& + EI \left(\begin{array}{l}
5\, {u_N}^{v} w''_N + 11\, {u_N}^{iv} w'''_N + 13\, u''_N {w_N}^{iv} + 8\, u''_N {w_N}^{v} \\
+2\, u'_N {w_N}^{vi} + w'_N {u_N}^{vi} + 26\, {w''_N}^2 {w_N}^{iv} + 16\, w'_N {w_N}^{v} w''_N \\
+28\, w'_N {w_N}^{iv} w'''_N + 2\, {w'_N}^2 {w_N}^{vi} + 36\, w''_N {w'''_N}^2
\end{array} \right) \\
& + \frac{EA}{L} \int_0^L \left(z' w'_N + \left(\tfrac{1}{2} w'_N\right)^2 \right) dx \left({w_N}^{iv} + z_0^{iv}\right) + \\
& 2 \frac{EA'}{L} \int_0^L \left(z' w'_N + \left(\tfrac{1}{2} w'_N\right)^2 \right) dx \left(w'''_N + z'''_0\right) + \\
& \frac{EA''}{L} \int_0^L \left(z' w'_N + \left(\tfrac{1}{2} w'_N\right)^2 \right) dx \left(w''_N + z''_0\right) + k_1 w''_N \\
& + k_2 \left(3 w''_N {w_N}^2 + 6 w_N {w'_N}^2\right)
\end{aligned}
\tag{2.17}
$$

With hepatic Vdw force given as;

$$
\left(F + (e_0 a)^2 \left(\nabla^2 F\right)\right) = \left(\sum_{\zeta=1}^{7} c_\zeta \left(w - w_i\right)^{\zeta} + (e_0 a)^2 \left(\nabla^2 \left[\sum_{\zeta=1}^{7} c_\zeta \left(w - w_i\right)^{\zeta} \right] \right) \right) \tag{2.18}
$$

While the generalized longitudinal vibration for the MWCNT becomes:

$$\begin{aligned}
& m\ddot{u}_N + [T_0 - G - EA_t]\, w'_N w''_N - (EA_t)\, u''_N \\
& -EA'_t\left(u'_N + \tfrac{1}{2}{w'_N}^2\right) + E\alpha\,(A\Delta T' + A'\Delta T) - \\
& \tfrac{E\alpha}{2}{w'_N}^2\,(A\Delta T' + A'\Delta T) - E\alpha A\Delta T w'_N w''_N - EI\left({w_N}^{iv} w'_N + w''_N w'''_N\right) + (e_o a)^2 \\
& \left[\begin{array}{l}
m\ddot{u}''_N + \left(\begin{array}{l} (T_0 - G - EA_t)\, w'_N {w_N}^{iv} + 3\,(T_0 - G - EA_t)\, w''_N w'''_N \\ -2EA'_t w'_N w'''_N - 2EA'_t {w''_N}^2 - EA''_t w'_N w''_N \end{array}\right) \\
+\left(\left(EA_t''\right) u''_N + 2\,(EA'_t)\, u'''_N + (EA_t)\, {u_N}^{iv}\right) \\
+E\left(A_t'''\left(u'_N + \tfrac{1}{2}{w'_N}^2\right) + 2A_t''\,(u''_N + w'_N w''_N) + A_t'\left(u'''_N + {w''_N}^2 + w'_N w'''_N\right)\right) \\
+E\alpha\,(3A''\Delta T' + 3A'\Delta T'' + A\Delta T''' + A'''\Delta T) \\
+\tfrac{E\alpha}{2}\left(\begin{array}{l} \left(\begin{array}{c} 3A''\Delta T' + 3A'\Delta T'' \\ +A\Delta T''' + A'''\Delta T \end{array}\right) {w'_N}^2 + 4\,(2A'\Delta T' + A\Delta T'' + A''\Delta T)\, w'_N w''_N \\ +2\,(A\Delta T' + A'\Delta T)\, {w''_N}^2 + 2\,(A\Delta T' + A'\Delta T)\, w'_N w'''_N \end{array}\right) \\
+E\left(\alpha\left(\begin{array}{l} A''\Delta T w'_N w''_N + 2A'\Delta T' w'_N w''_N + \\ 2A'\Delta T {w''_N}^2 + 2A'\Delta T w'_N w'''_N + \\ A\Delta T'' w'_N w''_N + 2A\Delta T' {w''_N}^2 \\ +2A\Delta T' w'_N w'''_N + 3A\Delta T w''_N w'''_N \\ +A\Delta T w'_N {w_N}^{iv} \end{array}\right) + I\left(\begin{array}{l} {w_N}^{vi} w'_N + \\ 3{w_N}^{v} w''_N + \\ 4{w_N}^{iv} w'''_N \end{array}\right)\right)
\end{array}\right] \\
& = F_N(x,t) + (e_o a)^2 \tfrac{\partial^2 F_N(x,t)}{\partial x^2},
\end{aligned} \tag{2.19}$$

The nonlinear model can be subjected to different boundary conditions with initial conditions expressed as;

$$w\,(\tau = 0) = a = A\cos\varpi\tau, \tag{2.20}$$

$$\dot{w}\,(\tau = 0) = 0, \tag{2.21}$$

Using the deflection, slope, bending moment and shear force, the following natural boundary conditions from Hamilton's principle are imposed;

Fixed-fixed supports

$$w|_{s=0} = 0, \tag{2.22}$$
$$w'|_{s=0} = 0, \tag{2.23}$$
$$w|_{s=l} = 0, \tag{2.24}$$
$$w'|_{s=l} = 0. \tag{2.25}$$

Fixed-free supports (Cantilever support)

$$w|_{s=0} = 0, \tag{2.26}$$
$$w'|_{s=0} = 0, \tag{2.27}$$
$$w''|_{s=l} = 0, \tag{2.28}$$
$$w'''|_{s=l} = 0. \tag{2.29}$$
$$\tag{2.30}$$

Fixed-simple supports

$$w|_{s=0} = 0, \tag{2.31}$$
$$w'|_{s=0} = 0, \tag{2.32}$$
$$w|_{s=l} = 0, \tag{2.33}$$
$$w''|_{s=l} = 0. \tag{2.34}$$

Simple-simple supports

$$
\begin{aligned}
w|_{s=0} &= 0, && (2.35)\\
w''|_{s=0} &= 0, && (2.36)\\
w|_{s=l} &= 0, && (2.37)\\
w''|_{s=l} &= 0. && (2.38)
\end{aligned}
$$

To fully establish the coupled relationship between the vibration models and the Navier Stokes equations describing the fluid, the transient behaviour of the MWCNTs and fluid flow under investigation are given by:

Continuity Equation (Mass conservation).

$$
\frac{\partial \rho}{\partial t} + \frac{1}{r}\frac{\partial}{\partial r}\left(\rho r U_r\right) + \frac{1}{r}\frac{\partial}{\partial \theta}\left(\rho U_\theta\right) + \frac{\partial}{\partial z}\left(\rho U_z\right) = 0. \tag{2.39}
$$

Momentum Equations (Momentum conservation).

r − Component,

$$
\begin{aligned}
&\frac{\partial(\rho U_r)}{\partial t} + U_r\frac{\partial}{\partial r}(\rho U_r) + \frac{U_\theta}{r}\frac{\partial}{\partial \theta}(\rho U_r) + U_z\frac{\partial}{\partial z}(\rho U_z) - \frac{\rho U_\theta^2}{r} = \rho g_r - \frac{\partial P}{\partial r} + \\
&\left[\frac{1}{r}\frac{\partial}{\partial r}(rU_r) + \frac{1}{r^2}\frac{\partial^2}{\partial \theta^2}(U_r) - \frac{2}{r^2}\frac{\partial}{\partial r}(U_\theta) + \frac{\partial^2}{\partial z^2}(U_r)\right] + \underbrace{\frac{\rho U_z^2}{R}\cos\theta}_{\text{Curvature for curved tube}}.
\end{aligned} \tag{2.40}
$$

θ − Component,

$$
\begin{aligned}
&\frac{\partial\left(\rho U_\theta\right)}{\partial t} + U_r\frac{\partial}{\partial r}\left(\rho U_\theta\right) + \frac{U_\theta}{r}\frac{\partial}{\partial \theta}\left(\rho U_\theta\right) + U_z\frac{\partial}{\partial z}\left(\rho U_\theta\right) - \frac{\rho U_r U_\theta}{r} = \rho g_\theta - \frac{1}{r}\frac{\partial P}{\partial \theta} + \\
&\quad \mu\left[\frac{\partial}{\partial r}\left(\frac{1}{r}\frac{\partial}{\partial r}\left(rU_\theta\right) + \frac{1}{r^2}\frac{\partial^2}{\partial \theta^2}\left(U_\theta\right) + \frac{2}{r^2}\frac{\partial}{\partial \theta}\left(U_r\right) + \frac{\partial^2}{\partial z^2}\left(U_\theta\right)\right)\right] - \underbrace{\frac{\rho U_z^2}{R} sin\theta}_{\substack{for \\ curved\,tube}}.
\end{aligned} \tag{2.41}
$$

z − Component,

$$
\begin{aligned}
&\frac{\partial\left(\rho U_z\right)}{\partial t} + U_r\frac{\partial}{\partial r}\left(\rho U_z\right) + \frac{U_\theta}{r}\frac{\partial}{\partial \theta}\left(\rho U_z\right) + U_z\frac{\partial}{\partial z}\left(\rho U_z\right) = \rho g_z - \frac{\partial P}{\partial z} + \\
&\qquad\qquad \mu\left[\frac{1}{r}\frac{\partial}{\partial r}\left(r\frac{\partial}{\partial z}\left(U_z\right)\right) + \frac{1}{r^2}\frac{\partial^2}{\partial \theta^2}\left(U_z\right) + \frac{\partial^2}{\partial z^2}\left(U_z\right)\right].
\end{aligned} \tag{2.42}
$$

Cattaneo-Christov Energy equation (Conservation of Energy)

On invoking the common thermal boundary layer approximations, the energy equation when there is no viscous dissipation is expressed as;

$$
\frac{\partial\left(\rho_f c_{p,f} T_f\right)}{\partial t} + U_r\frac{\partial}{\partial r}\left(\rho_f c_{p,f} T_f\right) + \frac{U_\theta}{r}\frac{\partial}{\partial \theta}\left(\rho_f c_{p,f} T_f\right) + U_z\frac{\partial}{\partial z}\left(\rho_f c_{p,f} T_f\right) = -\nabla. \tag{2.43}
$$

Cattaneo-Christov's heat flux equation is expressed as;

$$
\varepsilon\left[\frac{\partial q}{\partial t} + V.\nabla q - q.\nabla V + \left(\nabla.V\right)q\right] = -k\nabla T, \tag{2.44}
$$

V is the velocity vector. The equation above becomes the usual Fourier's heat transfer law when $\epsilon = 0$. For a constant density flow process, i.e., $\nabla \cdot \mathbf{U} = 0$, we have:

$$
q + \varepsilon\left[\frac{\partial q}{\partial t} + V.\nabla q - q.\nabla V\right] = -k\nabla T. \tag{2.45}
$$

Excluding q, the energy equation is obtained as in Equation (2.43):

$$\begin{gathered}\frac{\partial\left(T_f\right)}{\partial t}+U_r \frac{\partial}{\partial r}\left(T_f\right)+U_z \frac{\partial}{\partial z}\left(T_f\right)+ \\ \varepsilon\left[\begin{array}{l}U_r^2 \frac{\partial^2}{\partial r^2}\left(T_f\right)+U_z^2 \frac{\partial^2}{\partial z^2}\left(T_f\right)+2 U_r U_z \frac{\partial^2}{\partial r \partial z}\left(T_f\right)+U_r \frac{\partial}{\partial z}\left(U_f\right) \frac{\partial}{\partial z}\left(T_f\right)+ \\ U_r \frac{\partial}{\partial z}\left(U_z\right) \frac{\partial}{\partial r}\left(T_f\right)+U_z \frac{\partial}{\partial r}\left(U_f\right) \frac{\partial}{\partial z}\left(T_f\right)+U_z \frac{\partial}{\partial r}\left(U_z\right) \frac{\partial}{\partial r}\left(T_f\right)\end{array}\right] \\ =\alpha\left(\frac{\partial}{\partial r}\left(\frac{\partial T_f}{\partial r}\right)+\frac{1}{r}\left(\frac{\partial T_f}{\partial r}\right)\right).\end{gathered} \tag{2.46}$$

This heat flux equation (Cattaneo-Christov) helps anticipate the influences of thermal relaxation time on boundary layer phenomena.

Pressure continuity

$$\dot{P}+U P^{\prime}+\rho_f a^2\left(U^{\prime}-2 v \dot{u}^{\prime}\right)-2 v \rho_f a^2\left(w^{\prime} \dot{w}^{\prime}+U u^{\prime \prime}+U w^{\prime} w^{\prime \prime}\right)=0, \tag{2.47}$$

where

$$a^2=\frac{K / \rho_f}{1+\left\{\frac{K D_p}{E h}\right\}}.$$

Geometrical Equations (Change in areas).

$$\dot{A}_2+\frac{v \sqrt{A}_{t, 2} A_{t, 2}}{\sqrt{\pi} h}\left[\dot{u}_2^{\prime}+w^{\prime}{ }_2 \dot{w}_2^{\prime}\right]+\left(e_o a\right)^2\left\{\dot{A}_2^{\prime \prime}+\frac{v \sqrt{A}_{t, 2} A_{t, 2}}{\sqrt{\pi} h}\left[\dot{u}_2^{\prime}+w^{\prime}{ }_2 \dot{w}_2^{\prime}\right]\right\}=0, \tag{2.48}$$

$$\dot{A}_3+\frac{v \sqrt{A}_{t, 3} A_{t, 3}}{\sqrt{\pi} h}\left[\dot{u}_3^{\prime}+w^{\prime}{ }_3 \dot{w}_3^{\prime}\right]+\left(e_o a\right)^2\left\{\dot{A}_3^{\prime \prime}+\frac{v \sqrt{A}_{t, 3} A_{t, 3}}{\sqrt{\pi} h}\left[\dot{u}_3^{\prime}+w^{\prime}{ }_3 \dot{w}_3^{\prime}\right]\right\}=0, \tag{2.49}$$

$$\dot{A}_N+\frac{v \sqrt{A}_{t, N} A_{t, N}}{\sqrt{\pi} h}\left[\dot{u}_N^{\prime}+w^{\prime}{ }_N \dot{w}_N^{\prime}\right]+\left(e_o a\right)^2\left\{\dot{A}_N^{\prime \prime}+\frac{v \sqrt{A}_{t, N} A_{t, N}}{\sqrt{\pi} h}\left[\dot{u}_N^{\prime}+w^{\prime}{ }_N \dot{w}_N^{\prime}\right]\right\}=0. \tag{2.50}$$

Energy Equation of Multi-walled Nanotubes.

$$\tau_q \frac{\partial^2\left(\rho_1 c_{p, 1} T_1\right)}{\partial t^2}+\frac{\partial\left(\rho_1 c_{p, 1} T_1\right)}{\partial t}=\left[\frac{1}{r} \frac{\partial}{\partial r}\left(r K_{r, 1} \frac{\partial T_1}{\partial r}\right)+\frac{1}{r^2} \frac{\partial}{\partial \theta}\left(K_{\theta, 1} \frac{\partial T_1}{\partial \theta}\right)+\frac{\partial}{\partial z}\left(K_{z, 1} \frac{\partial T_1}{\partial z}\right)\right]+q^{\prime \prime \prime}, \tag{2.51}$$

$$\tau_q \frac{\partial^2\left(\rho_3 c_{p, 3} T_3\right)}{\partial t^2}+\frac{\partial\left(\rho_3 c_{p, 3} T_3\right)}{\partial t}=\left[\frac{1}{r} \frac{\partial}{\partial r}\left(r K_{r, 3} \frac{\partial T_3}{\partial r}\right)+\frac{1}{r^2} \frac{\partial}{\partial \theta}\left(K_{\theta, 3} \frac{\partial T_3}{\partial \theta}\right)+\frac{\partial}{\partial z}\left(K_{z, 3} \frac{\partial T_3}{\partial z}\right)\right]+q^{\prime \prime \prime}, \tag{2.52}$$

$$\tau_q \frac{\partial^2\left(\rho_N c_{p, N} T_N\right)}{\partial t^2}+\frac{\partial\left(\rho_1 c_{p, 1} T_1\right)}{\partial t}=\left[\frac{1}{r} \frac{\partial}{\partial r}\left(r K_{r, N} \frac{\partial T_N}{\partial r}\right)+\frac{1}{r^2} \frac{\partial}{\partial \theta}\left(K_{\theta, N} \frac{\partial T_1}{\partial \theta}\right)+\frac{\partial}{\partial z}\left(K_{z, N} \frac{\partial T_N}{\partial z}\right)\right]+q^{\prime \prime \prime}. \tag{2.53}$$

3. Analytical Solutions to the Governing Thermal-fluidic Equations

Relaxing the azimuth component because the tube under investigation is embedded in foundations, the Naiver Stoke's and energy equations for fluid flow through the MWCNTs are:

Continuity Equation (Mass conservation).

$$\frac{\partial \rho}{\partial t}+\frac{1}{r} \frac{\partial}{\partial r}\left(\rho r U_r\right)+\frac{\partial}{\partial z}\left(\rho U_z\right)=0. \tag{3.1}$$

Momentum Equations (Momentum Conservation).

r − Component,

$$\frac{\partial\left(\rho U_r\right)}{\partial t}+U_r\frac{\partial}{\partial r}\left(\rho U_r\right)+U_z\frac{\partial}{\partial z}\left(\rho U_z\right)=\rho g_r-\frac{\partial P}{\partial r}+\left[\frac{1}{r}\frac{\partial}{\partial r}\left(r\frac{\partial}{\partial r}U_r\right)+\frac{\partial^2}{\partial z^2}\left(U_r\right)\right]+\sigma_0 B^2 U_r+\underbrace{\frac{\rho U_z^2}{R}\cos\theta}_{\substack{curvature\,for\\ curved\,tube}}\ . \tag{3.2}$$

z − Component,

$$\frac{\partial\left(\rho U_z\right)}{\partial t}+U_r\frac{\partial}{\partial r}\left(\rho U_z\right)+U_z\frac{\partial}{\partial z}\left(\rho U_z\right)=\rho g_z-\frac{\partial P}{\partial z}+\sigma_0 B^2 U_z+\mu\left[\frac{1}{r}\frac{\partial}{\partial r}\left(r\frac{\partial}{\partial z}\left(U_z\right)\right)+\frac{\partial^2}{\partial z^2}\left(U_z\right)\right]. \tag{3.3}$$

Energy equations (Cattaneo-Christov) for the fluid (Energy conservation).

$$\frac{\partial\left(T_f\right)}{\partial t}+U_r\frac{\partial}{\partial r}\left(T_f\right)+U_z\frac{\partial}{\partial z}\left(T_f\right)\quad+\varepsilon\left[\begin{array}{l}U_r^2\frac{\partial^2}{\partial r^2}\left(T_f\right)+U_z^2\frac{\partial^2}{\partial z^2}\left(T_f\right)+2U_rU_z\frac{\partial^2}{\partial r\partial z}\left(T_f\right)+U_r\frac{\partial}{\partial z}\left(U_f\right)\frac{\partial}{\partial z}\left(T_f\right)+\\ U_r\frac{\partial}{\partial z}\left(U_z\right)\frac{\partial}{\partial r}\left(T_f\right)+U_z\frac{\partial}{\partial r}\left(U_f\right)\frac{\partial}{\partial z}\left(T_f\right)+U_z\frac{\partial}{\partial r}\left(U_z\right)\frac{\partial}{\partial r}\left(T_f\right)\end{array}\right]$$
$$=\alpha\left(\frac{\partial}{\partial r}\left(\frac{\partial T_f}{\partial r}\right)+\frac{1}{r}\left(\frac{\partial T_f}{\partial r}\right)\right). \tag{3.4}$$

Multi-walled nanotubes' Energy equation.

$$\tau_q\frac{\partial^2\left(\rho_N c_{p,N}T_N\right)}{\partial t^2}+\frac{\partial\left(\rho_N c_{p,N}T_N\right)}{\partial t}=\left[\frac{1}{r}\frac{\partial}{\partial r}\left(rK_{r,N}\frac{\partial T_N}{\partial r}\right)+\frac{\partial}{\partial z}\left(K_{z,N}\frac{\partial T_N}{\partial z}\right)\right]+q'''. \tag{3.5}$$

MWCNTs boundary and initial conditions are given as:

$$t=0,\quad T_i=T_0\quad i=1,2,3,\ldots,N.$$

Boundary and Interfacial conditions (for perfectly bonded nanotubes).

$$\begin{array}{lll} t>0 & , & T_i=T_{i+1},\\ t>0 & , & K_i\frac{\partial T_i}{\partial r}=K_{i+1}\frac{\partial T_i}{\partial r}\quad i=1,2,3,\ldots,N-1,\\ t>0 & , & K_1\frac{\partial T_1}{\partial r}=h_a\left(T_1-T_{in}\right)\quad r=r_{in},\\ t>0 & , & K_N\frac{\partial T_N}{\partial r}=h_b\left(T_{out}-T_N\right)\quad r=r_{out},\\ . & & \end{array}$$

Γ

Boundary and Interfacial conditions (for imperfectly bonded nanotubes).

$$\begin{array}{lll} t>0 & , & K_i\frac{\partial T_i}{\partial r}=h_i\left(T_{i+1}-T_i\right)\quad r=r_i,\\ t>0 & , & K_1\frac{\partial T_1}{\partial r}=h_a\left(T_1-T_{in}\right)\quad r=r_{in},\\ t>0 & , & K_N\frac{\partial T_N}{\partial r}=h_b\left(T_{out}-T_N\right)\quad r=r_{out}. \end{array}$$

Using the similarity function expressed in Equation (3.6);

$$\eta = \frac{1}{1-\beta t}\left(\frac{r}{a_0}\right)^2, U_r = -\frac{2vf(\eta)}{a_0\sqrt{(1-\beta t)\eta}}, U_z = -\frac{4vzf'(\eta)}{a_0^2(1-\beta t)}, \theta(\eta) = \frac{T_f - T_a}{T_0 - T_a}, \Theta_i(\eta) = \frac{T - T_\infty}{T_1 - T_\infty}. \tag{3.6}$$

The governing PDEs transmute into a system of ODEs describing fluid flow, fluid temperature, and heat transfer in the MWCNTs. These equations are exemplified in Equations (3.7)-(3.13):

$$\eta f''' + \lambda_1 f'' + \lambda_2 f f'' - \lambda_3 (f')^2 - S(\eta f'' + M f') = 0, \tag{3.7}$$

$$\eta\theta'' + \lambda_4\theta' + \Pr f\theta' - \Pr S\eta\theta' + N\eta(\theta')^2 + \Pr \eta Q\theta = 0, \tag{3.8}$$

$$\eta\Theta_1'' + \Theta_1' + Bi\lambda_5(\theta - \Theta_1) + \lambda_6 = 0, \tag{3.9}$$

$$\eta\Theta_i'' + \Theta_i' + Bi\lambda_5(\Theta_1 - \Theta_i) + \lambda_7 = 0, \tag{3.10}$$

$$\eta\Theta_n'' + \Theta_n' + Bi\lambda_5(\Theta_i - \Theta_n) + \lambda_8 = 0, \tag{3.11}$$

$$\begin{aligned} &\eta = 1, \quad f = A, f' = 1 + bf'', \quad \theta = 1 + c\theta', \\ &\eta = 0, \quad f' = 0, \quad \theta' = 0. \end{aligned} \tag{3.12}$$

Using N as the MWCNTs counter, the MWCNTs coupling conditions become;

$$\begin{aligned} &\Theta'_1 + Bi_a(\theta - \Theta_1) = 0, \\ &\Theta'_i + Bi_i(\Theta_1 - \Theta_i) = 0, \\ &\Theta'_n + Bi_b(\Theta_i - \Theta_n) = 0. \end{aligned} \tag{3.13}$$

Where the controlling parameters $S = \frac{\beta a_0^2}{4v}$, $\Pr = \frac{v}{\alpha}$, $N = \frac{\tau D(T_0 - T_w)}{\alpha T_w}$, $b = \frac{2N_0 v}{a_0}$, $c = \frac{2D_0}{a_0}$ are the dimensionless unsteady term, Prandtl number, thermophoreses term, velocity slip term and thermal slip term respectively.

3.1. **Concept of Differential transform method (DTM).** Due to the presence of nonlinear terms in the derived coupled governing equation, a method capable of transforming differential equations into another domain with a robust and easy way of representation is required. The differential transform method (DTM) possesses these attributes. DTM maps a governing equation into an algebraic domain and then obtains an inversion using a series summation method. This approximate analytical method generates a solution with the controlling parameters adequately conserved. The DTM recursive relation for transforming differential equation is shown in the Table 2 below [29, 48, 50]:

By applying the results shown in Table 2 to Equations (3.7)-(3.13) yield,

$$\begin{aligned} &\sum_{l=0}^{k}(l+1)(l+2)(l+3)F_{l+3}Z_{k-l} + \lambda_1(k+1)(k+2)F_{k+2} + \lambda_2\sum_{l=0}^{k}(l+1)(l+2)F_{l+2}F_{k-l} - \\ &\lambda_3\sum_{l=0}^{k}(l+1)F_{l+1}(k+1-l)F_{k+1-l} - S\sum_{l=0}^{k}(l+1)(l+2)F_{l+2}\delta(k-l) - SM(k+1)F_{k+1} = 0, \end{aligned} \tag{3.14}$$

$$\begin{aligned} &\sum_{l=0}^{k}(l+1)(l+2)\theta_{l+2}Z_{k-l} + \lambda_4(k+1)\theta_{k+1} + \Pr\sum_{l=0}^{k}(l+1)\theta_{l+1}F_{k-l} - \\ &\Pr S\sum_{l=0}^{k}(l+1)\theta_{l+1}\delta(k-l-1) + N\sum_{m=0}^{k}\left(\sum_{l=0}^{m}(l+1)\theta_{l+1}(m-l+1)\theta_{m-l+1}\delta(k-m-1)\right) = 0, \end{aligned} \tag{3.15}$$

Table 2. Some compiled DTM recursive relation.

S/N	DTM Expression
1	$Z(t) = U(t) \pm V(t), \quad Z(k) = U(k) \pm V(k).$
2	$Z(t) = \alpha U(t), \quad Z(k) = \alpha U(k).$
3	$Z(t) = \frac{dU(t)}{dt}, \quad Z(k) = (k+1)U[k+1].$
4	$Z(t) = \frac{d^2U(t)}{dt^2}, \quad Z(k) = (k+1)(k+2)U[k+2].$
5	$Z(t) = \frac{d^mU(t)}{dt^m}, \quad Z(k) = (k+1)(k+2)\cdots(k+m)U[k+m].$ or $\frac{(k+m)!}{k!}U[k+m].$
6	$Z(t) = U(t) * V(t), \quad Z(k) = \sum_{l=0}^{K} V[l]U[K-l].$
7	$Z(t) = t^m, \quad Z(k) = \delta(k-m) = \begin{cases} 1 & \text{if } k = m \\ 0 & \text{if } k \neq m \end{cases}$
8	$Z(t) = e^{\lambda t}, \quad Z(k) = \frac{\lambda^k}{k!} \quad D(e^{-\lambda t}) = \frac{-\lambda^k}{k!}$
9	$Z(t) = \sin(\omega t + \alpha), \quad Z(k) = \frac{\omega^k}{k!} \sin\left(\frac{\pi k}{2} + \alpha\right).$

$$\sum_{l=0}^{k} (l+1)(l+2)\,\Theta_{1_{l+2}} Z_{k-l} + (k+1)\,\Theta_{1_{k+1}} + Bi_a \lambda_5 \left(\theta_k - \Theta_{1_k}\right) + \lambda_6 \delta(k-1) = 0, \tag{3.16}$$

$$\sum_{l=0}^{k} (l+1)(l+2)\,\Theta_{i_{l+2}} Z_{k-l} + (k+1)\,\Theta_{i_{k+1}} + Bi_i \lambda_5 \left(\Theta_{1_k} - \Theta_{i_k}\right) + \lambda_7 \delta(k-1) = 0, \tag{3.17}$$

$$\sum_{l=0}^{k} (l+1)(l+2)\,\Theta_{n_{l+2}} Z_{k-l} + (k+1)\,\Theta_{n_{k+1}} + Bi_b \lambda_5 \left(\Theta_{i_k} - \Theta_{n_k}\right) + \lambda_8 \delta(k-1) = 0, \tag{3.18}$$

$$Z_{k+1} = (k+1)\, Z_{k+1} - \delta(k). \tag{3.19}$$

With transformed boundary conditions represented as;

$$\begin{array}{llll} F_0 = \beta_1, & F_1 = \beta_2, & F_2 = \beta_3, & \theta_0 = \beta_4, \\ \theta_1 = \beta_5, & \Theta_{1_0} = \beta_6, & \Theta_{1_1} = \beta_7, & \Theta_{i_0} = \beta_8, \\ \Theta_{i_1} = \beta_9, & \Theta_{n_0} = \beta_{10}, & \Theta_{n_1} = \beta_{11}, & Z_0 = \beta_{12}. \end{array} \tag{3.20}$$

Using the DTM recursive relations, the thermal-fluidic term-by-term solutions are obtained. Afterwards, the principle of DTM grouping is used on the term-by-term solutions and the desired thermal-fluidic solutions are summarized as;

$$\begin{array}{ll} f(\eta) = \sum_{k=0}^{N} F_k \eta^k & k = 0, 1, 2, 3, 4, 5, ..., \\ \theta(\eta) = \sum_{k=0}^{N} \theta_k \eta^k & k = 0, 1, 2, 3, 4, 5, ..., \\ \Theta_1(\eta) = \sum_{k=0}^{N} \chi_k \eta^k & k = 0, 1, 2, 3, 4, 5, ..., \\ \Theta_i(\eta) = \sum_{k=0}^{N} \chi_k \eta^k & k = 0, 1, 2, 3, 4, 5, ..., \\ \Theta_n(\eta) = \sum_{k=0}^{N} \chi_k \eta^k & k = 0, 1, 2, 3, 4, 5, ... \end{array} \tag{3.21}$$

Making necessary substitution, the desired thermofluidic solutions become:

$$f(\eta)=\left(\begin{array}{l}\beta_1+\beta_2\eta+\beta_3\eta^2+1/6\,\frac{\left(MS\beta_2-2\beta_1\beta_3\lambda_2+{\beta_2}^2\lambda_3+2S\beta_3-2\beta_3\lambda_1\right)\eta^3}{\beta_{12}}+\\ \frac{1}{24{\beta_{12}}^2}\left(\begin{array}{l}-MS\beta_1\beta_2\lambda_2+2{\beta_1}^2\beta_3{\lambda_2}^2-\beta_1{\beta_2}^2\lambda_2\lambda_3+MS^2\beta_2-MS\beta_2\lambda_1+\\ 2MS\beta_3\beta_{12}-4S\beta_1\beta_3\lambda_2+S{\beta_2}^2\lambda_3+4\beta_1\beta_3\lambda_1\lambda_2-{\beta_2}^2\lambda_1\lambda_3-\\ 2\beta_2\beta_3\beta_{12}\lambda_2+4\beta_2\beta_3\beta_{12}\lambda_3-MS\beta_2+2S^2\beta_3-4S\beta_3\lambda_1+\\ 2\beta_1\beta_3\lambda_2-{\beta_2}^2\lambda_3+2\beta_3{\lambda_1}^2-2S\beta_3+2\beta_3\lambda_1\end{array}\right)\eta^4+\\ \frac{1}{120{\beta_{12}}^3}\left(\begin{array}{l}MS{\beta_1}^2\beta_2{\lambda_2}^2-2{\beta_1}^3\beta_3{\lambda_2}^3+{\beta_1}^2{\beta_2}^2{\lambda_2}^2\lambda_3+M^2S^2\beta_2\beta_{12}-2MS^2\beta_1\beta_2\lambda_2+\\ 2MS\beta_1\beta_2\lambda_1\lambda_2-4MS\beta_1\beta_3\beta_{12}\lambda_2-2MS{\beta_2}^2\beta_{12}\lambda_2+3MS{\beta_2}^2\beta_{12}\lambda_3+\\ 6S{\beta_1}^2\beta_3{\lambda_2}^2-2S\beta_1{\beta_2}^2\lambda_2\lambda_3-6{\beta_1}^2\beta_3\lambda_1{\lambda_2}^2+2\beta_1{\beta_2}^2\lambda_1\lambda_2\lambda_3+\\ 6\beta_1\beta_2\beta_3\beta_{12}{\lambda_2}^2-8\beta_1\beta_2\beta_3\beta_{12}\lambda_2\lambda_3-2{\beta_2}^3\beta_{12}\lambda_2\lambda_3+2{\beta_2}^3\beta_{12}{\lambda_3}^2+\\ MS^3\beta_2-2MS^2\beta_2\lambda_1+4MS^2\beta_3\beta_{12}+3MS\beta_1\beta_2\lambda_2+MS\beta_2{\lambda_1}^2-\\ 4MS\beta_3\beta_{12}\lambda_1-6S^2\beta_1\beta_3\lambda_2+S^2{\beta_2}^2\lambda_3+12S\beta_1\beta_3\lambda_1\lambda_2-2S{\beta_2}^2\lambda_1\lambda_3-\\ 6S\beta_2\beta_3\beta_{12}\lambda_2+8S\beta_2\beta_3\beta_{12}\lambda_3-6{\beta_1}^2\beta_3{\lambda_2}^2+3\beta_1{\beta_2}^2\lambda_2\lambda_3-\\ 6\beta_1\beta_3{\lambda_1}^2\lambda_2+{\beta_2}^2{\lambda_1}^2\lambda_3+6\beta_2\beta_3\beta_{12}\lambda_1\lambda_2-8\beta_2\beta_3\beta_{12}\lambda_1\lambda_3-4{\beta_3}^2{\beta_{12}}^2\lambda_2+\\ 8{\beta_3}^2{\beta_{12}}^2\lambda_3-3MS^2\beta_2+3MS\beta_2\lambda_1-4MS\beta_3\beta_{12}+2S^3\beta_3-6S^2\beta_3\lambda_1+\\ 12S\beta_1\beta_3\lambda_2-3S{\beta_2}^2\lambda_3+6S\beta_3{\lambda_1}^2-12\beta_1\beta_3\lambda_1\lambda_2+3{\beta_2}^2\lambda_1\lambda_3+\\ 4\beta_2\beta_3\beta_{12}\lambda_2-8\beta_2\beta_3\beta_{12}\lambda_3-2\beta_3{\lambda_1}^3+2MS\beta_2-6S^2\beta_3+12S\beta_3\lambda_1-\\ 4\beta_1\beta_3\lambda_2+2{\beta_2}^2\lambda_3-6\beta_3{\lambda_1}^2+4S\beta_3-4\beta_3\lambda_1\end{array}\right)\eta^5\end{array}\right), \tag{3.22}$$

$$\theta(\eta)=\left(\begin{array}{l}\beta_4+\beta_5\eta-\frac{\beta_5(\Pr\beta_1+\lambda_4)\eta^2}{2\beta_{12}}-\frac{\beta_5\left(\begin{array}{l}-\overset{2}{\Pr}{\beta_1}^2+N\beta_5\beta_{12}-\Pr S\beta_{12}-\\ 2\Pr\beta_1\lambda_4+\Pr\beta_2\beta_{12}-\Pr\beta_1-{\lambda_4}^2-\lambda_4\end{array}\right)\eta^3}{6{\beta_{12}}^2}+\\ +\frac{\beta_5\left(\begin{array}{l}-\overset{3}{\Pr}{\beta_1}^3+5N\Pr\beta_1\beta_5\beta_{12}-3\overset{2}{\Pr}S\beta_1\beta_{12}-3\overset{2}{\Pr}{\beta_1}^2\lambda_4+3\overset{2}{\Pr}\beta_1\beta_2\beta_{12}+\\ 5N\beta_5\beta_{12}\lambda_4-3\overset{2}{\Pr}{\beta_1}^2-3\Pr S\beta_{12}\lambda_4-3\Pr\beta_1{\lambda_4}^2+3\Pr\beta_2\beta_{12}\lambda_4-\\ 2\Pr\beta_3{\beta_{12}}^2+2N\beta_5\beta_{12}-2\Pr S\beta_{12}-6\Pr\beta_1\lambda_4+2\Pr\beta_2\beta_{12}-\\ {\lambda_4}^3-2\Pr\beta_1-3{\lambda_4}^2-2\lambda_4\end{array}\right)\eta^4}{24{\beta_{12}}^3}+\ldots\end{array}\right), \tag{3.23}$$

$$\Theta_1(\eta)=\left(\begin{array}{l}\beta_6+\beta_7\eta-\frac{(Bi_a\beta_4\lambda_5-Bi_a\beta_6\lambda_5+\beta_7)\eta^2}{2\beta_{12}}+\\ \frac{\left(\begin{array}{l}-Bi_a\beta_5\beta_{12}\lambda_5+Bi_a\beta_7\beta_{12}\lambda_5+\\ 2Bi_a\beta_4\lambda_5-2Bi_a\beta_6\lambda_5-\beta_{12}\lambda_6+2\beta_7\end{array}\right)\eta^3}{6{\beta_{12}}^2}-\\ \frac{\left(\begin{array}{l}{Bi_a}^2\beta_4\beta_{12}{\lambda_5}^2-{Bi_a}^2\beta_6\beta_{12}{\lambda_5}^2-\\ Bi_a\Pr\beta_1\beta_5\beta_{12}\lambda_5-Bi_a\beta_5\beta_{12}\lambda_4\lambda_5-\\ 3Bi_a\beta_5\beta_{12}\lambda_5+4Bi_a\beta_7\beta_{12}\lambda_5+\\ 6Bi_a\beta_4\lambda_5-6Bi_a\beta_6\lambda_5-3\beta_{12}\lambda_6+6\beta_7\end{array}\right)\eta^4}{24{\beta_{12}}^3}+\ldots\end{array}\right), \tag{3.24}$$

$$\Theta_i(\eta) = \left(\begin{array}{l} \beta_8 + \beta_9 \eta - \frac{(Bi_i \beta_6 \lambda_5 - Bi_i \beta_8 \lambda_5 + \beta_9)\eta^2}{2\beta_{12}} + \\ \frac{\left(\begin{array}{l} -Bi_i \beta_7 \beta_{12} \lambda_5 + Bi_i \beta_9 \beta_{12} \lambda_5 + 2Bi_i \beta_6 \lambda_5 \\ -2Bi_i \beta_8 \lambda_5 - \beta_{12} \lambda_7 + 2\beta_9 \end{array} \right)\eta^3}{6{\beta_{12}}^2} + \\ \frac{\left(\begin{array}{l} Bi_a Bi_i \beta_4 \beta_{12} {\lambda_5}^2 - Bi_a Bi_i \beta_6 \beta_{12} {\lambda_5}^2 - \\ {Bi_i}^2 \beta_6 \beta_{12} {\lambda_5}^2 + {Bi_i}^2 \beta_8 \beta_{12} {\lambda_5}^2 + \\ 4Bi_i \beta_7 \beta_{12} \lambda_5 - 4Bi_i \beta_9 \beta_{12} \lambda_5 - \\ 6Bi_i \beta_6 \lambda_5 + 6Bi_i \beta_8 \lambda_5 + 3\beta_{12} \lambda_7 - 6\beta_9 \end{array} \right)\eta^4}{24{\beta_{12}}^3} + \ldots \end{array} \right), \tag{3.25}$$

$$\Theta_n(\eta) = \left(\begin{array}{l} \beta_{10} + \beta_{11} \eta - \frac{(Bi_b \beta_8 \lambda_5 - Bi_b \beta_{10} \lambda_5 + \beta_{11})\eta^2}{2\beta_{12}} + \\ \frac{(-Bi_b \beta_9 \beta_{12} \lambda_5 + Bi_b \beta_{11} \beta_{12} \lambda_5 + 2Bi_b \beta_8 \lambda_5 - 2Bi_b \beta_{10} \lambda_5 - \beta_{12} \lambda_8 + 2\beta_{11})\eta^3}{6{\beta_{12}}^2} - \\ \frac{\left(\begin{array}{l} {Bi_b}^2 \beta_8 \beta_{12} {\lambda_5}^2 - {Bi_b}^2 \beta_{10} \beta_{12} {\lambda_5}^2 - Bi_b Bi_i \beta_6 \beta_{12} {\lambda_5}^2 + Bi_b Bi_i \beta_8 \beta_{12} {\lambda_5}^2 - \\ 4Bi_b \beta_9 \beta_{12} \lambda_5 + 4Bi_b \beta_{11} \beta_{12} \lambda_5 + 6Bi_b \beta_8 \lambda_5 - 6Bi_b \beta_{10} \lambda_5 - 3\beta_{12} \lambda_8 + 6\beta_{11} \end{array} \right)\eta^4}{24{\beta_{12}}^3} \\ +\ldots \end{array} \right). \tag{3.26}$$

3.2. **Bulk Thermofluidic Variable.** The nonexistence of stream terms necessitate the need for bulk variables via averaging. This technique may also be employed for reducing independent variables into preferred forms. Considering internal flow through the MWCNTs under investigation, the thermal energy in transport is expressed as;

$$\begin{aligned} \dot{E}_t &= \int\limits_{A_c} \rho U c_p T dA_c = \dot{m} c_p T_b, \\ T_b &= \frac{\int\limits_{A_c} \rho U c_p T dA_c}{\dot{m} c_p} = \frac{\rho c_p \int\limits_{r_a}^{r_b} UT(2\pi r) dr}{\rho c_p \int\limits_{r_a}^{r_b} U(2\pi r) dr} = \frac{\int\limits_{r_a}^{r_b} UTrdr}{\int\limits_{r_a}^{r_b} Urdr}, \end{aligned} \tag{3.27}$$

given mean velocity as;

$$U_b = \frac{2}{(r_b^2 - r_a^2)} \int\limits_{r_a}^{r_b} Urdr, \tag{3.28}$$

The final bulk temperature turns out to be;

$$T_b = \frac{2}{U_b (r_b^2 - r_a^2)} \int\limits_{r_a}^{r_b} UTrdr, \tag{3.29}$$

Making necessary substitutions and simplifying after applying the averaging principle result in thermal-fluidic parameters (components) with similar coordinates of independent variables as present in the vibration model. This establishment consequently makes the coupling of the flow and vibration equations possible. The thermal-fluidic components that will be coupled with vibrations equations of motion are;

$$U_z\left(z,t\right)=\frac{1}{\left(r_b-r_a\right)}\left(\begin{array}{l}
4\,\frac{\beta_2 vz(r_b-r_a)}{{a_0}^2(-\beta t+1)}+\frac{8\beta_3 vz\left(-{r_a}^3+{r_b}^3\right)}{3{a_0}^4(-\beta t+1)^2}+\\
\frac{2\left(MS\beta_2-2\beta_1\beta_3\lambda_2+{\beta_2}^2\lambda_3+2S\beta_3-2\beta_3\lambda_1\right)vz\left(-{r_a}^5+{r_b}^5\right)}{5{a_0}^6(-\beta t+1)^3\beta_{12}}+\\
\frac{2\left(\begin{array}{l}
-MS\beta_1\beta_2\lambda_2+2{\beta_1}^2\beta_3{\lambda_2}^2-\beta_1{\beta_2}^2\lambda_2\lambda_3+\\
MS^2\beta_2-MS\beta_2\lambda_1+2MS\beta_3\beta_{12}-4S\beta_1\beta_3\lambda_2+\\
S{\beta_2}^2\lambda_3+4\beta_1\beta_3\lambda_1\lambda_2-{\beta_2}^2\lambda_1\lambda_3-2\beta_2\beta_3\beta_{12}\lambda_2+\\
4\beta_2\beta_3\beta_{12}\lambda_3-MS\beta_2+2S^2\beta_3-4S\beta_3\lambda_1+\\
2\beta_1\beta_3\lambda_2-{\beta_2}^2\lambda_3+2\beta_3{\lambda_1}^2-2S\beta_3+2\beta_3\lambda_1
\end{array}\right)vz\left(-{r_a}^7+{r_b}^7\right)}{21{a_0}^8(-\beta t+1)^4{\beta_{12}}^2}\\
\left(\begin{array}{l}
MS{\beta_1}^2\beta_2{\lambda_2}^2-2{\beta_1}^3\beta_3{\lambda_2}^3+{\beta_1}^2{\beta_2}^2{\lambda_2}^2\lambda_3+\\
M^2S^2\beta_2\beta_{12}-2MS^2\beta_1\beta_2\lambda_2+2MS\beta_1\beta_2\lambda_1\lambda_2-\\
4MS\beta_1\beta_3\beta_{12}\lambda_2-2MS{\beta_2}^2\beta_{12}\lambda_2+3MS{\beta_2}^2\beta_{12}\lambda_3+\\
6S{\beta_1}^2\beta_3{\lambda_2}^2-2S\beta_1{\beta_2}^2\lambda_2\lambda_3-6{\beta_1}^2\beta_3\lambda_1{\lambda_2}^2+\\
2\beta_1{\beta_2}^2\lambda_1\lambda_2\lambda_3+6\beta_1\beta_2\beta_3\beta_{12}{\lambda_2}^2-8\beta_1\beta_2\beta_3\beta_{12}\lambda_2\lambda_3-\\
2{\beta_2}^3\beta_{12}\lambda_2\lambda_3+2{\beta_2}^3\beta_{12}{\lambda_3}^2+MS^3\beta_2-\\
2MS^2\beta_2\lambda_1+4MS^2\beta_3\beta_{12}+3MS\beta_1\beta_2\lambda_2+\\
MS\beta_2{\lambda_1}^2-4MS\beta_3\beta_{12}\lambda_1-6S^2\beta_1\beta_3\lambda_2+S^2{\beta_2}^2\lambda_3+\\
12S\beta_1\beta_3\lambda_1\lambda_2-2S{\beta_2}^2\lambda_1\lambda_3-6S\beta_2\beta_3\beta_{12}\lambda_2+\\
8S\beta_2\beta_3\beta_{12}\lambda_3-6{\beta_1}^2\beta_3{\lambda_2}^2+3\beta_1{\beta_2}^2\lambda_2\lambda_3-\\
6\beta_1\beta_3{\lambda_1}^2\lambda_2+{\beta_2}^2{\lambda_1}^2\lambda_3+6\beta_2\beta_3\beta_{12}\lambda_1\lambda_2-\\
8\beta_2\beta_3\beta_{12}\lambda_1\lambda_3-4{\beta_3}^2{\beta_{12}}^2\lambda_2+8{\beta_3}^2{\beta_{12}}^2\lambda_3-\\
3MS^2\beta_2+3MS\beta_2\lambda_1-4MS\beta_3\beta_{12}+2S^3\beta_3-\\
6S^2\beta_3\lambda_1+12S\beta_1\beta_3\lambda_2-3S{\beta_2}^2\lambda_3+6S\beta_3{\lambda_1}^2-\\
12\beta_1\beta_3\lambda_1\lambda_2+3{\beta_2}^2\lambda_1\lambda_3+4\beta_2\beta_3\beta_{12}\lambda_2-\\
8\beta_2\beta_3\beta_{12}\lambda_3-2\beta_3{\lambda_1}^3+2MS\beta_2-\\
6S^2\beta_3+12S\beta_3\lambda_1-4\beta_1\beta_3\lambda_2+\\
2{\beta_2}^2\lambda_3-6\beta_3{\lambda_1}^2+4S\beta_3-4\beta_3\lambda_1
\end{array}\right)\frac{vz\left(-{r_a}^9+{r_b}^9\right)}{54{a_0}^{10}(-\beta t+1)^5{\beta_{12}}^3}
\end{array}\right), \tag{3.30}$$

and,

$$
\begin{aligned}
T_b\left(z,t\right) =& T_a + \frac{T_0 - T_a}{r_b - r_a} \\
&\left(\begin{array}{l}
\beta_4\left(r_b - r_a\right) + \frac{\beta_5\left(-r_a{}^3 + r_b{}^3\right)}{3a_0{}^2(-\beta t+1)} - \frac{\beta_5\left(\mathrm{Pr}\,\beta_1+\lambda_4\right)\left(-r_a{}^5+r_b{}^5\right)}{10a_0{}^4(-\beta t+1)^2\beta_{12}} \\
-\frac{\beta_5\left(\begin{array}{l} -\mathrm{Pr}^2\beta_1{}^2 + N\beta_5\beta_{12} - \mathrm{Pr}\,S\beta_{12} - 2\,\mathrm{Pr}\,\beta_1\lambda_4 \\ +\mathrm{Pr}\,\beta_2\beta_{12} - \mathrm{Pr}\,\beta_1 - \lambda_4{}^2 - \lambda_4 \end{array}\right)\left(-r_a{}^7+r_b{}^7\right)}{42a_0{}^6(-\beta t+1)^3\beta_{12}{}^2} \\
\frac{\beta_5\left(-r_a{}^9+r_b{}^9\right)}{216a_0{}^8(-\beta t+1)^4\beta_{12}{}^3}\left(\begin{array}{l}
-\mathrm{Pr}^3\beta_1{}^3 + 5N\,\mathrm{Pr}\,\beta_1\beta_5\beta_{12} - 3\,\mathrm{Pr}^2 S\beta_1\beta_{12} \\
-3\,\mathrm{Pr}^2\beta_1{}^2\lambda_4 + 3\,\mathrm{Pr}^2\beta_1\beta_2\beta_{12} \\
+5N\beta_5\beta_{12}\lambda_4 - 3\,\mathrm{Pr}^2\beta_1{}^2 - 3\,\mathrm{Pr}\,S\beta_{12}\lambda_4 \\
-3\,\mathrm{Pr}\,\beta_1\lambda_4{}^2 + 3\,\mathrm{Pr}\,\beta_2\beta_{12}\lambda_4 \\
-2\,\mathrm{Pr}\,\beta_3\beta_{12}{}^2 + 2N\beta_5\beta_{12} - 2\,\mathrm{Pr}\,S\beta_{12} - \\
6\,\mathrm{Pr}\,\beta_1\lambda_4 + 2\,\mathrm{Pr}\,\beta_2\beta_{12} - \lambda_4{}^3 - 2\,\mathrm{Pr}\,\beta_1 - 3\lambda_4{}^2 - 2\lambda_4
\end{array}\right) \\
-\frac{\beta_5\left(-r_a{}^{11}+r_b{}^{11}\right)}{1320a_0{}^{10}(-\beta t+1)^5\beta_{12}{}^4}\left(\begin{array}{l}
-\mathrm{Pr}^4\beta_1{}^4 + 17N\,\mathrm{Pr}^2\beta_1{}^2\beta_5\beta_{12} - 6\,\mathrm{Pr}^3 S\beta_1{}^2\beta_{12} \\
-4\,\mathrm{Pr}^3\beta_1{}^3\lambda_4 + 6\,\mathrm{Pr}^3\beta_1{}^2\beta_2\beta_{12} \\
+M\,\mathrm{Pr}\,S\beta_2\beta_{12}{}^2 - 6N^2\beta_5{}^2\beta_{12}{}^2 + \\
9N\,\mathrm{Pr}\,S\beta_5\beta_{12}{}^2 + 34N\,\mathrm{Pr}\,\beta_1\beta_5\beta_{12}\lambda_4 \\
-9N\,\mathrm{Pr}\,\beta_2\beta_5\beta_{12}{}^2 - 6\,\mathrm{Pr}^3\beta_1{}^3 - 3\,\mathrm{Pr}^2 S^2\beta_{12}{}^2 - \\
12\,\mathrm{Pr}^2 S\beta_1\beta_{12}\lambda_4 + 6\,\mathrm{Pr}^2 S\beta_2\beta_{12}{}^2 \\
-6\,\mathrm{Pr}^2\beta_1{}^2\lambda_4{}^2 + 12\,\mathrm{Pr}^2\beta_1\beta_2\beta_{12}\lambda_4 - \\
8\,\mathrm{Pr}^2\beta_1\beta_3\beta_{12}{}^2 - 3\,\mathrm{Pr}^2\beta_2{}^2\beta_{12}{}^2 - 2\,\mathrm{Pr}\,\beta_1\beta_3\beta_{12}{}^2\lambda_2 \\
+\mathrm{Pr}\,\beta_2{}^2\beta_{12}{}^2\lambda_3 + 23N\,\mathrm{Pr}\,\beta_1\beta_5\beta_{12} \\
+17N\beta_5\beta_{12}\lambda_4{}^2 - 14\,\mathrm{Pr}^2 S\beta_1\beta_{12} - 18\,\mathrm{Pr}^2\beta_1{}^2\lambda_4 \\
+14\,\mathrm{Pr}^2\beta_1\beta_2\beta_{12} + 2\,\mathrm{Pr}\,S\beta_3\beta_{12}{}^2 - 6\,\mathrm{Pr}\,S\beta_{12}\lambda_4{}^2 \\
-4\,\mathrm{Pr}\,\beta_1\lambda_4{}^3 + 6\,\mathrm{Pr}\,\beta_2\beta_{12}\lambda_4{}^2 - 2\,\mathrm{Pr}\,\beta_3\beta_{12}{}^2\lambda_1 \\
-8\,\mathrm{Pr}\,\beta_3\beta_{12}{}^2\lambda_4 + 23N\beta_5\beta_{12}\lambda_4 - 11\,\mathrm{Pr}^2\beta_1{}^2 \\
-14\,\mathrm{Pr}\,S\beta_{12}\lambda_4 - 18\,\mathrm{Pr}\,\beta_1\lambda_4{}^2 + 14\,\mathrm{Pr}\,\beta_2\beta_{12}\lambda_4 \\
-6\,\mathrm{Pr}\,\beta_3\beta_{12}{}^2 - \lambda_4{}^4 + 6N\beta_5\beta_{12} - 6\,\mathrm{Pr}\,S\beta_{12} \\
-22\,\mathrm{Pr}\,\beta_1\lambda_4 + 6\,\mathrm{Pr}\,\beta_2\beta_{12} - 6\lambda_4{}^3 - 6\,\mathrm{Pr}\,\beta_1 - 11\lambda_4{}^2 - 6\lambda_4
\end{array}\right)
\end{array}\right),
\end{aligned}
\tag{3.31}
$$

These bulk values will be substituted into the transverse and longitudinal vibration models of the CNT and solved together with deformation and pressure formulations using the transient differential transform method (TDTM) also known as the multi-dimensional differential transform method (MDTM). This is illustrated in Section 3.3.

3.3. **Analytical Solution of Coupled Vibration, Deformation and Pressure Models.** Since the bulk thermofluidic variables have been obtained, substituting into the vibration equations and applying the transient section of Table 2, the recursive relations for the vibration, deformation and pressure models become;

$$
\begin{aligned}
&m\left(h+1\right)\left(h+2\right)w_{k,h+2}+\left(c+A_f\sigma {B_0}^2(\cos\left(\varphi\right))^2\right)\left(h+1\right)w_{k,h+1}+\\
&2m_f\left(\Gamma\right)\xi_1\sum_{l=0}^{k}\left(\sum_{s=0}^{h}(l+1)w_{l+1,h-s+1}d\left(k-l-1,s\right)\right)+m_f\left(\Gamma\right)\xi_2\sum_{l=0}^{k}\left(\sum_{s=0}^{h}(l+1)w_{l+1,h-s}d\left(k-l-1,s\right)\right)+\\
&m_f\Gamma^2\xi_3\sum_{l=0}^{k}\left(\sum_{s=0}^{h}(l+1)w_{l+1,h-s}d\left(k-l-1,s\right)\right)-\left(T_0-G-k_p-\frac{{B_0}^2(\cos(\varphi))^2}{\mu_p}\right)\left(k+1\right)\left(k+2\right)w_{k+2,h}+\\
&\left(-2\delta v+1\right)\sum_{l=0}^{k}\left(\sum_{q=0}^{k-l}\left(\sum_{z=0}^{h}\left(\sum_{s=0}^{h-z}\left(l+1\right)\left(l+2\right)w_{l+2,h-z-s}P_{q,z}A_{k-l-q,s}\right)\right)\right)\\
&+m_f\Gamma^2\cos\left(\varphi\right)\xi_4\sum_{l=0}^{k}\left(\sum_{s=0}^{h}\left(l+1\right)\left(l+2\right)w_{l+2,h-s}d\left(k-l-2,s\right)\right)\\
&\left(T_0-G\right)\left(\begin{array}{l}
\sum_{l=0}^{k}\left(\sum_{s=0}^{h}\left(l+1\right)\left(l+2\right)u_{l+2,h-s}\left(k+1-l\right)w_{k+1-l,s}\right)\\
+\sum_{l=0}^{k}\left(\sum_{s=0}^{h}\left(l+1\right)\left(l+2\right)w_{l+2,h-s}\left(k+1-l\right)u_{k+1-l,s}\right)\\
+3/2\sum_{l=0}^{k}\left(\sum_{q=0}^{k-l}\left(\sum_{z=0}^{h}\left(\begin{array}{l}\sum_{s=0}^{h-z}\left(l+1\right)\left(l+2\right)w_{l+2,h-z-s}\left(q+1\right)\\ w_{q+1,z}\left(k+1-l-q\right)w_{k+1-l-q,s}\end{array}\right)\right)\right)
\end{array}\right)\\
&-\left(-2\delta v+1\right)\left(\begin{array}{l}
\sum_{l=0}^{k}\left(\sum_{q=0}^{k-l}\left(\sum_{g=0}^{k-l-q}\left(\sum_{j=0}^{h}\left(\sum_{z=0}^{h-j}\left(\begin{array}{l}\sum_{s=0}^{h-j-z}\left(l+1\right)\left(l+2\right)\\ u_{l+2,h-j-z-s}\left(q+1\right)w_{q+1,j}\\ P_{g,z}A_{k-l-q-g,s}\end{array}\right)\right)\right)\right)\right)\\
+\sum_{l=0}^{k}\left(\sum_{q=0}^{k-l}\left(\sum_{g=0}^{k-l-q}\left(\sum_{j=0}^{h}\left(\sum_{z=0}^{h-j}\left(\begin{array}{l}\sum_{s=0}^{h-j-z}\left(l+1\right)\left(l+2\right)\\ w_{l+2,h-j-z-s}\left(q+1\right)u_{q+1,j}\\ P_{g,z}A_{k-l-q-g,s}\end{array}\right)\right)\right)\right)\right)\\
+\frac{3}{3}\sum_{l=0}^{k}\sum_{q=0}^{k-l}\sum_{p=0}^{k-l-q}\sum_{g=0}^{k-l-q-p}\sum_{j=0}^{h}\sum_{z=0}^{h-j}\sum_{e=0}^{h-j-z}\sum_{s=0}^{h-j-z-e}\left(\begin{array}{l}\left(l+1\right)\left(l+2\right)\\ w_{l+2,h-j-z-e-s}\\ \left(q+1\right)w_{q+1,j}\\ \left(p+1\right)w_{p+1,z}\\ P_{g,e}A_{k-l-q-p-g,s}\end{array}\right)
\end{array}\right)\\
&+\left(\begin{array}{l}
\frac{3}{2}\sum_{l=0}^{k}\sum_{q=0}^{k-l}\sum_{g=0}^{k-l-q}\sum_{j=0}^{h}\sum_{z=0}^{h-j}\sum_{s=0}^{h-j-z}\begin{array}{l}\left(l+1\right)\left(l+2\right)\\ u_{l+2,h-j-z-s}\left(q+1\right)\\ w_{q+1,j}E_{g,z}A_{k-l-q-g,s}\end{array}\\
+\sum_{l=0}^{k}\sum_{q=0}^{k-l}\sum_{g=0}^{k-l-q}\sum_{j=0}^{h}\sum_{z=0}^{h-j}\sum_{s=0}^{h-j-z}\begin{array}{l}\left(l+1\right)\left(l+2\right)\\ w_{l+2,h-j-z-s}\left(q+1\right)\\ u_{q+1,j}E_{g,z}A_{k-l-q-g,s}\end{array}\\
+\sum_{l=0}^{k}\sum_{q=0}^{k-l}\sum_{p=0}^{k-l-q}\sum_{g=0}^{k-l-q-p}\sum_{j=0}^{h}\sum_{z=0}^{h-j}\sum_{e=0}^{h-j-z}\sum_{s=0}^{h-j-z-e}\begin{array}{l}\left(l+1\right)\left(l+2\right)\\ w_{l+2,h-j-z-e-s}\left(q+1\right)\\ w_{q+1,j}\left(p+1\right)\\ w_{p+1,z}E_{g,e}A_{k-l-q-p-g,s}\end{array}
\end{array}\right)\\
&\left(-2\delta v+1\right)\left(\left(\begin{array}{l}
\sum_{l=0}^{k}\left(\sum_{q=0}^{k-l}\left(\sum_{z=0}^{h}\left(\sum_{s=0}^{h-z}(l+1)w_{l+1,h-z-s}P_{q,z}A_{k-l-q,s}\right)\right)\right)\\
-\sum_{l=0}^{k}\sum_{q=0}^{k-l}\sum_{g=0}^{k-l-q}\sum_{j=0}^{h}\sum_{z=0}^{h-j}\sum_{s=0}^{h-j-z}\begin{array}{l}\left(l+1\right)w_{l+1,h-j-z-s}\left(q+1\right)\\ u_{q+1,j}P_{g,z}A_{k-l-q-g,s}\end{array}\\
-1/2\sum_{l=0}^{k}\sum_{q=0}^{k-l}\sum_{p=0}^{k-l-q}\sum_{g=0}^{k-l-q-p}\sum_{j=0}^{h}\sum_{z=0}^{h-j}\sum_{e=0}^{h-j-z}\sum_{s=0}^{h-j-z-e}\begin{array}{l}\left(l+1\right)\\ w_{l+1,h-j-z-e-s}\left(q+1\right)\\ w_{q+1,j}\left(p+1\right)\\ w_{p+1,z}P_{g,e}A_{k-l-q-p-g,s}\end{array}
\end{array}\right)\right)
\end{aligned}
$$

$$
-E\left(\begin{array}{l}
\sum_{l=0}^{k}\left(\sum_{q=0}^{k-l}\left(\sum_{z=0}^{h}\left(\sum_{s=0}^{h-z}(l+1)w_{l+1,h-z-s}\left(q+1\right)u_{q+1,z}A_{k-l-q,s}\right)\right)\right)+\\
1/2\sum_{l=0}^{k}\left(\sum_{q=0}^{k-l}\left(\sum_{g=0}^{k-l-q}\left(\sum_{j=0}^{h}\left(\sum_{z=0}^{h-j}\left(\begin{array}{l}\sum_{s=0}^{h-j-z}(l+1)w_{l+1,h-j-z-s}\left(q+1\right)\\ w_{q+1,j}\left(g+1\right)w_{g+1,z}A_{k-l-q-g,s}\end{array}\right)\right)\right)\right)\right)
\end{array}\right)
$$

$$
+E\alpha\left(\begin{array}{l}
\sum_{l=0}^{k}\left(\sum_{q=0}^{k-l}\left(\sum_{z=0}^{h}\left(\sum_{s=0}^{h-z}(l+1)w_{l+1,h-z-s}T_{q,z}A_{k-l-q,s}\right)\right)\right)\\
-\sum_{l=0}^{k}\sum_{q=0}^{k-l}\sum_{g=0}^{k-l-q}\sum_{j=0}^{h}\sum_{z=0}^{h-j}\sum_{s=0}^{h-j-z}\begin{array}{l}\left(l+1\right)w_{l+1,h-j-z-s}\\ \left(q+1\right)u_{q+1,j}T_{g,z}A_{k-l-q-g,s}\end{array}\\
-1/2\sum_{l=0}^{k}\sum_{q=0}^{k-l}\sum_{p=0}^{k-l-q}\sum_{g=0}^{k-l-q-p}\sum_{j=0}^{h}\sum_{z=0}^{h-j}\sum_{e=0}^{h-j-z}\sum_{s=0}^{h-j-z-e}\begin{array}{l}\left(l+1\right)\\ w_{l+1,h-j-z-e-s}\\ \left(q+1\right)w_{q+1,j}\\ \left(p+1\right)w_{p+1,z}T_{g,e}A_{k-l-q-p-g,s}\end{array}
\end{array}\right)
$$

$$
+E\alpha\left(\begin{array}{l}
\sum_{l=0}^{k}\left(\sum_{q=0}^{k-l}\left(\sum_{z=0}^{h}\left(\sum_{s=0}^{h-z}(l+1)w_{l+1,h-z-s}\left(q+1\right)T_{q+1,z}A_{k-l-q,s}\right)\right)\right)-\\
\sum_{l=0}^{k}\sum_{q=0}^{k-l}\sum_{g=0}^{k-l-q}\sum_{j=0}^{h}\sum_{z=0}^{h-j}\sum_{s=0}^{h-j-z}\begin{array}{l}\left(l+1\right)w_{l+1,h-j-z-s}\left(q+1\right)u_{q+1,j}\\ \left(g+1\right)T_{g,z}A_{k-l-q-g,s}\end{array}\\
-1/2\sum_{l=0}^{k}\sum_{q=0}^{k-l}\sum_{p=0}^{k-l-q}\sum_{g=0}^{k-l-q-p}\sum_{j=0}^{h}\sum_{z=0}^{h-j}\sum_{e=0}^{h-j-z}\begin{array}{l}\left(l+1\right)w_{l+1,h-j-z-e-s}\left(q+1\right)\\ w_{q+1,j}\left(p+1\right)w_{p+1,z}\left(g+1\right)\\ T_{g+1,e}A_{k-l-q-p-g,s}\end{array}
\end{array}\right)
$$

$$
+E\alpha\left(\begin{array}{l}
\sum_{l=0}^{k}\left(\sum_{q=0}^{k-l}\left(\sum_{z=0}^{h}\left(\sum_{s=0}^{h-z}(l+1)w_{l+1,h-z-s}T_{q,z}\left(k+1-l-q\right)A_{k+1-l-q,s}\right)\right)\right)\\
-\sum_{l=0}^{k}\sum_{q=0}^{k-l}\sum_{g=0}^{k-l-q}\sum_{j=0}^{h}\sum_{z=0}^{h-j}\sum_{s=0}^{h-j-z}\begin{array}{l}\left(l+1\right)w_{l+1,h-j-z-s}\left(q+1\right)u_{q+1,j}\\ T_{g,z}\left(k+1-l-q-g\right)A_{k+1-l-q-g,s}\end{array}-\\
1/2\sum_{l=0}^{k}\sum_{q=0}^{k-l}\sum_{p=0}^{k-l-q}\sum_{g=0}^{k-l-q-p}\sum_{j=0}^{h}\sum_{z=0}^{h-j}\sum_{e=0}^{h-j-z}\begin{array}{l}\left(l+1\right)w_{l+1,h-j-z-e-s}\left(q+1\right)w_{q+1,j}\\ \left(p+1\right)w_{p+1,z}T_{g,e}\\ \left(k+1-l-q-p-g\right)A_{k+1-l-q-p-g,s}\end{array}
\end{array}\right)
$$

$$
-E\alpha\left(\begin{array}{l}
\sum_{l=0}^{k}\sum_{q=0}^{k-l}\sum_{p=0}^{k-l-q}\sum_{g=0}^{k-l-q-p}\sum_{j=0}^{h}\sum_{z=0}^{h-j}\sum_{e=0}^{h-j-z}\begin{array}{l}(l+1)\,w_{l+1,h-j-z-e-s}\,(q+1)\,w_{q+1,j}\,(p+1)\\ (p+2)\,u_{p+2,z}T_{g,e}\,(k+1-l-q-p-g)\\ A_{k+1-l-q-p-g,s}\end{array}\\
+\sum_{l=0}^{k}\sum_{q=0}^{k-l}\sum_{p=0}^{k-l-q}\sum_{g=0}^{k-l-q-p}\sum_{j=0}^{h}\sum_{z=0}^{h-j}\sum_{e=0}^{h-j-z}\begin{array}{l}(l+1)\,w_{l+1,h-j-z-e-s}\,(q+1)\,w_{q+1,j}\\ (p+1)\,(p+2)\,w_{p+2,z}T_{g,e}\\ (k+1-l-q-p-g)\,A_{k+1-l-q-p-g,s}\end{array}
\end{array}\right)
$$

$$
+\left(IE+\frac{iB_0{}^2(\sin(\varphi))^2}{\mu_p}\right)(k+1)\,(k+2)\,(k+3)\,(k+4)\,w_{k+4,h}
$$

$$
-EI\left(\begin{array}{l}
\left(\begin{array}{l}
3\sum_{l=0}^{k}\left(\sum_{s=0}^{h}(l+1)\,(l+2)\,(l+3)\,u_{l+3,h-s}\,(k+1-l)\,(k+2-l)\,w_{k+2-l,s}\right)\\
+4\sum_{l=0}^{k}\left(\sum_{s=0}^{h}(l+1)\,(l+2)\,(l+3)\,w_{l+3,h-s}\,(k+1-l)\,(k+2-l)\,u_{k+2-l,s}\right)\\
+2\sum_{l=0}^{k}\left(\sum_{s=0}^{h}(l+1)\,(l+2)\,(l+3)\,(l+4)\,w_{l+4,h-s}\,(k+1-l)\,u_{k+1-l,s}\right)\\
+\sum_{l=0}^{k}\left(\sum_{s=0}^{h}(l+1)\,(l+2)\,(l+3)\,(l+4)\,u_{l+4,h-s}\,(k+1-l)\,w_{k+1-l,s}\right)
\end{array}\right)\\
2\sum_{l=0}^{k}\left(\sum_{q=0}^{k-l}\left(\sum_{z=0}^{h}\left(\begin{array}{l}\sum_{s=0}^{h-z}(l+1)\,(l+2)\,(l+3)\,(l+4)\,w_{l+4,h-z-s}\\ (q+1)\,T_{q+1,z}\,(k+1-l-q)\,w_{k+1-l-q,s}\end{array}\right)\right)\right)\\
+8\sum_{l=0}^{k}\left(\sum_{q=0}^{k-l}\left(\sum_{z=0}^{h}\left(\begin{array}{l}\sum_{s=0}^{h-z}(l+1)\,(l+2)\,(l+3)\,w_{l+3,h-z-s}\,(q+1)\,(q+2)\\ w_{q+2,z}\,(k+1-l-q)\,w_{k+1-l-q,s}\end{array}\right)\right)\right)\\
+2\sum_{l=0}^{k}\left(\sum_{q=0}^{k-l}\left(\sum_{z=0}^{h}\left(\begin{array}{l}\sum_{s=0}^{h-z}(l+1)\,(l+2)\,w_{l+2,h-z-s}\,(q+1)\,(q+2)\\ w_{q+2,z}\,(k+1-l-q)\,(k+2-l-q)\,w_{k+2-l-q,s}\end{array}\right)\right)\right)
\end{array}\right)
$$

$$
-E\left(\xi_5\sum_{l=0}^{k}\left(\sum_{s=0}^{h}(l+1)\,(l+2)\,w_{l+2,h-s}A_{k,s}\right)+\xi_6A_{k,h}\right)+k_1w_{k,h}+
$$

$$
k_2\sum_{l=0}^{k}\left(\sum_{q=0}^{k-l}\left(\sum_{z=0}^{h}\left(\sum_{s=0}^{h-z}w_{l,h-z-s}w_{q,z}w_{k-l-q,s}\right)\right)\right)
$$

$$
+{(e_0a)}^2\left(\begin{array}{l}
+\left(IE+\frac{iB_0{}^2(\sin(\varphi))^2}{\mu_p}\right)(k+1)\\
(k+2)(k+3)\\
(k+4)(k+5)(k+6)\,w_{k+6,h}\\
-E\left(\begin{array}{l}
\sum\limits_{l=0}^{k}\left(\sum\limits_{q=0}^{k-l}\left(\sum\limits_{z=0}^{h}\left(\begin{array}{l}\sum\limits_{s=0}^{h-z}(l+1)(l+2)(k+3)\,w_{l+3,h-z-s}\\(q+1)\,u_{q+1,z}A_{k-l-q,s}\end{array}\right)\right)\right)\\
+1/2\sum\limits_{l=0}^{k}\left(\sum\limits_{q=0}^{k-l}\left(\sum\limits_{g=0}^{k-l-q}\left(\sum\limits_{j=0}^{h}\left(\sum\limits_{z=0}^{h-j}\left(\begin{array}{l}\sum\limits_{s=0}^{h-j-z}(l+1)w_{l+1,h-j-z-s}(q+1)\\w_{q+1,j}(g+1)\,w_{g+1,z}A_{k-l-q-g,s}\end{array}\right)\right)\right)\right)\right)
\end{array}\right)\\
+E\alpha\left(\begin{array}{l}
\sum\limits_{l=0}^{k}\left(\sum\limits_{q=0}^{k-l}\left(\sum\limits_{z=0}^{h}\left(\begin{array}{l}\sum\limits_{s=0}^{h-z}(l+1)(l+2)(k+3)\\w_{l+3,h-z-s}T_{q,z}A_{k-l-q,s}\end{array}\right)\right)\right)\\
-\sum\limits_{l=0}^{k}\sum\limits_{q=0}^{k-l}\sum\limits_{g=0}^{k-l-q}\sum\limits_{j=0}^{h}\sum\limits_{z=0}^{h-j}\sum\limits_{s=0}^{h-j-z}\begin{array}{l}(l+1)\,w_{l+1,h-j-z-s}(q+1)\\u_{q+1,j}T_{g,z}A_{k-l-q-g,s}\end{array}\\
-1/2\sum\limits_{l=0}^{k}\sum\limits_{q=0}^{k-l}\sum\limits_{p=0}^{k-l-q}\sum\limits_{g=0}^{k-l-q-p}\sum\limits_{j=0}^{h}\sum\limits_{z=0}^{h-j}\sum\limits_{e=0}^{h-j-z}\sum\limits_{s=0}^{h-j-z-e}\begin{array}{l}(l+1)\,w_{l+1,h-j-z-e-s}\\(q+1)\,w_{q+1,j}\\(p+1)\,w_{p+1,z}T_{g,e}A_{k-l-q-p-g,s}\end{array}
\end{array}\right)\\
+E\alpha\left(\begin{array}{l}
\sum\limits_{l=0}^{k}\left(\sum\limits_{q=0}^{k-l}\left(\sum\limits_{z=0}^{h}\left(\sum\limits_{s=0}^{h-z}(l+1)w_{l+1,h-z-s}(q+1)\,T_{q+1,z}A_{k-l-q,s}\right)\right)\right)\\
-\sum\limits_{l=0}^{k}\sum\limits_{q=0}^{k-l}\sum\limits_{g=0}^{k-l-q}\sum\limits_{j=0}^{h}\sum\limits_{z=0}^{h-j}\sum\limits_{s=0}^{h-j-z}\begin{array}{l}(l+1)\,w_{l+1,h-j-z-s}(q+1)\,u_{q+1,j}\\(g+1)\,T_{g,z}A_{k-l-q-g,s}\end{array}\\
-1/2\sum\limits_{l=0}^{k}\sum\limits_{q=0}^{k-l}\sum\limits_{p=0}^{k-l-q}\sum\limits_{g=0}^{k-l-q-p}\sum\limits_{j=0}^{h}\sum\limits_{z=0}^{h-j}\sum\limits_{e=0}^{h-j-z}\begin{array}{l}(l+1)\,w_{l+1,h-j-z-e-s}(q+1)\\w_{q+1,j}(p+1)\,w_{p+1,z}\\(g+1)\,T_{g+1,e}A_{k-l-q-p-g,s}\end{array}
\end{array}\right)\\
+E\alpha\left(\begin{array}{l}
\sum\limits_{l=0}^{k}\left(\sum\limits_{q=0}^{k-l}\left(\sum\limits_{z=0}^{h}\left(\begin{array}{l}\sum\limits_{s=0}^{h-z}(l+1)(l+2)(k+3)\,w_{l+3,h-z-s}T_{q,z}\\(k+1-l-q)\,A_{k+1-l-q,s}\end{array}\right)\right)\right)\\
-\sum\limits_{l=0}^{k}\sum\limits_{q=0}^{k-l}\sum\limits_{g=0}^{k-l-q}\sum\limits_{j=0}^{h}\sum\limits_{z=0}^{h-j}\sum\limits_{s=0}^{h-j-z}\begin{array}{l}(l+1)\,w_{l+1,h-j-z-s}(q+1)\,u_{q+1,j}\\T_{g,z}(k+1-l-q-g)\,A_{k+1-l-q-g,s}\end{array}-\\
1/2\sum\limits_{l=0}^{k}\sum\limits_{q=0}^{k-l}\sum\limits_{p=0}^{k-l-q}\sum\limits_{g=0}^{k-l-q-p}\sum\limits_{j=0}^{h}\sum\limits_{z=0}^{h-j}\sum\limits_{e=0}^{h-j-z}\begin{array}{l}(l+1)\,w_{l+1,h-j-z-e-s}(q+1)\\w_{q+1,j}(p+1)\,w_{p+1,z}T_{g,e}\\(k+1-l-q-p-g)\,A_{k+1-l-q-p-g,s}\end{array}
\end{array}\right)\\
-E\alpha\left(\begin{array}{l}
\sum\limits_{l=0}^{k}\sum\limits_{q=0}^{k-l}\sum\limits_{p=0}^{k-l-q}\sum\limits_{g=0}^{k-l-q-p}\sum\limits_{j=0}^{h}\sum\limits_{z=0}^{h-j}\sum\limits_{e=0}^{h-j-z}\begin{array}{l}(l+1)\,w_{l+1,h-j-z-e-s}(q+1)\,w_{q+1,j}\\(p+1)(p+2)\,u_{p+2,z}T_{g,e}\left(\begin{array}{l}k+1-l-\\q-p-g\end{array}\right)\\A_{k+1-l-q-p-g,s}\end{array}\\
+\sum\limits_{l=0}^{k}\sum\limits_{q=0}^{k-l}\sum\limits_{p=0}^{k-l-q}\sum\limits_{g=0}^{k-l-q-p}\sum\limits_{j=0}^{h}\sum\limits_{z=0}^{h-j}\sum\limits_{e=0}^{h-j-z}\begin{array}{l}(l+1)\,w_{l+1,h-j-z-e-s}\\(q+1)\,w_{q+1,j}(p+1)(p+2)\\w_{p+2,z}T_{g,e}(k+1-l-q-p-g)\\A_{k+1-l-q-p-g,s}\end{array}
\end{array}\right)\\
+J_5
\end{array}\right)
$$

$$
+(e_0a)^2
\left(\begin{array}{l}
m\left(h+1\right)\left(h+2\right)w_{k+2,h+2}+\\
\left(c+A_f\sigma {B_0}^2(\cos\left(\varphi\right))^2\right)\left(h+1\right)w_{k+2,h+1}\\
+2m_f\left(\Gamma\right)\xi_1\sum_{l=0}^{k}\left(\sum_{s=0}^{h}(l+1)w_{l+1,h-s+1}d\left(k-l-1,s\right)\right)\\
+m_f\left(\Gamma\right)\xi_2\sum_{l=0}^{k}\left(\sum_{s=0}^{h}(l+1)\left(l+2\right)\left(l+3\right)w_{l+3,h-s}d\left(k-l-1,s\right)\right)\\
+m_f\Gamma^2\xi_3\sum_{l=0}^{k}\left(\sum_{s=0}^{h}(l+1)\left(l+2\right)\left(l+3\right)w_{l+3,h-s}d\left(k-l-1,s\right)\right)\\
-\left(T_0-G-k_p-\frac{{B_0}^2(\cos(\varphi))^2}{\mu_p}\right)\left(k+1\right)\left(k+2\right)\\
\left(l+3\right)\left(l+4\right)w_{k+4,h}+\left(-2\delta v+1\right)\sum_{l=0}^{k}\left(\sum_{q=0}^{k-l}\left(\sum_{z=0}^{h}\left(\begin{array}{l}\sum_{s=0}^{h-z}\left(l+1\right)\left(l+2\right)\\ w_{l+2,h-z-s}P_{q,z}A_{k-l-q,s}\end{array}\right)\right)\right)\\
+m_f\Gamma^2\cos\left(\varphi\right)\xi_4\sum_{l=0}^{k}\left(\sum_{s=0}^{h}\left(l+1\right)\left(l+2\right)w_{l+2,h-s}d\left(k-l-2,s\right)\right)\left(T_0-G\right)\\
\left(\begin{array}{l}
\sum_{l=0}^{k}\left(\sum_{s=0}^{h}\left(l+1\right)\left(l+2\right)u_{l+2,h-s}\left(k+1-l\right)w_{k+1-l,s}\right)\\
+\sum_{l=0}^{k}\left(\sum_{s=0}^{h}\left(l+1\right)\left(l+2\right)w_{l+2,h-s}\left(k+1-l\right)u_{k+1-l,s}\right)\\
+3/2\sum_{l=0}^{k}\left(\sum_{q=0}^{k-l}\left(\sum_{z=0}^{h}\left(\begin{array}{l}\sum_{s=0}^{h-z}\left(l+1\right)\left(l+2\right)w_{l+2,h-z-s}\left(q+1\right)\\ w_{q+1,z}\left(k+1-l-q\right)w_{k+1-l-q,s}\end{array}\right)\right)\right)
\end{array}\right)\\
-\left(-2\delta v+1\right)\\
\left(\begin{array}{l}
\sum_{l=0}^{k}\left(\sum_{q=0}^{k-l}\left(\sum_{g=0}^{k-l-q}\left(\sum_{j=0}^{h}\left(\sum_{z=0}^{h-j}\left(\begin{array}{l}\sum_{s=0}^{h-j-z}\left(l+1\right)\left(l+2\right)\\ u_{l+2,h-j-z-s}\left(q+1\right)w_{q+1,j}\\ P_{g,z}A_{k-l-q-g,s}\end{array}\right)\right)\right)\right)\right)\\
+\sum_{l=0}^{k}\left(\sum_{q=0}^{k-l}\left(\sum_{g=0}^{k-l-q}\left(\sum_{j=0}^{h}\left(\sum_{z=0}^{h-j}\left(\begin{array}{l}\sum_{s=0}^{h-j-z}\left(l+1\right)\left(l+2\right)w_{l+2,h-j-z-s}\\ \left(q+1\right)u_{q+1,j}P_{g,z}A_{k-l-q-g,s}\end{array}\right)\right)\right)\right)\right)\\
+\frac{3}{3}\sum_{l=0}^{k}\sum_{q=0}^{k-l}\sum_{p=0}^{k-l-q}\sum_{g=0}^{k-l-q-p}\sum_{j=0}^{h}\sum_{z=0}^{h-j}\sum_{e=0}^{h-j-z}\sum_{s=0}^{h-j-z-e}\left(\begin{array}{l}\left(l+1\right)\left(l+2\right)\\ w_{l+2,h-j-z-e-s}\left(q+1\right)w_{q+1,j}\\ \left(p+1\right)w_{p+1,z}P_{g,e}A_{k-l-q-p-g,s}\end{array}\right)
\end{array}\right)\\
+J_6
\end{array}\right)
$$

$$= TDTMtr\left(F + e_0 a\left(\nabla^2 F\right)\right) = TDTMtr\left(\sum_{\zeta=1}^{7} c_\zeta \left(w - w_i\right)^{\zeta} + e_0 a\left(\nabla^2\left[\sum_{\zeta=1}^{7} c_\zeta \left(w - w_i\right)^{\zeta}\right]\right)\right), \tag{3.32}$$

Where,

$$J_5 = \\ -EI\left(\begin{array}{l}
\left(\begin{array}{l}
3\sum_{l=0}^{k}\left(\begin{array}{l}\sum_{s=0}^{h}(l+1)(l+2)(l+3)\\ (k+4)(k+5)\,u_{l+5,h-s}(k+1-l)(k+2-l)\,w_{k+2-l,s}\end{array}\right)\\
+4\sum_{l=0}^{k}\left(\begin{array}{l}\sum_{s=0}^{h}(l+1)(l+2)(l+3)\\ (l+4)(k+5)\,w_{l+5,h-s}(k+1-l)(k+2-l)\,u_{k+2-l,s}\end{array}\right)\\
+2\sum_{l=0}^{k}\left(\begin{array}{l}\sum_{s=0}^{h}(l+1)(l+2)(l+3)\\ (l+4)(k+5)(k+6)\,w_{l+6,h-s}(k+1-l)\,u_{k+1-l,s}\end{array}\right)\\
+\sum_{l=0}^{k}\left(\begin{array}{l}\sum_{s=0}^{h}(l+1)(l+2)(l+3)\\ (l+4)(k+5)(k+6)\,u_{l+6,h-s}(k+1-l)\,w_{k+1-l,s}\end{array}\right)
\end{array}\right)\\
2\sum_{l=0}^{k}\left(\sum_{q=0}^{k-l}\left(\sum_{z=0}^{h}\left(\begin{array}{l}\sum_{s=0}^{h-z}(l+1)(l+2)(l+3)\\ (l+4)(k+5)(k+6)\,w_{l+6,h-z-s}\\ (q+1)\,T_{q+1,z}(k+1-l-q)\,w_{k+1-l-q,s}\end{array}\right)\right)\right)\\
+8\sum_{l=0}^{k}\left(\sum_{q=0}^{k-l}\left(\sum_{z=0}^{h}\left(\begin{array}{l}\sum_{s=0}^{h-z}(l+1)(l+2)(l+3)\\ (l+4)(k+5)\,w_{l+5,h-z-s}(q+1)\\ (q+2)\,w_{q+2,z}(k+1-l-q)\,w_{k+1-l-q,s}\end{array}\right)\right)\right)\\
+2\sum_{l=0}^{k}\left(\sum_{q=0}^{k-l}\left(\sum_{z=0}^{h}\left(\begin{array}{l}\sum_{s=0}^{h-z}(l+1)(l+2)(l+3)(k+4)\\ w_{l+4,h-z-s}(q+1)(q+2)\,w_{q+2,z}\\ (k+1-l-q)(k+2-l-q)\,w_{k+2-l-q,s}\end{array}\right)\right)\right)
\end{array}\right) \\
-E\left(\xi_5\sum_{l=0}^{k}\left(\sum_{s=0}^{h}(l+1)(l+2)\,w_{l+2,h-s}A_{k,s}\right)+\xi_6 A_{k,h}\right)+ \\
k_1\sum_{s=0}^{h-z}(l+1)(l+2)\,w_{k+2,h} \\
+6k_2\sum_{l=0}^{k}\left(\sum_{q=0}^{k-l}\left(\sum_{z=0}^{h}\left(\sum_{s=0}^{h-z}\sum_{s=0}^{h-z}(l+1)w_{l+1,h-z-s}(q+1)\,w_{q+1,z}w_{k-l-q,s}\right)\right)\right) \\
+3k_2\sum_{l=0}^{k}\left(\sum_{q=0}^{k-l}\left(\sum_{z=0}^{h}\left(\sum_{s=0}^{h-z}\sum_{s=0}^{h-z}(l+1)(l+2)\,w_{l+2,h-z-s}w_{q,z}w_{k-l-q,s}\right)\right)\right), \tag{3.33}$$

$$
\begin{aligned}
&J_6 = \\
&+\left(\begin{array}{l}
\frac{3}{2}\sum_{l=0}^{k}\sum_{q=0}^{k-l}\sum_{g=0}^{k-l-q}\sum_{j=0}^{h}\sum_{z=0}^{h-j}\sum_{s=0}^{h-j-z} \begin{array}{l}(l+1)(l+2)(l+3)(l+4)\,u_{l+4,h-j-z-s}\\ (q+1)\,w_{q+1,j}E_{g,z}A_{k-l-q-g,s}\end{array}\\
+\sum_{l=0}^{k}\sum_{q=0}^{k-l}\sum_{g=0}^{k-l-q}\sum_{j=0}^{h}\sum_{z=0}^{h-j}\sum_{s=0}^{h-j-z} \begin{array}{l}(l+1)(l+2)(l+3)(l+4)\,w_{l+4,h-j-z-s}\\ (q+1)\,u_{q+1,j}E_{g,z}A_{k-l-q-g,s}\end{array}\\
+\sum_{l=0}^{k}\sum_{q=0}^{k-l}\sum_{p=0}^{k-l-q}\sum_{g=0}^{k-l-q-p}\sum_{j=0}^{h}\sum_{z=0}^{h-j}\sum_{e=0}^{h-j-z}\sum_{s=0}^{h-j-z-e} \begin{array}{l}(l+1)(l+2)\\ (l+3)(l+4)\,w_{l+4,h-j-z-e-s}\\ (q+1)\,w_{q+1,j}\,(p+1)\\ w_{p+1,z}E_{g,e}A_{k-l-q-p-g,s}\end{array}
\end{array}\right)\\
&(-2\delta v+1)\\
&\left(\left(\begin{array}{l}
\sum_{l=0}^{k}\left(\sum_{q=0}^{k-l}\left(\sum_{z=0}^{h}\left(\begin{array}{l}\sum_{s=0}^{h-z}(l+1)w_{l+1,h-z-s}\\ P_{q,z}A_{k-l-q,s}\end{array}\right)\right)\right) - \sum_{l=0}^{k}\sum_{q=0}^{k-l}\sum_{g=0}^{k-l-q}\sum_{j=0}^{h}\sum_{z=0}^{h-j}\sum_{s=0}^{h-j-z} \begin{array}{l}(l+1)\,w_{l+1,h-j-z-s}\\ (q+1)\\ u_{q+1,j}P_{g,z}A_{k-l-q-g,s}\end{array}\\
-1/2\sum_{l=0}^{k}\sum_{q=0}^{k-l}\sum_{p=0}^{k-l-q}\sum_{g=0}^{k-l-q-p}\sum_{j=0}^{h}\sum_{z=0}^{h-j}\sum_{e=0}^{h-j-z}\sum_{s=0}^{h-j-z-e} \begin{array}{l}(l+1)\,w_{l+1,h-j-z-e-s}\,(q+1)\\ w_{q+1,j}\,(p+1)\,w_{p+1,z}P_{g,e}A_{k-l-q-p-g,s}\end{array}
\end{array}\right)\right),
\end{aligned}
\tag{3.34}
$$

For tubes not in contact with fluid (i.e., for $N > 1$), the fluid velocity transform in the vibration model becomes nullified.
Similarly, the longitudinal vibration model transforms into;

$$
\begin{aligned}
&m\,(h+1)\,(h+2)\,u_{k,h+2}+\\
&2m_f\,(\Gamma)\,\xi_1\sum_{l=0}^{k}\left(\sum_{s=0}^{h}(l+1)\,(l+2)\,u_{l+2,h-s+1}d\,(k-l-1,s)\right)\\
&+m_f\,(\Gamma)\,\xi_2\sum_{l=0}^{k}\left(\begin{array}{l}\sum_{s=0}^{h}(l+1)\,(l+2)\\ (l+3)\,u_{l+3,h-s+1}d\,(k-l-1,s+1)\end{array}\right)\\
&+m_f\,(\Gamma)\,\xi_2 d\,(k-1,h)+m_f\Gamma^2\xi_1\xi_3\,(d\,(k,h)+(h+1)\,u_{k,h+1})\\
&(T_0-G-EA_t)\sum_{l=0}^{k}\left(\sum_{s=0}^{h}(l+1)\,(l+2)\,w_{l+2,h-s}\,(k+1-l)\,w_{1,s}\right)\\
&-EA_t\,(k+1)\,(k+2)\,u_{k+2,h}+\\
&m_f\Gamma^2{\xi_1}^2\sum_{l=0}^{k}\left(\begin{array}{l}\sum_{s=0}^{h}(l+1)\,(l+2)\,u_{l+2,h-s+1}\\ d\,(k-l-1,s)\end{array}\right)\\
&-(-2v\delta+1)\left(\begin{array}{l}\sum_{l=0}^{k}\left(\sum_{s=0}^{h}(l+1)A_{l+1,h-s}P_{k-l,s}\right)+\\ \sum_{l=0}^{k}\left(\sum_{s=0}^{h}(l+1)P_{l+1,h-s}A_{k-l,s}\right)\end{array}\right)\\
&+(-2v\delta+1)\sum_{l=0}^{k}\sum_{q=0}^{k-l}\sum_{g=0}^{k-l-q}\sum_{j=0}^{h}\sum_{z=0}^{h-j}\sum_{s=0}^{h-j-z}\begin{array}{l}(l+1)\,(l+2)\,w_{l+2,h-j-z-s}\\ (q+1)\,w_{q+1,j}P_{g,z}A_{k-l-q-g,s}\end{array}\\
&-EA_t\left((k+1)\,u_{k+1,h}+1/2\sum_{l=0}^{k}\left(\begin{array}{l}\sum_{s=0}^{h}(l+1)w_{l+1,h-s}\\ (k+1-l)\,w_{1,s}\end{array}\right)\right)
\end{aligned}
$$

$$
\begin{aligned}
&-\frac{(-2v\delta+1)}{2}\left(\begin{array}{l}\sum_{l=0}^{k}\sum_{q=0}^{k-l}\sum_{g=0}^{k-l-q}\sum_{j=0}^{h}\sum_{z=0}^{h-j}\sum_{s=0}^{h-j-z}\begin{array}{l}(l+1)\,w_{l+1,h-j-z-s}\,(q+1)\,w_{q+1,j}\\(g+1)\,P_{g+1,z}A_{k-l-q-g,s}\end{array}\\+\sum_{l=0}^{k}\sum_{q=0}^{k-l}\sum_{g=0}^{k-l-q}\sum_{j=0}^{h}\sum_{z=0}^{h-j}\sum_{s=0}^{h-j-z}\begin{array}{l}(l+1)\,w_{l+1,h-j-z-s}\,(q+1)\,w_{q+1,j}\\P_{g,z}\,(k+1-l-q-g)\,A_{k+1-l-q-g,s}\end{array}\end{array}\right)\\
&+E\alpha\left(\sum_{l=0}^{k}\left(\sum_{s=0}^{h}(l+1)T_{l+1,h-s}A_{k-l,s}\right)+\sum_{l=0}^{k}\left(\begin{array}{l}\sum_{s=0}^{h}(l+1)\\A_{l+1,h-s}T_{k-l,s}\end{array}\right)\right)\\
&-E\alpha\sum_{l=0}^{k}\sum_{q=0}^{k-l}\sum_{g=0}^{k-l-q}\sum_{j=0}^{h}\sum_{z=0}^{h-j}\sum_{s=0}^{h-j-z}\begin{array}{l}(l+1)\,(l+2)\,w_{l+2,h-j-z-s}\\(q+1)\,w_{q+1,j}T_{g,z}\\(k+1-l-q-g)\,A_{k+1-l-q-g,s}\end{array}\\
&-EI\left(\begin{array}{l}\sum_{l=0}^{k}\left(\begin{array}{l}\sum_{s=0}^{h}(l+1)\,(l+2)\\(l+3)\,(l+4)\,w_{l+4,h-s}\,(k+1-l)\,w_{k-2l+1,s}\end{array}\right)\\+\sum_{l=0}^{k}\left(\begin{array}{l}\sum_{s=0}^{h}(l+1)\,(l+2)\,(l+3)\,w_{l+3,h-s}\\(k+1-l)\,(k+2-l)\,w_{k+2-l,s}\end{array}\right)\end{array}\right)
\end{aligned}
$$

$$
\begin{gathered}
+(e_0 a)^2 \\
\left(\begin{array}{l}
m\,(h+1)\,(h+2)\,u_{k+2,h+2}+ \\
2m_f\,(\Gamma)\,\xi_1 \sum\limits_{l=0}^{k}\left(\begin{array}{l}\sum\limits_{s=0}^{h}(l+1)\,(l+2) \\ (l+3)\,(l+4) \\ u_{l+4,h-s+1}d\,(k-l-1,s)\end{array}\right) \\
+m_f\,(\Gamma)\,\xi_2 \sum\limits_{l=0}^{k}\left(\begin{array}{l}\sum\limits_{s=0}^{h}(l+1)\,(l+2) \\ (l+3)\,(l+4)\,(l+5)\,u_{l+5,h-s+1}d\,(k-l-1,s+1)\end{array}\right) \\
+m_f\,(\Gamma)\,\xi_2 d\,(k-1,h)+m_f\Gamma^2\xi_1\xi_3\,(d\,(k,h)+(h+1)\,u_{k+2,h+1}) \\
(T_0-G-EA_t)\sum\limits_{l=0}^{k}\left(\sum\limits_{s=0}^{h}(l+1)\,(l+2)\,(l+3)\,(l+4)\,w_{l+4,h-s}\,(k+1-l)\,w_{1,s}\right) \\
-EA_t\,(k+1)\,(k+2)\,(l+3)\,(l+4)\,u_{k+4,h}+ \\
m_f\Gamma^2{\xi_1}^2\sum\limits_{l=0}^{k}\left(\sum\limits_{s=0}^{h}(l+1)\,(l+2)\,(l+3)\,(l+4)\,u_{l+4,h-s+1}d\,(k-l-1,s)\right) \\
-\,(-2v\delta+1)\left(\begin{array}{l}\sum\limits_{l=0}^{k}\left(\sum\limits_{s=0}^{h}(l+1)\,(l+2)\,(l+3)\,A_{l+3,h-s}P_{k-l,s}\right) \\ +\sum\limits_{l=0}^{k}\left(\sum\limits_{s=0}^{h}(l+1)\,(l+2)\,(l+3)\,P_{l+3,h-s}A_{k-l,s}\right)\end{array}\right) \\
+\,(-2v\delta+1)\sum\limits_{l=0}^{k}\sum\limits_{q=0}^{k-l}\sum\limits_{g=0}^{k-l-q}\sum\limits_{j=0}^{h}\sum\limits_{z=0}^{h-j}\sum\limits_{s=0}^{h-j-z}\begin{array}{l}(l+1)\,(l+2) \\ (l+3)\,(l+4)\,w_{l+4,h-j-z-s} \\ (q+1)\,w_{q+1,j}P_{g,z}A_{k-l-q-g,s}\end{array} \\
-EA_t\left((k+1)\,(l+2)\,(l+3)\,u_{k+3,h}+1/2\sum\limits_{l=0}^{k}\left(\begin{array}{l}\sum\limits_{s=0}^{h}(l+1) \\ (l+2) \\ (l+3)\,w_{l+3,h-s}\,(k+1-l)\,w_{1,s}\end{array}\right)\right) \\
-\frac{(-2v\delta+1)}{2}\left(\begin{array}{l}\sum\limits_{l=0}^{k}\sum\limits_{q=0}^{k-l}\sum\limits_{g=0}^{k-l-q}\sum\limits_{j=0}^{h}\sum\limits_{z=0}^{h-j}\sum\limits_{s=0}^{h-j-z}\begin{array}{l}(l+1)\,w_{l+1,h-j-z-s}\,(q+1) \\ w_{q+1,j}\,(g+1)\,P_{g+1,z}A_{k-l-q-g,s}\end{array} \\ +\sum\limits_{l=0}^{k}\sum\limits_{q=0}^{k-l}\sum\limits_{g=0}^{k-l-q}\sum\limits_{j=0}^{h}\sum\limits_{z=0}^{h-j}\sum\limits_{s=0}^{h-j-z}\begin{array}{l}(l+1)\,w_{l+1,h-j-z-s}\,(q+1) \\ w_{q+1,j}P_{g,z}\,(k+1-l-q-g)\,A_{k+1-l-q-g,s}\end{array}\end{array}\right) \\
+E\alpha\left(\sum\limits_{l=0}^{k}\left(\sum\limits_{s=0}^{h}(l+1)\,(l+2)\,(l+3)T_{l+3,h-s}A_{k-l,s}\right)+\sum\limits_{l=0}^{k}\left(\begin{array}{l}\sum\limits_{s=0}^{h}(l+1)\,(l+2) \\ (l+3)\,A_{l+3,h-s}T_{k-l,s}\end{array}\right)\right) \\
-E\alpha\sum\limits_{l=0}^{k}\sum\limits_{q=0}^{k-l}\sum\limits_{g=0}^{k-l-q}\sum\limits_{j=0}^{h}\sum\limits_{z=0}^{h-j}\sum\limits_{s=0}^{h-j-z}\begin{array}{l}(l+1)\,(l+2) \\ (l+3)\,(l+4)\,w_{l+4,h-j-z-s}\,(q+1)\,w_{q+1,j}T_{g,z} \\ (k+1-l-q-g)\,A_{k+1-l-q-g,s}\end{array} \\
-EI\left(\begin{array}{l}\sum\limits_{l=0}^{k}\left(\begin{array}{l}\sum\limits_{s=0}^{h}(l+1)\,(l+2)\,(l+3) \\ (l+4)\,(l+5)\,(l+6)\,w_{l+6,h-s}\,(k+1-l)\,w_{k-2l+1,s}\end{array}\right) \\ +\sum\limits_{l=0}^{k}\left(\begin{array}{l}\sum\limits_{s=0}^{h}(l+1)\,(l+2)\,(l+3) \\ (l+4)\,(l+5)\,w_{l+5,h-s}\,(k+1-l)\,(k+2-l)\,w_{k+2-l,s}\end{array}\right)\end{array}\right)
\end{array}\right) \\
=TDTMtr\left(F+e_0a\left(\nabla^2F\right)\right)=TDTMtr\left(\sum_{\zeta=1}^{7}c_\zeta\,(w-w_i)^{\zeta}+e_0a\left(\nabla^2\left[\sum_{\zeta=1}^{7}c_\zeta\,(w-w_i)^{\zeta}\right]\right)\right), \qquad (3.35)
\end{gathered}
$$

The transformed pressure model is;

$$
\begin{aligned}
&(h+1)\,P_{k,h+1}+\xi_1\sum_{l=0}^{k}\left(\sum_{s=0}^{h}(l+1)P_{l+1,h-s}d\,(k-l-1,s)\right)+\rho_f a^2\left(\xi_1 d\,(k,h)-2v\,(k+1)\,u_{k+1,h+1}\right)\\
&-2v\rho_f a^2\left(\sum_{l=0}^{k}\left(\sum_{s=0}^{h}(l+1)w_{l+1,h-s+1}\,(k+1-l)\,w_{k+1-l,s}\right)\right.\\
&+\xi_1\sum_{l=0}^{k}\left(\sum_{s=0}^{h}(l+1)\,(l+2)\,u_{l+2,h-s}d\,(k-l-1,s)\right)\\
&+\xi_1\sum_{l=0}^{k}\left(\sum_{q=0}^{k-l}\left(\sum_{z=0}^{h}\left(\sum_{s=0}^{h-z}(l+1)\,(l+2)\,w_{l+2,h-z-s}\,(q+1)\right)\right.\right.\\
&\left.\left.\left.\times w_{q+1,z}\,(k+1-l-q)\,d\,(k-1-l-q,s)\right)\right)\right)=0.
\end{aligned}
\tag{3.36}
$$

With transformed area model given as;

$$
\begin{aligned}
&(h+1)\,A_{N\,k,h+1}+\frac{vA_t^{\,3/2}\left((k+1)u_{k+1,h+1}+\sum\limits_{l=0}^{k}\left(\sum\limits_{s=0}^{h}(l+1)w_{l+1,h-s+1}(k+1-l)w_{k+1-l,s}\right)\right)}{\pi H}\\
&+e_0 a\left((k+1)\,(k+2)\,A_{N\,k+2,h+1}+\frac{vA_t^{\,3/2}\left((k+1)u_{k+1,h+1}+\sum\limits_{l=0}^{k}\left(\sum\limits_{s=0}^{h}(l+1)w_{l+1,h-s+1}(k+1-l)w_{k+1-l,s}\right)\right)}{\pi H}\right)=0.
\end{aligned}
\tag{3.37}
$$

The above transformed equations are recapitulated for different counter values and boundary conditions using MAPLE 16. The obtained analytical solutions are summarized as;

$$
\begin{aligned}
&w\,(z,t)=\sum_{k}^{N}\sum_{h=0}^{N}w_{k,h}z^k t^h \qquad k=h=0,1,2,3,4,5,...\\
&u\,(z,t)=\sum_{k}^{N}\sum_{h=0}^{N}u_{k,h}z^k t^h \qquad k=h=0,1,2,3,4,5,...\\
&P\,(z,t)=\sum_{k}^{N}\sum_{h=0}^{N}P_{k,h}z^k t^h \qquad k=h=0,1,2,3,4,5,...\\
&A\,(z,t)=\sum_{k}^{N}\sum_{h=0}^{N}A_{k,h}z^k t^h \qquad k=h=0,1,2,3,4,5,...
\end{aligned}
\tag{3.38}
$$

Which in expanded form becomes;

$$w_{z,t}=\left(\begin{array}{l}
azt^{7}+azt^{6}+azt^{5}+azt^{4}+azt^{3}+azt^{2}+bz^{3}t^{7}+bz^{3}t^{6}+bz^{3}t^{5}+bz^{3}t^{4}+bz^{3}t^{3}+bz^{3}t^{2}\\
-\frac{m\Gamma\xi_1\xi_3 az^{5}}{60}\left(IE+\frac{I{B_0}^{2}(\sin(\varphi))^{2}}{\mu_p}\right)^{-1}-\frac{\left(6ma+2\left(c+A_f\sigma {B_0}^{2}(\cos(\varphi))^{2}\right)a\right)z^{5}t}{120}\left(IE+\frac{I{B_0}^{2}(\sin(\varphi))^{2}}{\mu_p}\right)^{-1}\\
-\frac{z^{5}t^{2}}{120}\left(\begin{array}{l}12ma+3\left(c+A_f\sigma {B_0}^{2}(\cos(\varphi))^{2}\right)a-\\ 6\left(T_0-G-k_p-\frac{{B_0}^{2}(\cos(\varphi))^{2}}{\mu_p}\right)b+k_1a\end{array}\right)\left(IE+\frac{I{B_0}^{2}(\sin(\varphi))^{2}}{\mu_p}\right)^{-1}\\
-\frac{z^{5}t^{3}}{120}\left(\begin{array}{l}20ma+4\left(c+A_f\sigma {B_0}^{2}(\cos(\varphi))^{2}\right)a-\\ 6\left(T_0-G-k_p-\frac{{B_0}^{2}(\cos(\varphi))^{2}}{\mu_p}\right)b+k_1a\end{array}\right)\left(IE+\frac{I{B_0}^{2}(\sin(\varphi))^{2}}{\mu_p}\right)^{-1}\\
-\frac{z^{5}t^{4}}{120}\left(\begin{array}{l}30ma+5\left(c+A_f\sigma {B_0}^{2}(\cos(\varphi))^{2}\right)a-\\ 6\left(T_0-G-k_p-\frac{{B_0}^{2}(\cos(\varphi))^{2}}{\mu_p}\right)b+\\ 6\left(T_0-G\right)ba+k_1a\end{array}\right)\left(IE+\frac{I{B_0}^{2}(\sin(\varphi))^{2}}{\mu_p}\right)^{-1}\\
-\frac{z^{5}t^{5}}{120}\left(\begin{array}{l}42ma+6\left(c+A_f\sigma {B_0}^{2}(\cos(\varphi))^{2}\right)a-\\ 6\left(T_0-G-k_p-\frac{{B_0}^{2}(\cos(\varphi))^{2}}{\mu_p}\right)b+\\ 12\left(T_0-G\right)ba+k_1a\end{array}\right)\left(IE+\frac{I{B_0}^{2}(\sin(\varphi))^{2}}{\mu_p}\right)^{-1}\\
-\frac{z^{5}t^{6}}{120}\left(\begin{array}{l}56ma+7\left(c+A_f\sigma {B_0}^{2}(\cos(\varphi))^{2}\right)a-\\ 6\left(T_0-G-k_p-\frac{{B_0}^{2}(\cos(\varphi))^{2}}{\mu_p}\right)b+\\ \left(T_0-G\right)\left(9a^{2}b+18ab\right)+k_1a\end{array}\right)\left(iE+\frac{i{B_0}^{2}(\sin(\varphi))^{2}}{\mu_p}\right)^{-1}\\
-\frac{z^{5}t^{7}}{120}\left(\begin{array}{l}72ma+8\left(c+A_f\sigma {B_0}^{2}(\cos(\varphi))^{2}\right)a-\\ 6\left(T_0-G-k_p-\frac{{B_0}^{2}(\cos(\varphi))^{2}}{\mu_p}\right)b\end{array}\right)-\frac{(T_0-G)}{30}baz^{6}t^{4}\left(IE+\frac{I{B_0}^{2}(\sin(\varphi))^{2}}{\mu_p}\right)^{-1}\\
-\frac{1}{15}\left(T_0-G\right)baz^{6}t^{5}\left(IE+\frac{I{B_0}^{2}(\sin(\varphi))^{2}}{\mu_p}\right)^{-1}-\frac{1}{10}\left(T_0-G\right)baz^{6}t^{6}\left(IE+\frac{I{B_0}^{2}(\sin(\varphi))^{2}}{\mu_p}\right)^{-1}\\
-\frac{2}{15}\left(T_0-G\right)baz^{6}t^{7}\left(IE+\frac{I{B_0}^{2}(\sin(\varphi))^{2}}{\mu_p}\right)^{-1}
\end{array}\right)$$

$$+(e_0a)^2\left(\begin{array}{l}
-\frac{maz^5}{60}\left(IE+\frac{IB_0{}^2(\sin(\varphi))^2}{\mu_p}\right)^{-1}-\frac{\left(6ma+2\left(c+A_f\sigma B_0{}^2(\cos(\varphi))^2\right)a\right)z^5t}{120}\left(IE+\frac{IB_0{}^2(\sin(\varphi))^2}{\mu_p}\right)^{-1}\\
-\frac{z^5t^2}{120}\left(\begin{array}{l}12ma+3\left(c+A_f\sigma B_0{}^2(\cos(\varphi))^2\right)a-\\ 6\left(T_0-G-k_p-\frac{B_0{}^2(\cos(\varphi))^2}{\mu_p}\right)b+k_1a\end{array}\right)\left(IE+\frac{IB_0{}^2(\sin(\varphi))^2}{\mu_p}\right)^{-1}\\
-\frac{z^5t^3}{120}\left(\begin{array}{l}20ma+4\left(c+A_f\sigma B_0{}^2(\cos(\varphi))^2\right)a-\\ 6\left(T_0-G-k_p-\frac{B_0{}^2(\cos(\varphi))^2}{\mu_p}\right)b+k_1a\end{array}\right)\left(IE+\frac{IB_0{}^2(\sin(\varphi))^2}{\mu_p}\right)^{-1}\\
-\frac{z^5t^4}{120}\left(\begin{array}{l}30ma+5\left(c+A_f\sigma B_0{}^2(\cos(\varphi))^2\right)a-\\ 6\left(T_0-G-k_p-\frac{B_0{}^2(\cos(\varphi))^2}{\mu_p}\right)b+\\ 6\left(T_0-G\right)ba+k_1a\end{array}\right)\left(IE+\frac{IB_0{}^2(\sin(\varphi))^2}{\mu_p}\right)^{-1}\\
-\frac{z^5t^5}{120}\left(\begin{array}{l}42ma+6\left(c+A_f\sigma B_0{}^2(\cos(\varphi))^2\right)a-\\ 6\left(T_0-G-k_p-\frac{B_0{}^2(\cos(\varphi))^2}{\mu_p}\right)b+\\ 12\left(T_0-G\right)ba+k_1a\end{array}\right)\left(IE+\frac{IB_0{}^2(\sin(\varphi))^2}{\mu_p}\right)^{-1}\\
-\frac{z^5t^6}{120}\left(\begin{array}{l}56ma+7\left(c+A_f\sigma B_0{}^2(\cos(\varphi))^2\right)a-\\ 6\left(T_0-G-k_p-\frac{B_0{}^2(\cos(\varphi))^2}{\mu_p}\right)b+\\ \left(T_0-G\right)\left(9a^2b+18ab\right)+k_1a\end{array}\right)\left(iE+\frac{iB_0{}^2(\sin(\varphi))^2}{\mu_p}\right)^{-1}\\
-\frac{z^5t^7}{120}\left(\begin{array}{l}72ma+8\left(c+A_f\sigma B_0{}^2(\cos(\varphi))^2\right)a-\\ 6\left(T_0-G-k_p-\frac{B_0{}^2(\cos(\varphi))^2}{\mu_p}\right)b\end{array}\right)-\frac{(T_0-G)}{30}baz^6t^4\left(IE+\frac{IB_0{}^2(\sin(\varphi))^2}{\mu_p}\right)^{-1}\\
-\frac{1}{15}\left(T_0-G\right)baz^6t^5\left(iE+\frac{iB_0{}^2(\sin(\varphi))^2}{\mu_p}\right)^{-1}-\frac{1}{10}\left(T_0-G\right)baz^6t^6\left(IE+\frac{IB_0{}^2(\sin(\varphi))^2}{\mu_p}\right)^{-1}
\end{array}\right) \tag{3.39}$$

$$u_{z,t}=\left(\begin{array}{l}
azt^5+azt^4+azt^3+azt^2+bz^3t^5+bz^3t^4+bz^3t^3+bz^3t^2+1/24m_f\Gamma^2\xi_1\xi_3z^4\\
-\frac{1}{24}\left(EA_taz^4t^2+EA_taz^4t^3+EA_t\left(a+1/2a^2\right)z^4t^4\right)\\
-\frac{1}{24}EA_t\left(a^2+a\right)z^4t^5+\left(\frac{m_f(\Gamma)\xi_2}{120}+\frac{ma}{60}\right)z^5+\left(\frac{m_f\Gamma^2\xi_1\xi_3a}{60}+\frac{1}{20}ma\right)z^5t+\\
\left(\frac{1}{40}m_f\Gamma^2\xi_1\xi_3a-\frac{1}{20}EA_tb+\frac{1}{10}ma\right)z^5t^2\\
+\left(\frac{1}{30}m_f\Gamma^2\xi_1\xi_3a-\frac{1}{20}EA_tb+\frac{1}{6}ma\right)z^5t^3\\
+\left(\begin{array}{l}\frac{1}{4}ma+1/24m_f\Gamma^2\xi_1\xi_3a+\frac{1}{20}\left(T_0-G-EA_t\right)ba\\ -\frac{1}{20}EA_tb-\frac{EA_ta^2}{120}-\frac{3}{10}EIb^2\end{array}\right)z^5t^4\\
+\left(\begin{array}{l}\frac{7ma}{20}+\frac{1}{20}m_f\Gamma^2\xi_1\xi_3a+\frac{1}{10}\left(T_0-G-EA_t\right)ba\\ -\frac{1}{20}EA_tb-\frac{EA_ta^2}{60}-\frac{3}{5}EIb^2\end{array}\right)z^5t^5\\
-\frac{EA_tm_f\Gamma^2\xi_1\xi_3z^6}{720}+\left(\begin{array}{l}\frac{(T_0-G-EA_t)m_f\Gamma^2\xi_1\xi_3a}{720}\\ +\frac{EA_t{}^2a}{720}-\frac{EA_tb}{120}-\frac{1}{40}EIbm_f\Gamma^2\xi_1\xi_3\end{array}\right)z^6t^2\\
+\left(\frac{(T_0-G-EA_t)m_f\Gamma^2\xi_1\xi_3a}{720}+\frac{EA_t{}^2a}{720}-\frac{EA_tb}{120}-\frac{1}{40}EIbm_f\Gamma^2\xi_1\xi_3\right)z^6t^3\\
+\left(\begin{array}{l}\left(T_0-G-EA_t\right)\frac{\left(12ba-\frac{1}{2}EA_ta^2+\frac{1}{2}m_f\Gamma^2\xi_1\xi_3a\right)}{360}\\ +\frac{EA_t{}^2\left(a+\frac{1}{2}a^2\right)}{720}-\frac{EA_t\left(3b+\frac{3}{2}a^2+\frac{3}{2}ba\right)}{360}\\ -\frac{EI\left(9\Gamma^2bm_f\xi_1\xi_3-9EA_tab\right)}{360}\end{array}\right)z^6t^4\\
+\left(\begin{array}{l}\frac{(T_0-G-EA_t)\left(-EA_ta^2+24ba+\frac{1}{2}m_f\Gamma^2\xi_1\xi_3a\right)}{360}+\frac{EA_t{}^2\left(a^2+a\right)}{720}\\ -\frac{EA_t\left(3a^2+3ba+3b\right)}{360}-\frac{EI\left(9\Gamma^2bm_f\xi_1\xi_3-18EA_tab\right)}{360}\end{array}\right)z^6t^5
\end{array}\right.$$

$$
+(e_0 a)^2 \left(\begin{array}{l}
-\frac{1}{24} EA_t \left(a^2+a\right) z^4 t^5 + \left(\frac{m_f(\Gamma)\xi_2}{120} + \frac{ma}{60}\right) z^5 + \left(\frac{m_f \Gamma^2 \xi_1 \xi_3 a}{60} + \frac{1}{20} ma\right) z^5 t + \\
\left(\frac{1}{40} m_f \Gamma^2 \xi_1 \xi_3 a - \frac{1}{20} EA_t b + \frac{1}{10} ma\right) z^5 t^2 \\
+ \left(\frac{1}{30} m_f \Gamma^2 \xi_1 \xi_3 a - \frac{1}{20} EA_t b + 1/6 ma\right) z^5 t^3 \\
+ \left(\begin{array}{l} 1/4 ma + 1/24 m_f \Gamma^2 \xi_1 \xi_3 a + 1/20 \left(T_0 - G - EA_t\right) ba \\ -1/20 EA_t b - \frac{EA_t a^2}{120} - 3/10 EI b^2 \end{array} \right) z^5 t^4 \\
+ \left(\begin{array}{l} \frac{7ma}{20} + 1/20 m_f \Gamma^2 \xi_1 \xi_3 a + 1/10 \left(T_0 - G - EA_t\right) ba \\ -1/20 EA_t b - \frac{EA_t a^2}{60} - \\ 3/5 EI b^2 \end{array} \right) z^5 t^5 \\
-\frac{EA_t m_f \Gamma^2 \xi_1 \xi_3 z^6}{720} + \left(\begin{array}{l} \frac{(T_0-G-EA_t) m_f \Gamma^2 \xi_1 \xi_3 a}{720} \\ + \frac{{EA_t}^2 a}{720} - \frac{EA_t b}{120} - 1/40 EI b m_f \Gamma^2 \xi_1 \xi_3 \end{array} \right) z^6 t^2 \\
+ \left(\frac{(T_0-G-EA_t) m_f \Gamma^2 \xi_1 \xi_3 a}{720} + \frac{{EA_t}^2 a}{720} - \frac{EA_t b}{120} - 1/40 EI b m_f \Gamma^2 \xi_1 \xi_3 \right) z^6 t^3 \\
+ \left(\begin{array}{l} \left(T_0 - G - EA_t\right) \frac{\left(12ba - 1/2 EA_t a^2 + 1/2 m_f \Gamma^2 \xi_1 \xi_3 a\right)}{360} \\ + \frac{{EA_t}^2 \left(a + 1/2 a^2\right)}{720} - \frac{EA_t \left(3b + 3/2 a^2 + 3/2 ba\right)}{360} \\ - \frac{EI \left(9 \Gamma^2 b m_f \xi_1 \xi_3 - 9 EA_t ab\right)}{360} \end{array} \right) z^6 t^4 \\
+ \left(\begin{array}{l} \frac{(T_0-G-EA_t)\left(-EA_t a^2 + 24ba + 1/2 m_f \Gamma^2 \xi_1 \xi_3 a\right)}{360} + \frac{{EA_t}^2 \left(a^2 + a\right)}{720} \\ - \frac{EA_t \left(3a^2 + 3ba + 3b\right)}{360} - \frac{EI \left(9 \Gamma^2 b m_f \xi_1 \xi_3 - 18 EA_t ab\right)}{360} \end{array} \right) z^6 t^5,
\end{array} \right) \tag{3.40}
$$

$$
P_{z,t} = \left(\begin{array}{l}
ct^3 + ct^2 + P_{0,1} t + \xi_p - \frac{\left(a^2 \rho_f \xi_1 + P_{0,1}\right) z}{\xi_1} + 2 \frac{\left(a^3 \rho_f v - c\right) zt}{\xi_1} + \frac{\left(2a^3 \rho_f v - 3c\right) zt^2}{\xi_1} \\
+2 \frac{\left(a^4 \rho_f v + a^3 \rho_f v - 2c\right) zt^3}{\xi_1} - \frac{\left(a^3 \rho_f v - c\right) z^2}{{\xi_1}^2} - \frac{\left(2a^3 \rho_f v - 3c\right) z^2 t}{{\xi_1}^2} \\
-3 \frac{\left(a^4 \rho_f v + a^3 \rho_f v - 2c\right) z^2 t^2}{{\xi_1}^2} - 2 \frac{\left(4a^4 \rho_f v + 2a^3 \rho_f v - 5c\right) z^2 t^3}{{\xi_1}^2} \\
+ \frac{\left(2a^3 \rho_f v - 3c\right) z^3}{3{\xi_1}^3} + 2 \frac{\left(a^2 b \rho_f v {\xi_1}^2 + a^4 \rho_f v + a^3 \rho_f v - 2c\right) z^3 t}{{\xi_1}^3} \\
+2 \frac{\left(\begin{array}{l} a^2 b \rho_f v {\xi_1}^2 + 4a^4 \rho_f v + \\ 2a^3 \rho_f v - 5c \end{array} \right) z^3 t^2}{{\xi_1}^3} + 2 \frac{\left(\begin{array}{l} 6a^3 b \rho_f v {\xi_1}^2 + 3a^2 b \rho_f v {\xi_1}^2 + \\ 30a^4 \rho_f v + 10a^3 \rho_f v - 30c \end{array} \right) z^3 t^3}{3{\xi_1}^3} \\
- \frac{\left(\begin{array}{l} a^2 b \rho_f v {\xi_1}^2 + a^4 \rho_f v + \\ a^3 \rho_f v - 2c \end{array} \right) z^4}{2{\xi_1}^4} - \frac{\left(\begin{array}{l} -2a^2 \rho_f v {\xi_1}^3 u_{4,2} + a^2 b \rho_f v {\xi_1}^2 + \\ 4a^4 \rho_f v + 2a^3 \rho_f v - 5c \end{array} \right) z^4 t}{{\xi_1}^4} \\
- \frac{\left(6a^3 b \rho_f v {\xi_1}^2 - 4a^2 \rho_f v {\xi_1}^3 u_{4,3} + 3a^2 b \rho_f v {\xi_1}^2 + 30a^4 \rho_f v + 10a^3 \rho_f v - 30c\right) z^4 t^2}{2{\xi_1}^4} \\
- \frac{\left(\begin{array}{l} -4a^3 \rho_f v {\xi_1}^3 u_{4,2} + 8a^3 b \rho_f v {\xi_1}^2 \\ -2a^2 \rho_f v {\xi_1}^3 u_{4,4} + \\ 2a^2 b \rho_f v {\xi_1}^2 + 40a^4 \rho_f v \\ +10a^3 \rho_f v - 35c \end{array} \right) z^4 t^3}{{\xi_1}^4} + P_{5,3} z^5 t^3 + P_{5,2} z^5 t^2 + P_{5,1} z^5 t + \xi_p z^5 + \ldots
\end{array} \right), \tag{3.41}
$$

$$A_{N\,z,t} = \begin{pmatrix} et^3 + et^2 + \xi_A t + A_{N\,0,0} + gzt^3 + gzt^2 + \xi_A zt + A_{N\,1,0} z - \frac{\xi_A z^2}{2e_0 a} \\ - \frac{\left(A_t{}^{3/2} a^2 e_0 v + v A_t{}^{3/2} a + 2e\pi H\right) z^2 t}{2\pi H e_0 a} - \frac{\left(A_t{}^{3/2} a^2 e_0 v + v A_t{}^{3/2} a + 3e\pi H\right) z^2 t^2}{2\pi H e_0 a} \\ - \frac{\left(A_t{}^{3/2} a^2 e_0 v + v A_t{}^{3/2} a^2 + v A_t{}^{3/2} a + 4e\pi H\right) z^2 t^3}{2\pi H e_0 a} - \frac{\xi_A z^3}{6(e_0 a)} \\ - \frac{gz^3 t}{3e_0 a} - \frac{gz^3 t^2}{2e_0 a} - \frac{2gz^3 t^3}{3e_0 a} + \frac{\left(A_t{}^{3/2} a^2 e_0 v + v A_t{}^{3/2} a + 2e\pi H\right) z^4}{24\pi H e_0{}^2 a^2} \\ + \frac{\left(-3e_0{}^2 a^2 v A_t{}^{3/2} b + A_t{}^{3/2} a^2 e_0 v - 3e_0 a v A_t{}^{3/2} b + v A_t{}^{3/2} a + 3e\pi H\right) z^4 t}{12\pi H e_0{}^2 a^2} \\ + \frac{\left(-2e_0{}^2 a^2 v A_t{}^{3/2} b + A_t{}^{3/2} a^2 e_0 v - 2e_0 a v A_t{}^{3/2} b + v A_t{}^{3/2} a^2 + v A_t{}^{3/2} a + 4e\pi H\right) z^4 t^2}{8\pi H e_0{}^2 a^2} + \\ \frac{\begin{pmatrix} -3e_0{}^2 a^2 v A_t{}^{3/2} b - 6A_t{}^{3/2} a^2 e_0 v b + \\ 2A_t{}^{3/2} a^2 e_0 v - 3e_0 a v A_t{}^{3/2} b + \\ 4v A_t{}^{3/2} a^2 + 2v A_t{}^{3/2} a + 10e\pi H \end{pmatrix} z^4 t^3}{12\pi H e_0{}^2 a^2} + \frac{gz^5}{60 e_0{}^2 a^2} + \frac{\begin{pmatrix} -4e_0{}^2 a^2 v A_t{}^{3/2} u_{4,2} - \\ 4e_0 a v A_t{}^{3/2} u_{4,2} + g\pi H \end{pmatrix} z^5 t}{20\pi H e_0{}^2 a^2} \\ + \frac{\left(-2e_0{}^2 a^2 v A_t{}^{3/2} u_{4,3} - 2e_0 a v A_t{}^{3/2} u_{4,3} + g\pi H\right) z^5 t^2}{10\pi H e_0{}^2 a^2} \\ + \frac{\left(-6e_0{}^2 a^2 v A_t{}^{3/2} u_{4,4} - 12A_t{}^{3/2} a^2 e_0 v u_{4,2} - 6e_0 a v A_t{}^{3/2} u_{4,4} + 5g\pi H\right) z^5 t^3}{30\pi H e_0{}^2 a^2} \end{pmatrix}, \tag{3.42}$$

Where,

$$\xi_1 = \frac{1}{(r_b - r_a)} \begin{pmatrix} 4\frac{\beta_2 v (r_b - r_a)}{a_0{}^2(-\beta+1)} + \frac{8\beta_3 v\left(-r_a{}^3 + r_b{}^3\right)}{3a_0{}^4(-\beta+1)^2} + \\ \frac{2\left(MS\beta_2 - 2\beta_1\beta_3\lambda_2 + \beta_2{}^2\lambda_3 + 2S\beta_3 - 2\beta_3\lambda_1\right) v\left(-r_a{}^5 + r_b{}^5\right)}{5a_0{}^6(-\beta+1)^3\beta_{12}} + \\ \frac{2\begin{pmatrix} -MS\beta_1\beta_2\lambda_2 + 2\beta_1{}^2\beta_3\lambda_2{}^2 - \beta_1\beta_2{}^2\lambda_2\lambda_3 + \\ MS^2\beta_2 - MS\beta_2\lambda_1 + 2MS\beta_3\beta_{12} - 4S\beta_1\beta_3\lambda_2 + \\ S\beta_2{}^2\lambda_3 + 4\beta_1\beta_3\lambda_1\lambda_2 - \beta_2{}^2\lambda_1\lambda_3 - 2\beta_2\beta_3\beta_{12}\lambda_2 + \\ 4\beta_2\beta_3\beta_{12}\lambda_3 - MS\beta_2 + 2S^2\beta_3 - 4S\beta_3\lambda_1 + \\ 2\beta_1\beta_3\lambda_2 - \beta_2{}^2\lambda_3 + 2\beta_3\lambda_1{}^2 - 2S\beta_3 + 2\beta_3\lambda_1 \end{pmatrix} v\left(-r_a{}^7 + r_b{}^7\right)}{21a_0{}^8(-\beta+1)^4\beta_{12}{}^2} \\ \begin{pmatrix} MS\beta_1{}^2\beta_2\lambda_2{}^2 - 2\beta_1{}^3\beta_3\lambda_2{}^3 + \beta_1{}^2\beta_2{}^2\lambda_2{}^2\lambda_3 + \\ M^2S^2\beta_2\beta_{12} - 2MS^2\beta_1\beta_2\lambda_2 + 2MS\beta_1\beta_2\lambda_1\lambda_2 - \\ 4MS\beta_1\beta_3\beta_{12}\lambda_2 - 2MS\beta_2{}^2\beta_{12}\lambda_2 + 3MS\beta_2{}^2\beta_{12}\lambda_3 + \\ 6S\beta_1{}^2\beta_3\lambda_2{}^2 - 2S\beta_1\beta_2{}^2\lambda_2\lambda_3 - 6\beta_1{}^2\beta_3\lambda_1\lambda_2{}^2 + \\ 2\beta_1\beta_2{}^2\lambda_1\lambda_2\lambda_3 + 6\beta_1\beta_2\beta_3\beta_{12}\lambda_2{}^2 - 8\beta_1\beta_2\beta_3\beta_{12}\lambda_2\lambda_3 - \\ 2\beta_2{}^3\beta_{12}\lambda_2\lambda_3 + 2\beta_2{}^3\beta_{12}\lambda_3{}^2 + MS^3\beta_2 - \\ 2MS^2\beta_2\lambda_1 + 4MS^2\beta_3\beta_{12} + 3MS\beta_1\beta_2\lambda_2 + \\ MS\beta_2\lambda_1{}^2 - 4MS\beta_3\beta_{12}\lambda_1 - 6S^2\beta_1\beta_3\lambda_2 + S^2\beta_2{}^2\lambda_3 + \\ 12S\beta_1\beta_3\lambda_1\lambda_2 - 2S\beta_2{}^2\lambda_1\lambda_3 - 6S\beta_2\beta_3\beta_{12}\lambda_2 + \\ 8S\beta_2\beta_3\beta_{12}\lambda_3 - 6\beta_1{}^2\beta_3\lambda_2{}^2 + 3\beta_1\beta_2{}^2\lambda_2\lambda_3 - \\ 6\beta_1\beta_3\lambda_1{}^2\lambda_2 + \beta_2{}^2\lambda_1{}^2\lambda_3 + 6\beta_2\beta_3\beta_{12}\lambda_1\lambda_2 - \\ 8\beta_2\beta_3\beta_{12}\lambda_1\lambda_3 - 4\beta_3{}^2\beta_{12}{}^2\lambda_2 + 8\beta_3{}^2\beta_{12}{}^2\lambda_3 - \\ 3MS^2\beta_2 + 3MS\beta_2\lambda_1 - 4MS\beta_3\beta_{12} + 2S^3\beta_3 - \\ 6S^2\beta_3\lambda_1 + 12S\beta_1\beta_3\lambda_2 - 3S\beta_2{}^2\lambda_3 + 6S\beta_3\lambda_1{}^2 - \\ 12\beta_1\beta_3\lambda_1\lambda_2 + 3\beta_2{}^2\lambda_1\lambda_3 + 4\beta_2\beta_3\beta_{12}\lambda_2 - \\ 8\beta_2\beta_3\beta_{12}\lambda_3 - 2\beta_3\lambda_1{}^3 + 2MS\beta_2 - \\ 6S^2\beta_3 + 12S\beta_3\lambda_1 - 4\beta_1\beta_3\lambda_2 + \\ 2\beta_2{}^2\lambda_3 - 6\beta_3\lambda_1{}^2 + 4S\beta_3 - 4\beta_3\lambda_1 \end{pmatrix} \frac{v\left(-r_a{}^9 + r_b{}^9\right)}{54a_0{}^{10}(-\beta+1)^5\beta_{12}{}^3} \end{pmatrix}, \tag{3.43}$$

and,

$$
\xi_3 = \left(\begin{array}{l}
\beta_4 \left(r_b - r_a \right) + \frac{\beta_5 \left(-{r_a}^3 + {r_b}^3 \right)}{3{a_0}^2(-\beta+1)} - \frac{\beta_5 \left(\mathrm{Pr}\,\beta_1 + \lambda_4 \right)\left(-{r_a}^5 + {r_b}^5 \right)}{10{a_0}^4(-\beta+1)^2\beta_{12}} \\
- \frac{\beta_5 \left(\begin{array}{l} -\overset{2}{\mathrm{Pr}}\,{\beta_1}^2 + N\beta_5\beta_{12} - \mathrm{Pr}\,S\beta_{12} - 2\,\mathrm{Pr}\,\beta_1\lambda_4 \\ +\mathrm{Pr}\,\beta_2\beta_{12} - \mathrm{Pr}\,\beta_1 - {\lambda_4}^2 - \lambda_4 \end{array} \right)\left(-{r_a}^7 + {r_b}^7 \right)}{42{a_0}^6(-\beta+1)^3{\beta_{12}}^2} \\
\frac{\beta_5 \left(-{r_a}^9 + {r_b}^9 \right)}{216{a_0}^8(-\beta+1)^4{\beta_{12}}^3} \left(\begin{array}{l}
-\overset{3}{\mathrm{Pr}}\,{\beta_1}^3 + 5N\,\mathrm{Pr}\,\beta_1\beta_5\beta_{12} - 3\,\overset{2}{\mathrm{Pr}}\,S\beta_1\beta_{12} \\
-3\,\overset{2}{\mathrm{Pr}}\,{\beta_1}^2\lambda_4 + 3\,\overset{2}{\mathrm{Pr}}\,\beta_1\beta_2\beta_{12} \\
+5N\beta_5\beta_{12}\lambda_4 - 3\,\overset{2}{\mathrm{Pr}}\,{\beta_1}^2 - 3\,\mathrm{Pr}\,S\beta_{12}\lambda_4 \\
-3\,\mathrm{Pr}\,\beta_1{\lambda_4}^2 + 3\,\mathrm{Pr}\,\beta_2\beta_{12}\lambda_4 \\
-2\,\mathrm{Pr}\,\beta_3{\beta_{12}}^2 + 2N\beta_5\beta_{12} - 2\,\mathrm{Pr}\,S\beta_{12} - \\
6\,\mathrm{Pr}\,\beta_1\lambda_4 + 2\,\mathrm{Pr}\,\beta_2\beta_{12} - {\lambda_4}^3 - 2\,\mathrm{Pr}\,\beta_1 - 3{\lambda_4}^2 - 2\lambda_4
\end{array} \right) \\
- \frac{\beta_5 \left(-{r_a}^{11} + {r_b}^{11} \right)}{1320{a_0}^{10}(-\beta+1)^5{\beta_{12}}^4} \left(\begin{array}{l}
-\overset{4}{\mathrm{Pr}}\,{\beta_1}^4 + 17N\,\overset{2}{\mathrm{Pr}}\,{\beta_1}^2\beta_5\beta_{12} - 6\,\overset{3}{\mathrm{Pr}}\,S{\beta_1}^2\beta_{12} \\
-4\,\overset{3}{\mathrm{Pr}}\,{\beta_1}^3\lambda_4 + 6\,\overset{3}{\mathrm{Pr}}\,{\beta_1}^2\beta_2\beta_{12} \\
+M\,\mathrm{Pr}\,S\beta_2{\beta_{12}}^2 - 6N^2{\beta_5}^2{\beta_{12}}^2 + \\
9N\,\mathrm{Pr}\,S\beta_5{\beta_{12}}^2 + 34N\,\mathrm{Pr}\,\beta_1\beta_5\beta_{12}\lambda_4 \\
-9N\,\mathrm{Pr}\,\beta_2\beta_5{\beta_{12}}^2 - 6\,\overset{3}{\mathrm{Pr}}\,{\beta_1}^3 - 3\,\overset{2}{\mathrm{Pr}}\,S^2{\beta_{12}}^2 - \\
12\,\overset{2}{\mathrm{Pr}}\,S\beta_1\beta_{12}\lambda_4 + 6\,\overset{2}{\mathrm{Pr}}\,S\beta_2{\beta_{12}}^2 \\
-6\,\overset{2}{\mathrm{Pr}}\,{\beta_1}^2{\lambda_4}^2 + 12\,\overset{2}{\mathrm{Pr}}\,\beta_1\beta_2\beta_{12}\lambda_4 - \\
8\,\overset{2}{\mathrm{Pr}}\,\beta_1\beta_3{\beta_{12}}^2 - 3\,\overset{2}{\mathrm{Pr}}\,{\beta_2}^2{\beta_{12}}^2 - 2\,\mathrm{Pr}\,\beta_1\beta_3{\beta_{12}}^2\lambda_2 \\
+\mathrm{Pr}\,{\beta_2}^2{\beta_{12}}^2\lambda_3 + 23N\,\mathrm{Pr}\,\beta_1\beta_5\beta_{12} \\
+17N\beta_5\beta_{12}{\lambda_4}^2 - 14\,\overset{2}{\mathrm{Pr}}\,S\beta_1\beta_{12} - 18\,\overset{2}{\mathrm{Pr}}\,{\beta_1}^2\lambda_4 \\
+14\,\overset{2}{\mathrm{Pr}}\,\beta_1\beta_2\beta_{12} + 2\,\mathrm{Pr}\,S\beta_3{\beta_{12}}^2 - 6\,\mathrm{Pr}\,S\beta_{12}{\lambda_4}^2 \\
-4\,\mathrm{Pr}\,\beta_1{\lambda_4}^3 + 6\,\mathrm{Pr}\,\beta_2\beta_{12}{\lambda_4}^2 - 2\,\mathrm{Pr}\,\beta_3{\beta_{12}}^2\lambda_1 \\
-8\,\mathrm{Pr}\,\beta_3{\beta_{12}}^2\lambda_4 + 23N\beta_5\beta_{12}\lambda_4 - 11\,\overset{2}{\mathrm{Pr}}\,{\beta_1}^2 \\
-14\,\mathrm{Pr}\,S\beta_{12}\lambda_4 - 18\,\mathrm{Pr}\,\beta_1{\lambda_4}^2 + 14\,\mathrm{Pr}\,\beta_2\beta_{12}\lambda_4 \\
-6\,\mathrm{Pr}\,\beta_3{\beta_{12}}^2 - {\lambda_4}^4 + 6N\beta_5\beta_{12} - 6\,\mathrm{Pr}\,S\beta_{12} \\
-22\,\mathrm{Pr}\,\beta_1\lambda_4 + 6\,\mathrm{Pr}\,\beta_2\beta_{12} - 6{\lambda_4}^3 - 6\,\mathrm{Pr}\,\beta_1 - 11{\lambda_4}^2 - 6\lambda_4
\end{array} \right)
\end{array} \right). \tag{3.44}
$$

These analytical solutions are treated using after treatment technique and then used to carry out the parametric study. The fundamental frequency is attained by generating sets of equations using the natural boundary conditions derived from Hamilton's principle. The equations are put in the form described in Equation (3.45);

$$\begin{bmatrix} \Gamma_{11}\left(\omega, \beta, \psi, e_0a, Ha, z, k, EI, ...\right) & \Gamma_{12}\left(\omega, \beta, \psi, e_0a, Ha, z, k, EI, ...\right) \\ \Gamma_{21}\left(\omega, \beta, \psi, e_0a, Ha, z, k, EI, ...\right) & \Gamma_{22}\left(\omega, \beta, \psi, e_0a, Ha, z, k, EI, ...\right) \end{bmatrix} \begin{bmatrix} \Lambda_1 \\ \Lambda_2 \end{bmatrix} = \begin{bmatrix} F_1^{BC} \\ F_2^{BC} \end{bmatrix}, \tag{3.45}$$

Conditioning the determinant of the stability matrix to varnish, the characteristic equation is obtained. This equation is used to obtain the eigen values of the system under investigation.

4. RESULTS AND DISCUSSION

4.1. **The Present Study's Verifications and Validations.** The section presents firstly validations for the novel thermal-fluidic induced nonlinear vibrations models. This will be accomplished by means of experimental validation as well as comparison with results from previous studies. A checklist is presented and used to establish the novelty in the present work Sections 4.1.1-4.1.2. Subsequently, using the developed MATLAB and MAPLE codes, parametric studies and sensitivity analysis are performed. Then, thermal-fluidic results as well as their impacts on MWCNT temperature variation, deformation, flow pressure and transverse and longitudinal dynamic responses are presented, analyzed and discussed Sections 4.1.3-4.1.15.

4.1.1. *Verification of the present study with Belhadj et al. (2017).* The dimensional fundamental frequency models in this study are reduced and used to recover that of Belhadj et al. [6] nanotube model with excellent agreements established as enumerated in Table 3, Table 4, Table 5, Table 6 and Table 7:

Table 3. Comparison of the present study with the exact solution of Belhadj et al. (2017) for pinned-pinned condition.

Mode 1
Frequency of the Single-walled carbon nanotube (THz)

Length (nm)	Belhadj et al. (2017)	Present Study
1	0.300	0.300
2	0.211	0.209
3	0.206	0.204
4	0.202	0.202
5	0.201	0.200

Table 4. Comparison of the present study with exact solution of Belhadj et al. (2017) for pinned - pinned condition.

Mode 2
Frequency of the Single-walled carbon nanotube (THz)

Length (nm)	Belhadj et al. (2017)	Present Study
1	1.000	1.000
2	0.612	0.614
3	0.409	0.407
4	0.304	0.302
5	0.200	0.200

Table 5. Comparison of the present study with exact solution of Belhadj et al. (2017) for pinned - pinned condition.

Mode 3
Frequency of the Single-walled carbon nanotube (THz)

Length (nm)	Belhadj et al. (2017)	Present Study
1	2.500	2.500
2	1.603	1.601
3	0.707	0.703
4	0.515	0.513
5	0.200	0.200

Table 6. Comparison of the present study with exact solution of Belhadj et al. (2017) for pinned - pinned condition.

Mode 4
Frequency of the Single-walled carbon nanotube (THz)

Length (nm)	Belhadj et al. (2017)	Present Study
1	-	4.000
2	-	2.501
3	-	0.912
4	-	0.603
5	-	0.200

Table 7. Comparison of the present study with exact solution of Belhadj et al. (2017) for pinned - pinned condition.

Mode 5
Frequency of the Single-walled carbon nanotube (THz)

Length (nm)	Belhadj et al. (2017)	Present Study
1	-	5.000
2	-	4.511
3	-	1.010
4	-	0.821
5	-	0.200

Table 8. Validation table using the Work of Filiz and Aydogdu (2010).

Frequency Parameter

Mode	Filiz and Aydogdu (2010)	Present Study	Percentage error (%)
1	3.132	3.133	0.03192848
2	6.245	6.246	0.01601281
3	9.331	9.333	0.02143393

4.1.2. *Validation using the Work of Filiz and Aydogdu (2010).* On reducing model in the present study to recover that of an axial vibration of carbon nanotube using nonlocal elasticity, the Filiz and Aydogdu [14] SWCNT model is recovered. The obtained relationship for the SWCNT amplitude and length as well as frequency parameters and mode numbers are then used for validation as depicted in Figure 2 and Table 8 respectively.

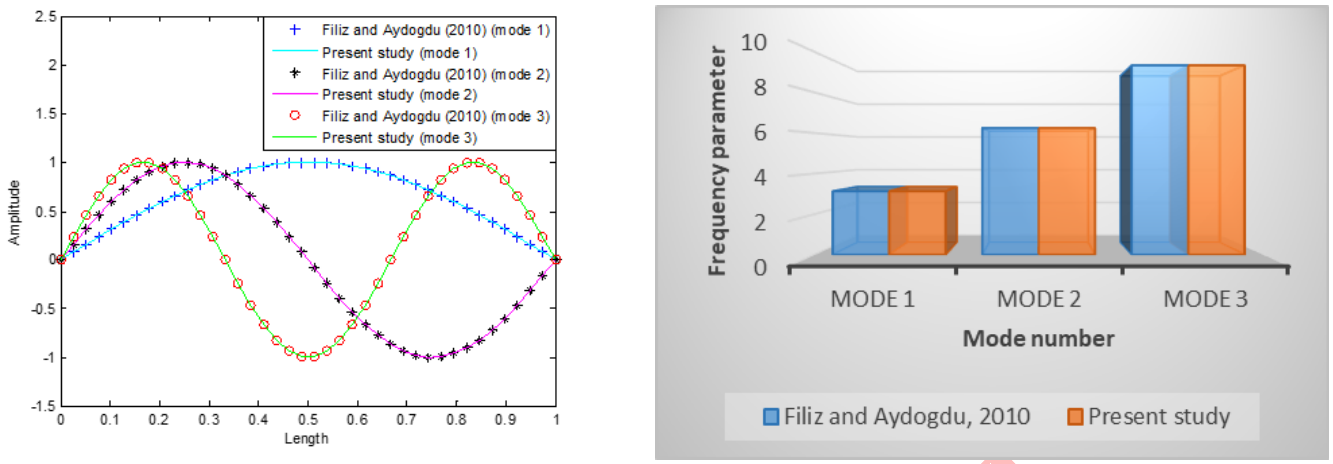

*(a) *(b)

FIGURE 2. Validation using the Work of Filiz and Aydogdu (2010).

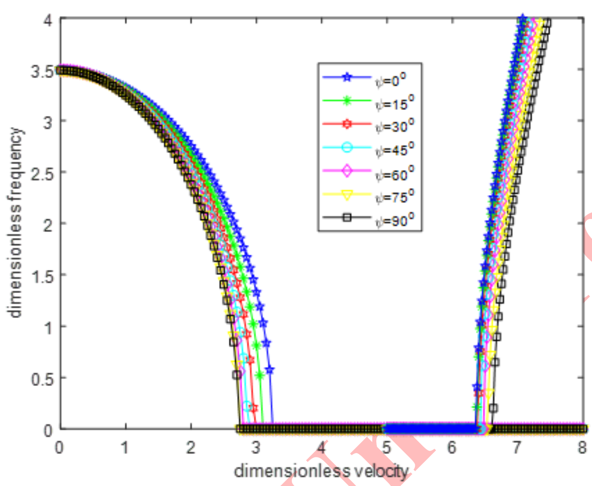

FIGURE 3. Influence of junction angle on MWCNT's stability for linear pre- and post-bifurcation.

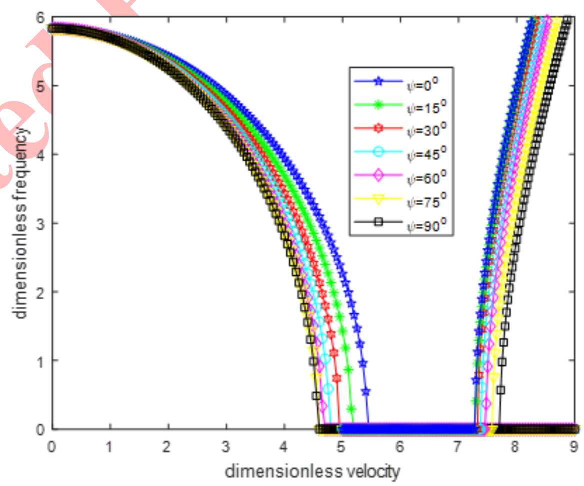

FIGURE 4. Influence of junction angle on MWCNT's stability for Nonlinear pre- and post-bifurcation

4.1.3. ***Influence of Junction angle and Mass Ratio on Stability of the MWCNT***. Figure 3 and Figure 4 portray the impacts of junction angles on nanotubes' stability curve. The desired stability parts of the plots are the parabolic sections which continue to reduce with increasing velocity of flow. These regions denote stable domains. The critical flow velocity ranges for linear and nonlinear stability analyses are 2.69 to 3.18 and 4.17 to 5.17 respectively. From the plots, it is evident that nonlinear analysis provides better stability as it provides shorter bifurcation and regains stability faster before finally passing through the divergence of flutter. Meanwhile, Figure 5 and Figure 6 describe the impacts of mass ratio on both the imaginary and real parts of the nonlinear dimensionless frequency. These effects are better felt for the higher velocity of flow through the tubes. Figure 5 shows how an increase in

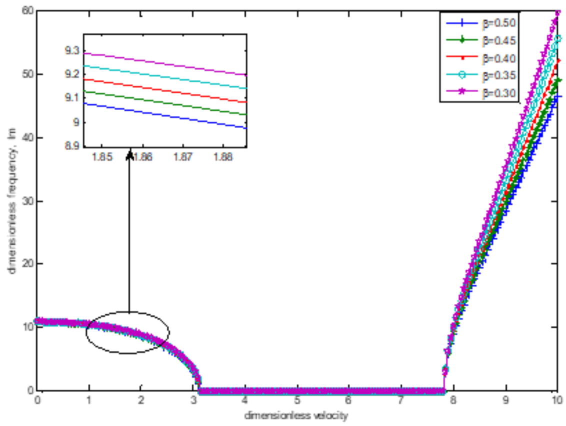

FIGURE 5. Effect of mass ratio on MWCNT stability.

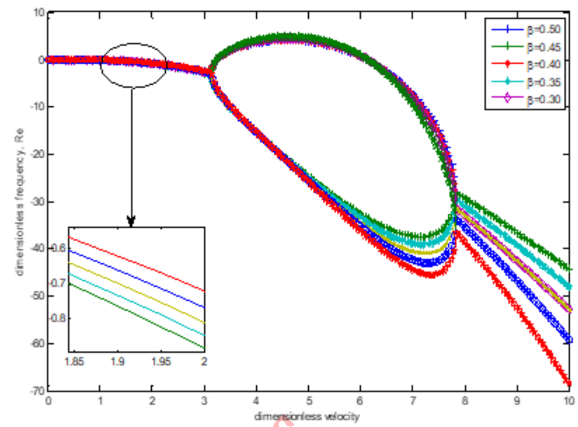

FIGURE 6. Influence of mass ratio on nanotubes' damping.

mass ratio reduces the system's stability while Figure 6 symbolizes the required damping for stability. The established critical value for mass ratio is 0.40 as its continuous augmentation gives synonymous effects when it is lower than 0.40.

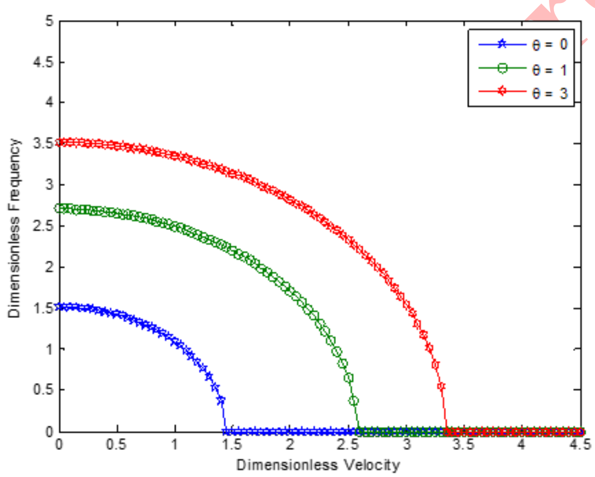

FIGURE 7. Effect of temperature change on the stability of the MWCNT for linear Winkler foundation and without magnetic effect.

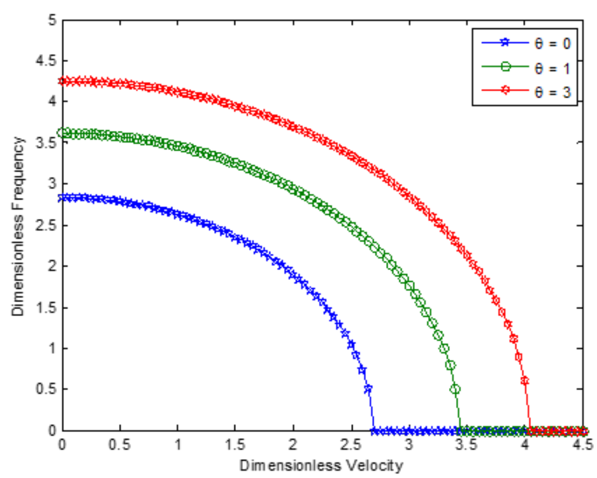

FIGURE 8. Effect of temperature change on the stability of the MWCNT for Nonlinear Winkler foundation and without magnetic effect.

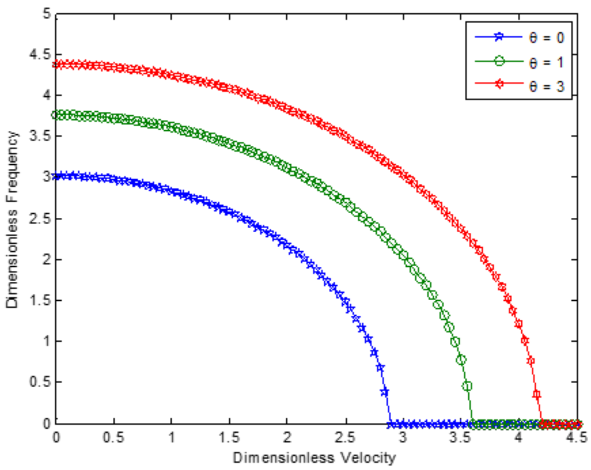

FIGURE 9. Effect of temperature change on the stability of the MWCNT for linear Pasternak foundation and without magnetic effect.

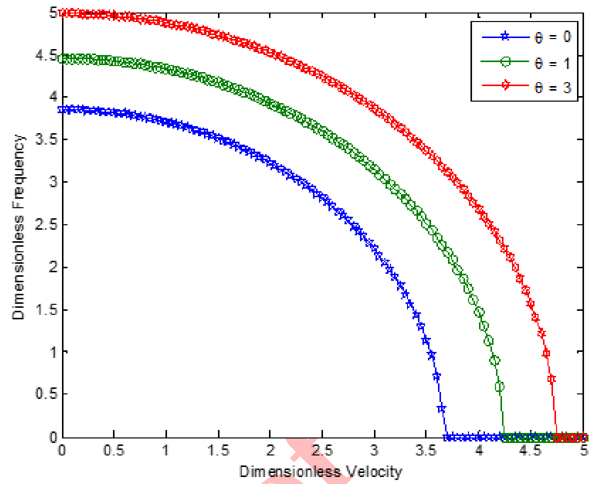

FIGURE 10. Effect of temperature change on the stability of the MWCNT for Nonlinear Pasternak foundation and without magnetic effect.

4.1.4. *Influence of Temperature Change on Stability of the MWCNT without Magnetic Effect.*

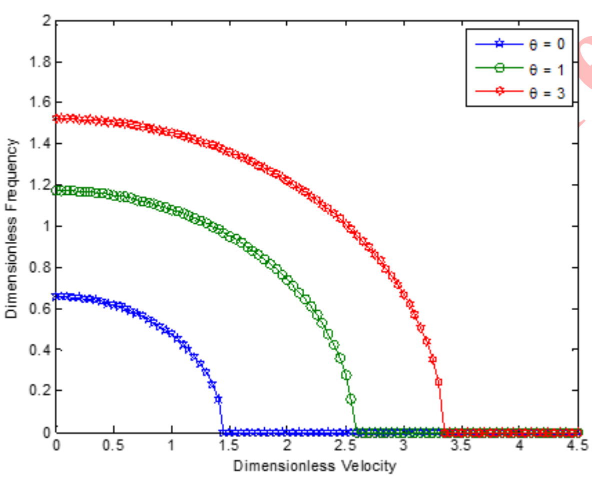

FIGURE 11. Effect of temperature change on the stability of the MWCNT for linear Winkler foundation and with magnetic effect.

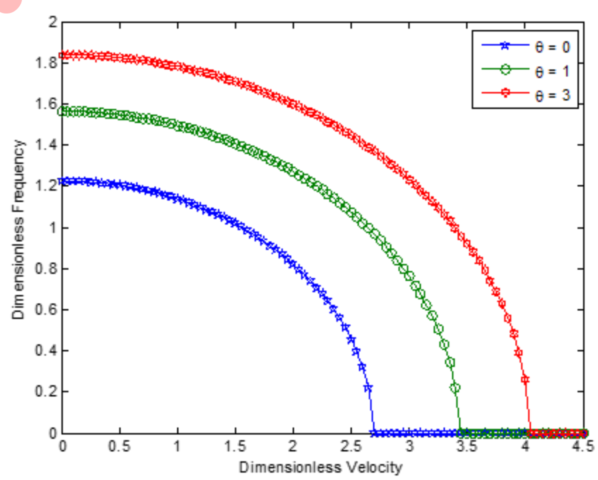

FIGURE 12. Effect of temperature change on the stability of the MWCNT for Nonlinear Winkler foundation and with magnetic effect.

4.1.5. *Influence of Temperature Change on Stability of the MWCNT with Magnetic Effect.* Figures 7-14 depict the influences of temperature change on the dimensionless frequency of the MWCNT embedded in Winkler and Pasternak

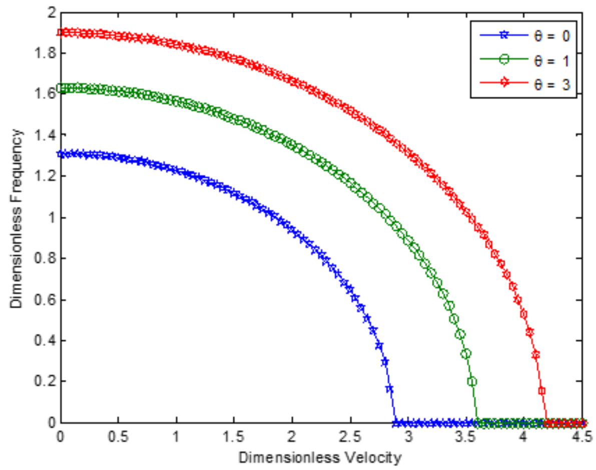

FIGURE 13. Effect of temperature change on the stability of the MWCNT for linear Pasternak foundation and with magnetic effect.

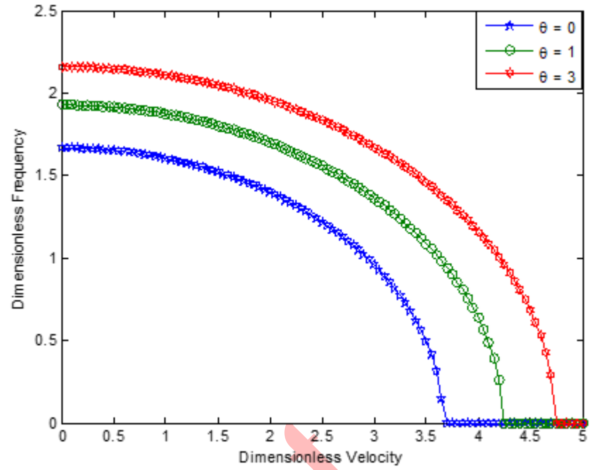

FIGURE 14. Effect of temperature change on the stability of the MWCNT for Nonlinear Pasternak foundation and with magnetic effect.

foundations with and without magnetic effect. It is observed that the dimensionless frequency and dimensionless velocity increases with increasing temperature change. When the magnetic effect is considered, the stability of the CNT increases because the dimensionless frequency of the system reduces for the same flow velocity range as that of when there is no magnetic effect.

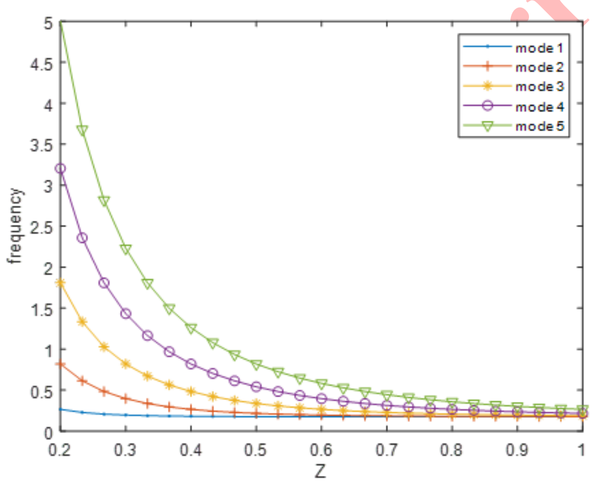

FIGURE 15. Effect of modal number on the frequency of the MWCNT.

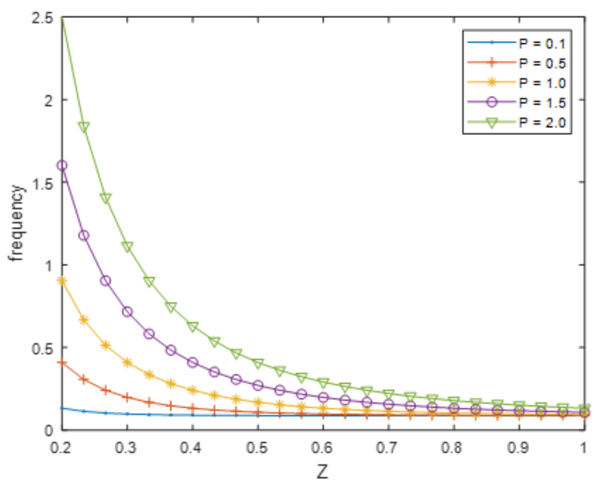

FIGURE 16. Effect of pressure on the frequency of the MWCNT.

4.1.6. *Effects of Modal Number, Pressure, Foundation and Mass Ratio on Frequency of the MWCNT.* Figures 15–16 depict the influence of modal number and flow pressure on the frequency of the MWCNT. A careful study helps visualizes the effect of these two important parameters on stability of the CNT. The frequency of CNT which is a vital parameter in stability study reaches some THz when dimensionalized and continues to increase as the modal number increases. This astonishing property enables CNT to offer an exceptional optical and mechanical properties although there is always need to dampen the frequency to an application limit. Furthermore, a synonymous effect is realized as the induced pressure by the fluid increases. These two parameters as a result of their tremendous effects on frequency may be used to annul the effect of mass ration when one of them is desired based on the requirement of the engineering design and applications.

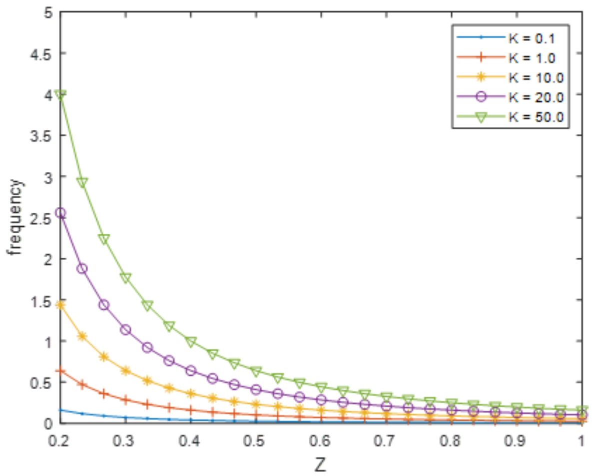

FIGURE 17. Effect of foundation parameter on the frequency of the MWCNT.

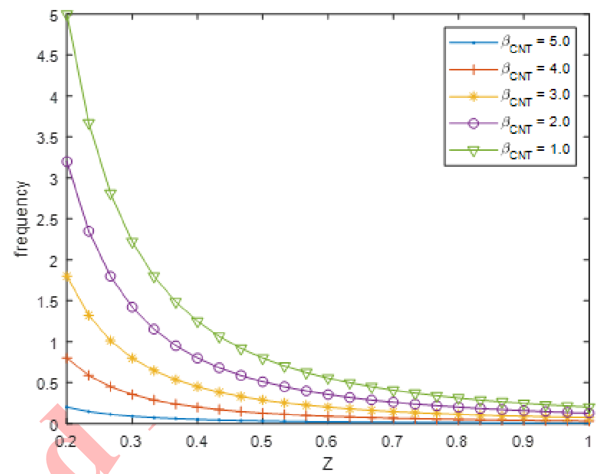

FIGURE 18. Effect of mass on the frequency of the MWCNT.

Figures 17–18 depict the impact of foundation variable and mass on the excitation frequency of the CNT.

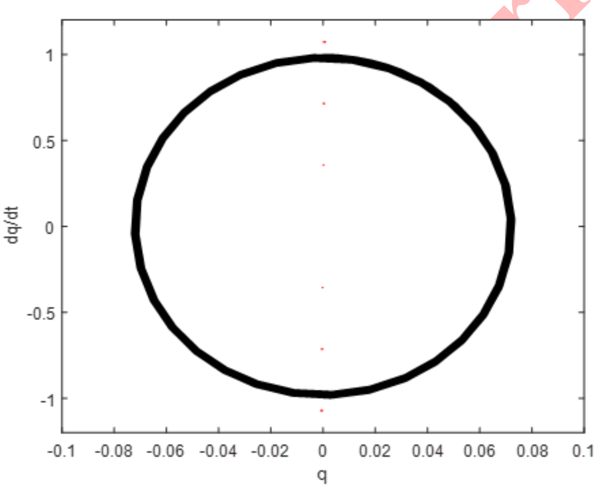

FIGURE 19. Phase-plane plot for linear vibration.

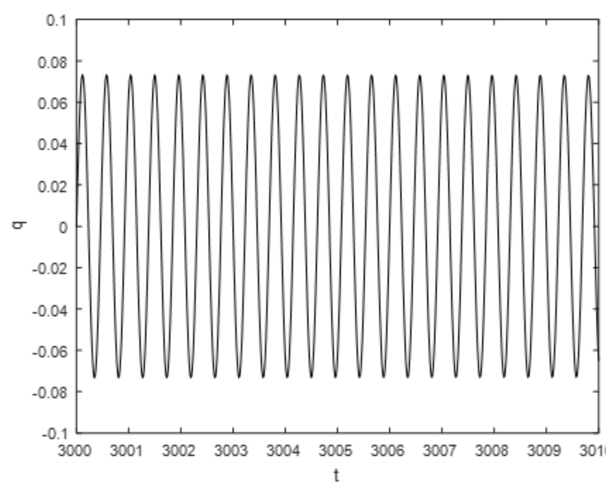

FIGURE 20. Linear vibration history.

From the plots, it is obvious that an increase in foundation variable or parameter as well as a reduction in the mass of the carbon nanotube increases its frequency. For both parameters, extreme values should be avoided to prevent

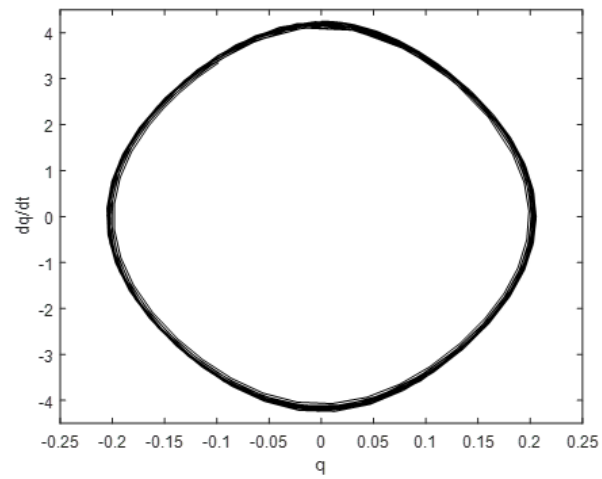

FIGURE 21. Phase-plane plot for nonlinear vibration.

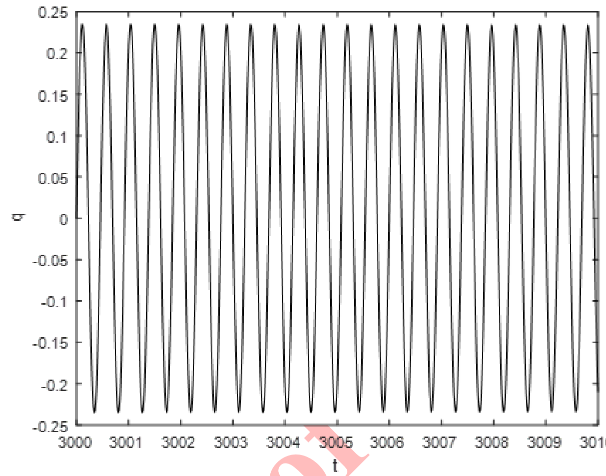

FIGURE 22. . Nonlinear vibration history.

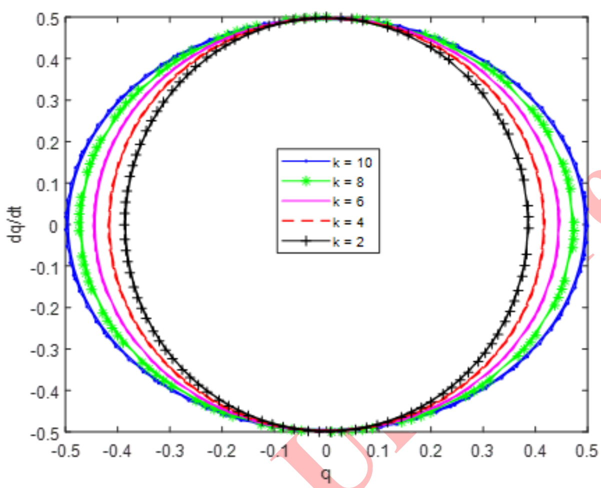

FIGURE 23. Foundation effect for B = 0.

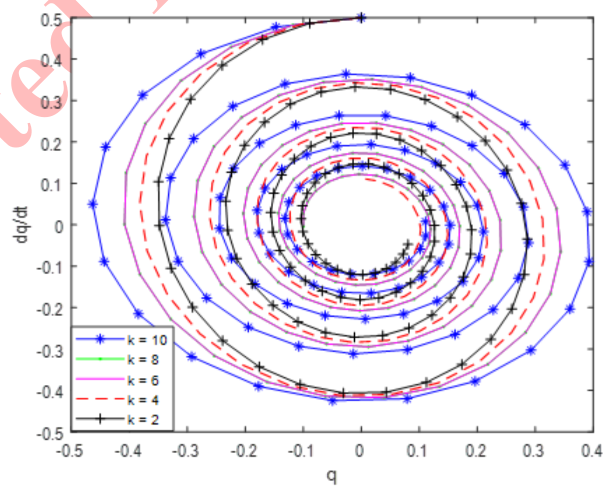

FIGURE 24. Foundation effect for B = 10.

instability for very low values of the foundation parameter and over excitation or resonance for very high values. Moderate and intelligent choice of the mass of the CNT may also be used to annul the above-mentioned effects. The corresponding phase plane plots for qualitative stability analyses are presented in Figures 19–30.

4.1.7. *Impact of Plug and Fully Coupled Flow Induced Vibration on Transverse Response of the MWCNT..*

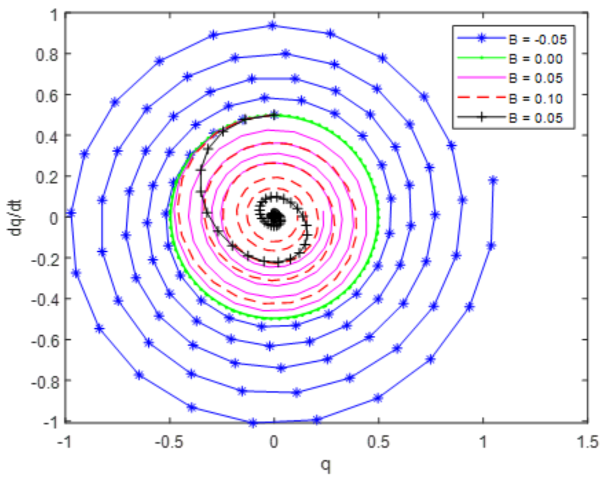

FIGURE 25. Phase-plane with small negative damping.

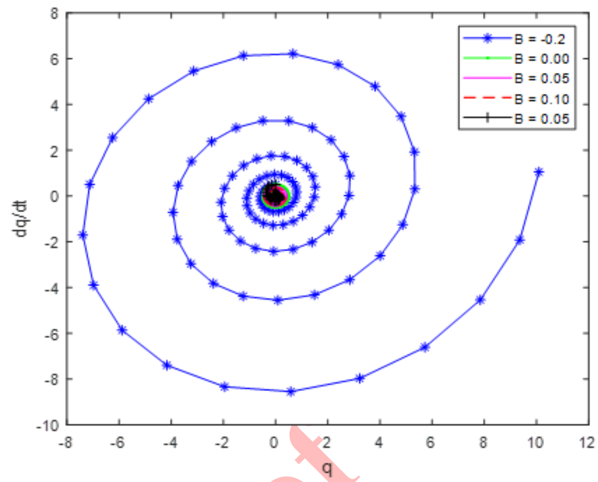

FIGURE 26. Phase-plane with large negative damping.

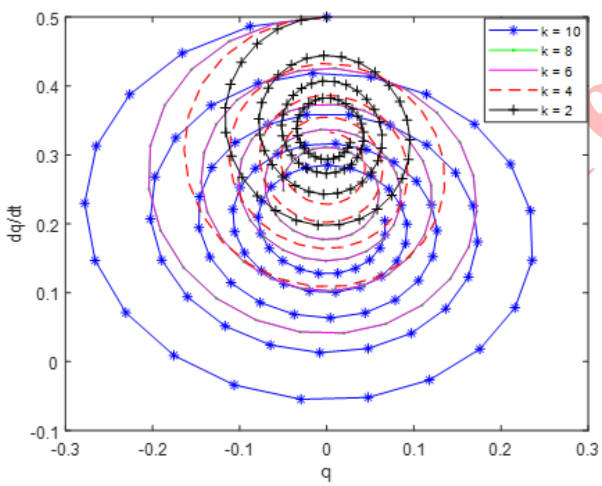

FIGURE 27. Foundation effect on forced vibration with damping.

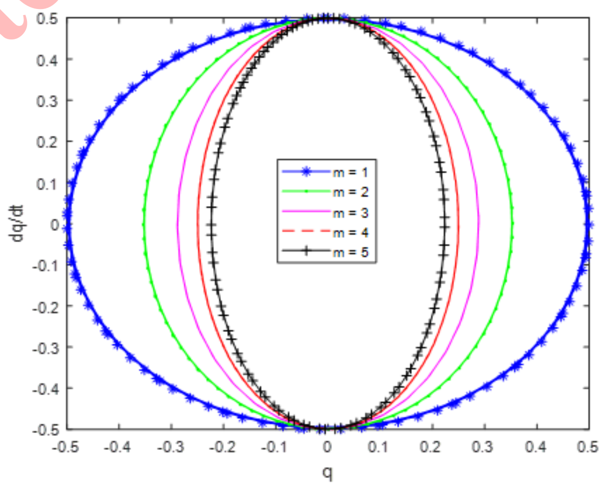

FIGURE 28. Mass effect on MWCNT stability.

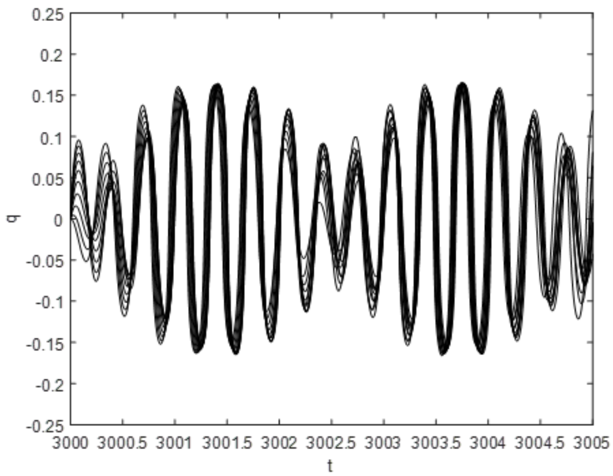

FIGURE 29. Beat phenomenon with magnetic effect.

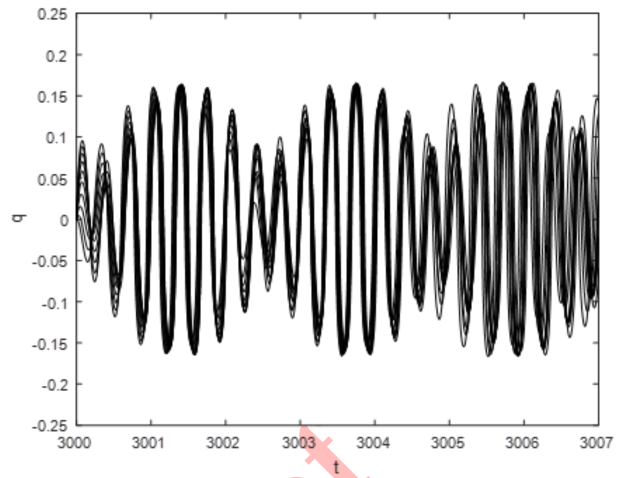

FIGURE 30. Beat phenomenon without magnetic effect.

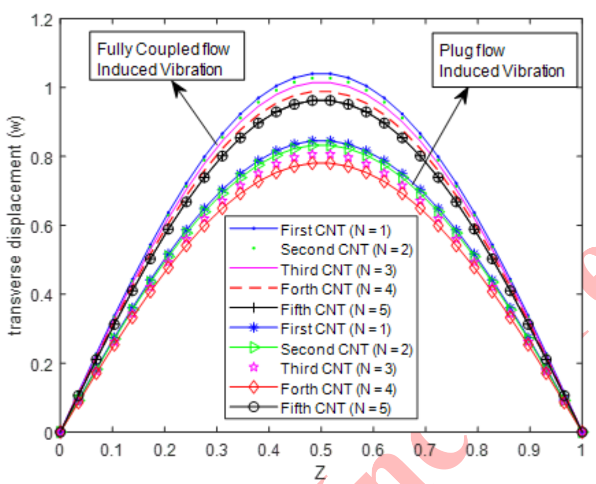

FIGURE 31. For pinned-pinned support.

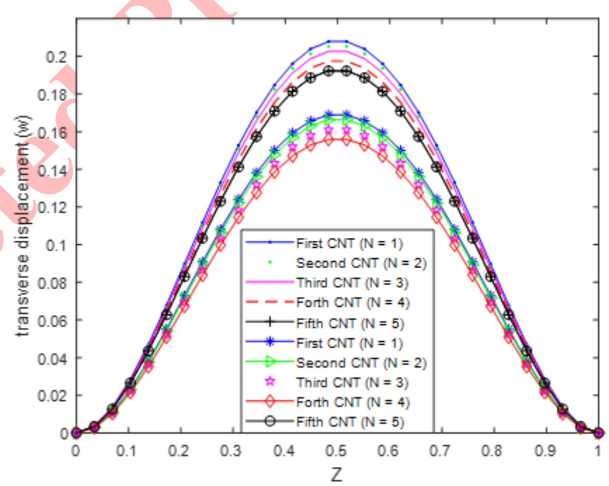

FIGURE 32. For clamped-clamped support.

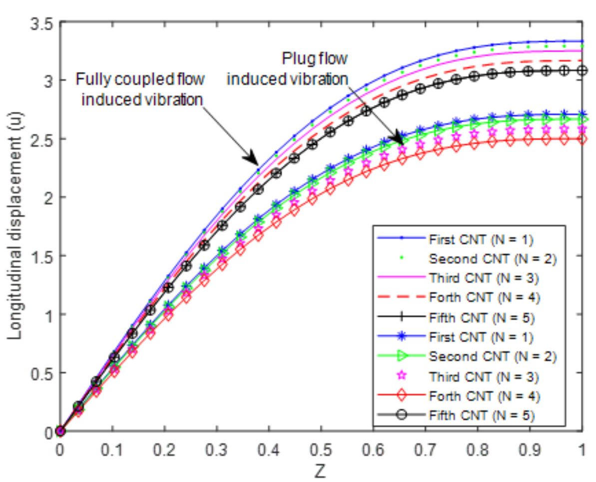

FIGURE 35. For pinned support.

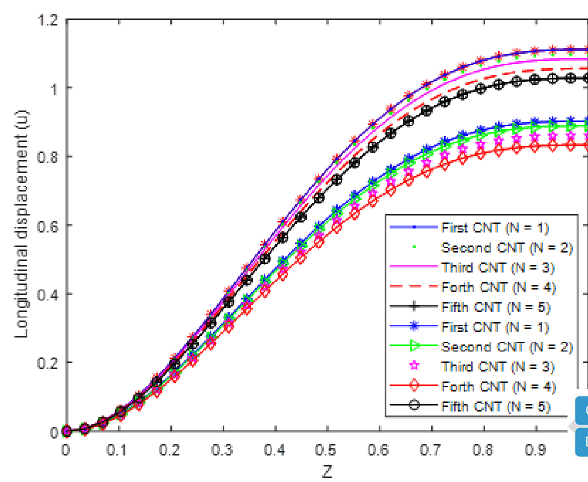

FIGURE 36. For clamped support.

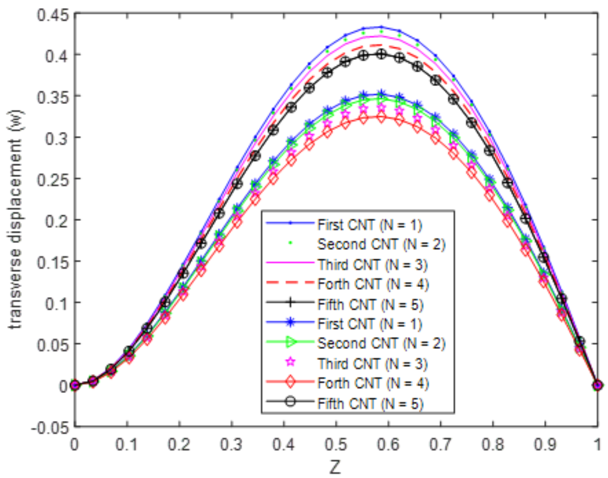

FIGURE 33. For clamped-pinned support.

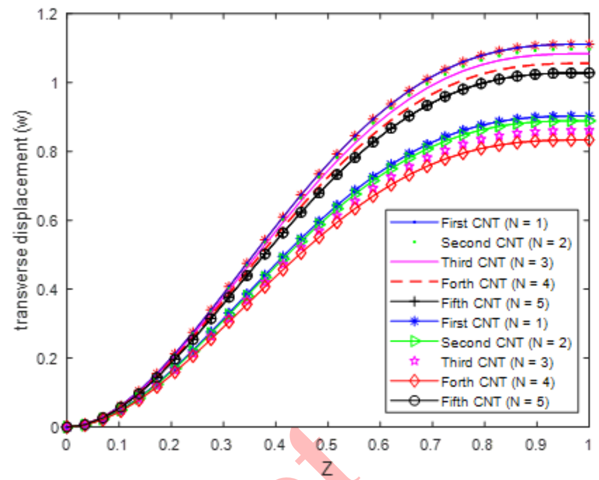

FIGURE 34. For clamped-free support.

4.1.8. ***Impact of Plug and Fully Coupled Flow Induced Vibration on Longitudinal Response of the MWCNT***. Figures 31–36 depict the impact of plug and fully coupled flow induced vibration on steady state response of the MWCNT for different boundary conditions. The clamped-free support gives the highest steady state response while clamped-clamped gives the least. In design and practical applications, the plug flow assumption should be discouraged as it deviates from actual working processes by over 11 percent. This leads to under design and consequently system's failure when in contact with real flow dynamics.

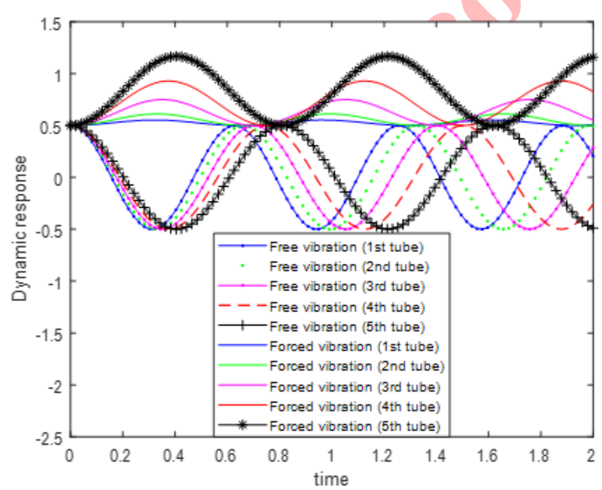

FIGURE 37. : Midpoint Deflection history of the MWCNT when B = 0.

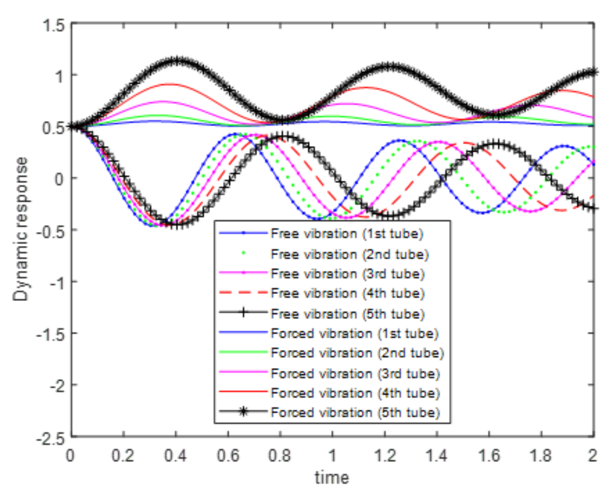

FIGURE 38. Midpoint Deflection history of the MWCNT when B = 1.

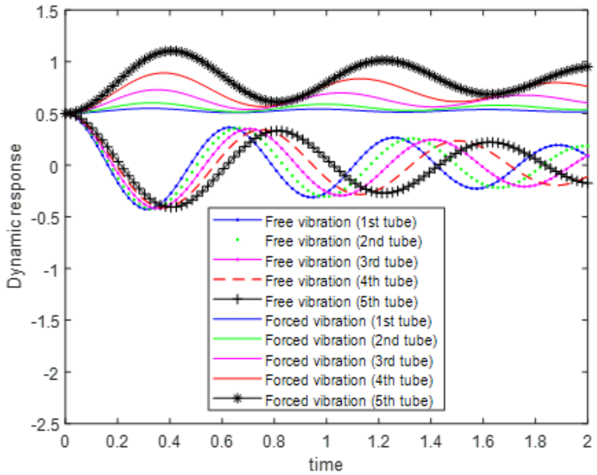

FIGURE 39. Midpoint Deflection history of the MWCNT when B = 2.

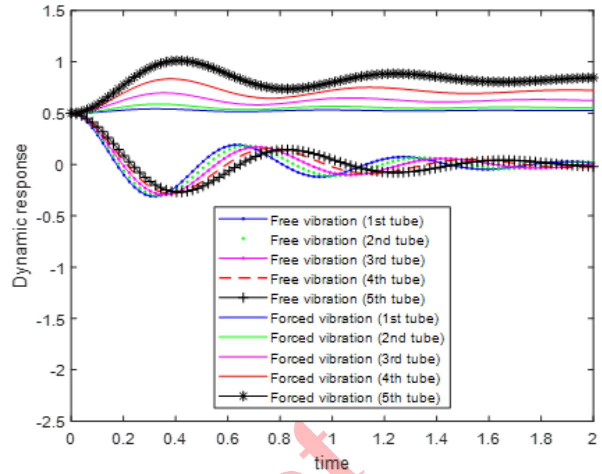

FIGURE 40. Midpoint Deflection history of the MWCNT when B = 4.

4.1.9. ***Effect of Magnetic Term on Midpoint Deflection History of the MWCNT.*** Figures 37–38 depict the effect of magnetic field on the Midpoint Deflection time history of the MWCNT for free and forced vibration. CNTs under free vibration vibrate with a constant amplitude and natural frequency as shown in Figure 37. When the magnetic effect is included, the responses begin to damp as the magnetic term increases. Additionally, the inner tube gives the highest displacement both for free and forced vibration.

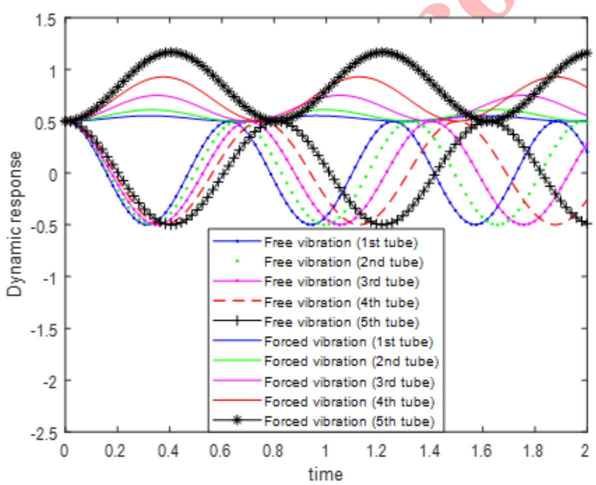

FIGURE 41. Midpoint Deflection history of the MWCNT when $\Delta\theta = 0$.

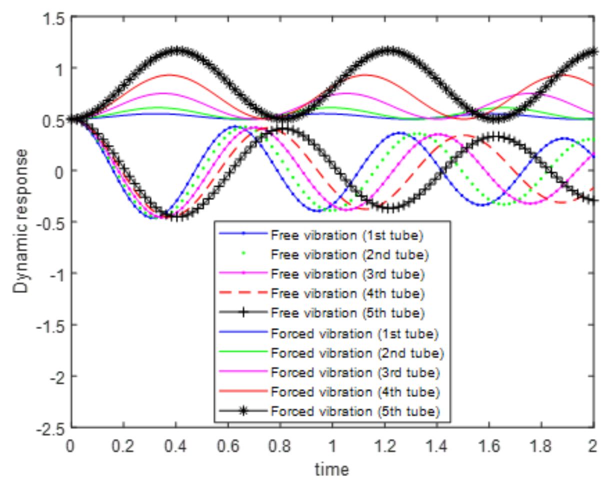

FIGURE 42. Midpoint Deflection history of the MWCNT when $\Delta\theta = 0.5$.

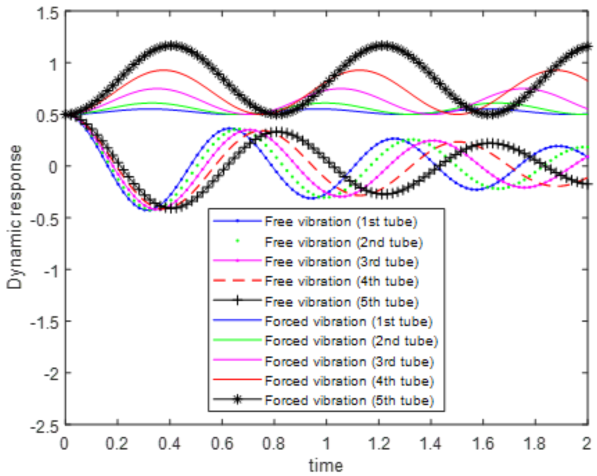

FIGURE 43. Midpoint Deflection history of the MWCNT when $\Delta\theta = 1$.

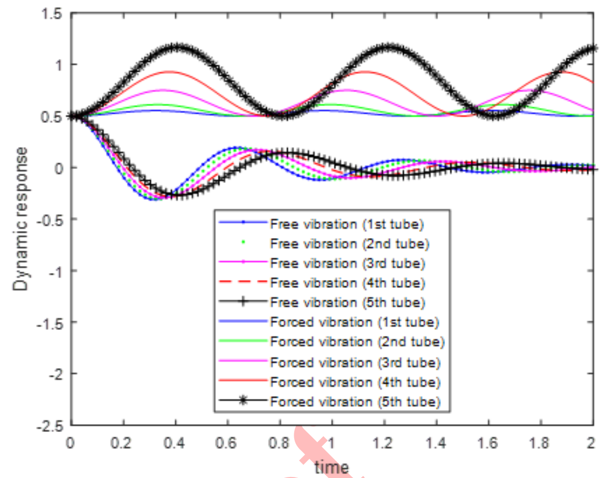

FIGURE 44. Midpoint Deflection history of the MWCNT when $\Delta\theta = 2$.

4.1.10. ***Effect of Temperature Change on the Deflection of MWCNT.*** Figures 41–44 show the impact of temperature change on the Midpoint Deflection time history of the MWCNT for free and forced vibration. An increase in temperature attenuates the dynamic response of the CNTs for free vibration with negligible effect on forced vibration. The reason for attenuation in free vibration is because of the reduction in system's stiffness which results in frequency reduction. However, this loss in stiffness is augmented by the induced external agent during forced vibration. The forcing function acts as a restoring agent by increasing the amplitude of damped vibration to the initial case.

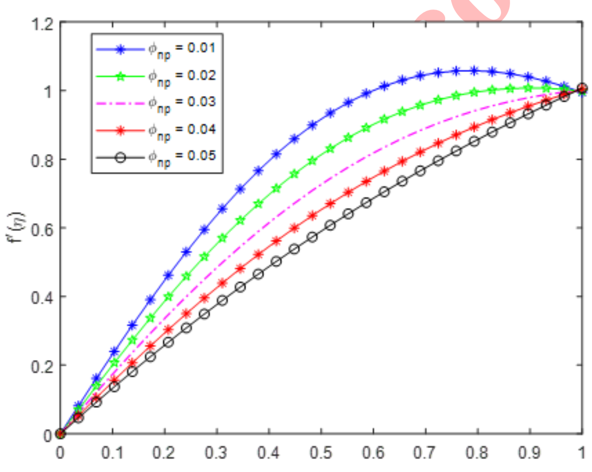

FIGURE 45. Effect of nanoparticles on velocity profile.

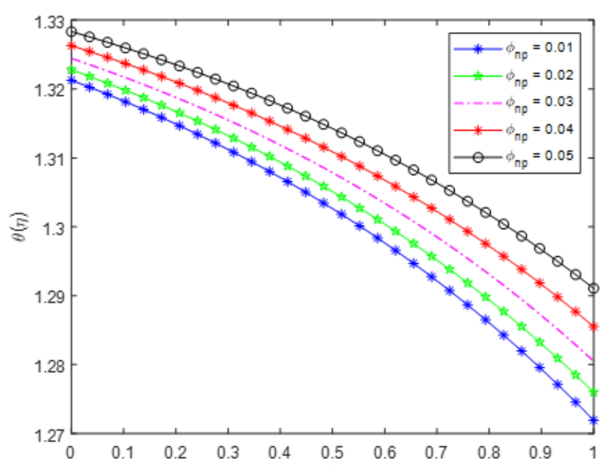

FIGURE 46. Effect of nanoparticles on temperature profile.

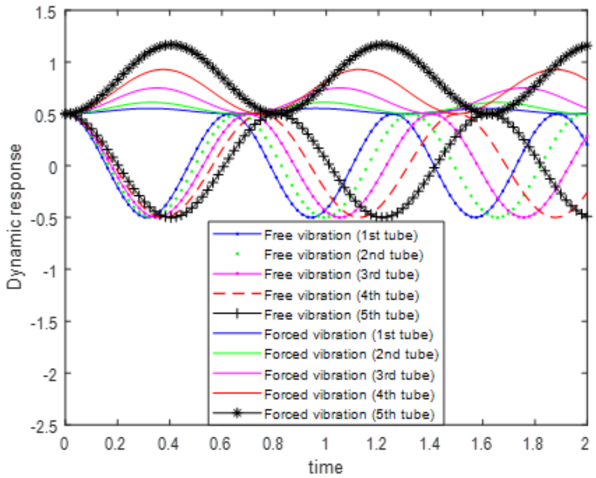

FIGURE 47. Midpoint Deflection history of the MWCNT when $\phi_{np} = 0.01$.

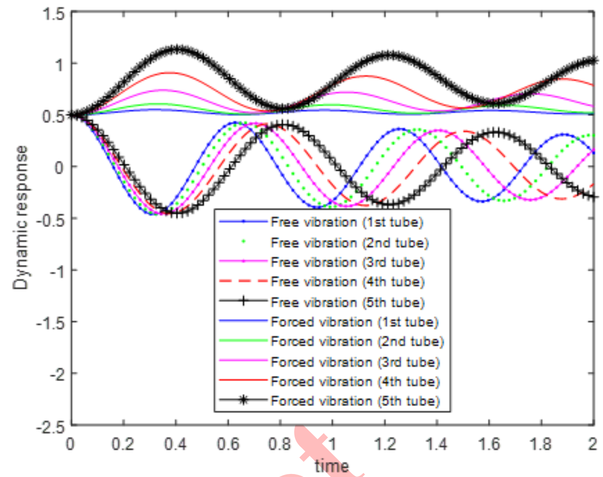

FIGURE 48. Midpoint Deflection history of the MWCNT when $\phi_{np} = 0.02$.

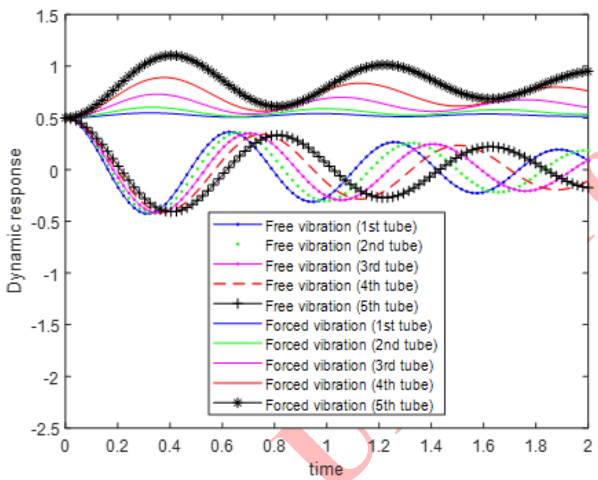

FIGURE 49. Midpoint Deflection history of the MWCNT when $\phi_{np} = 0.03$.

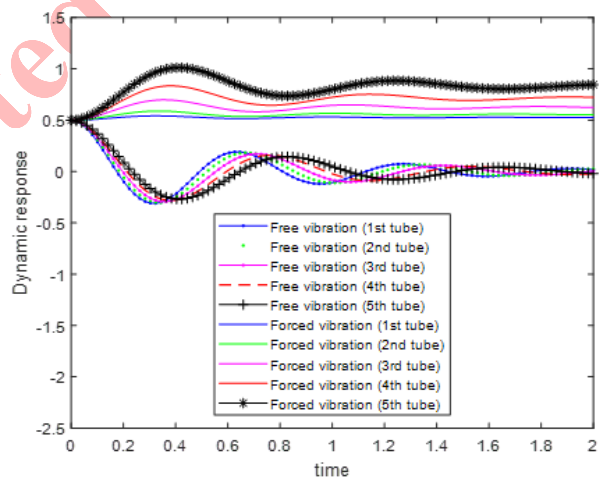

FIGURE 50. Midpoint Deflection history of the MWCNT when $\phi_{np} = 0.04$.

4.1.11. ***Effect of Nano-Particles on Thermofluidic and Midpoint Deflection Curve.*** Figures 45–50 depict the effect of nanoparticles on the velocity profile, temperature profile and midpoint deflection time history of the MWCNT for free and forced vibration. An augmentation in volume fraction of nanoparticles decreases the flow profile owing to the presence of drag introduced by Lorentz force from the magnetic field. However, an opposite impact is observed on temperature plots as augmentation in volume fraction of nanoparticles increases thermal profiles. As nanoparticles volume fraction is increased, the dynamic response of the MWCNT begins to attenuate. Although, the inner tube gives the highest displacement both for free and forced vibration, nanoparticles can generally be used to dampen vibration.

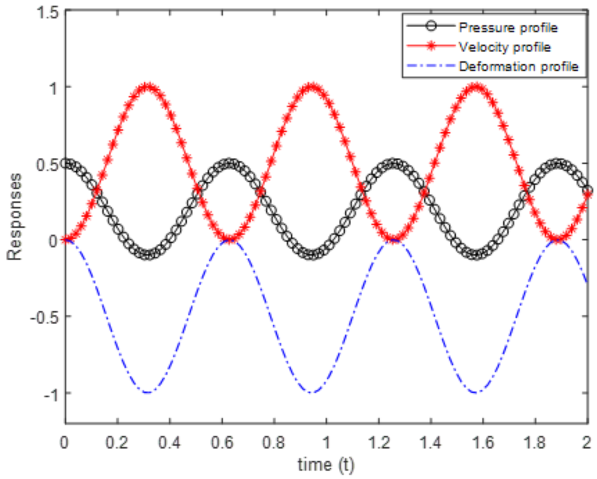

FIGURE 51. Pressure, Velocity and Deformation Profile without magnetic ter.0

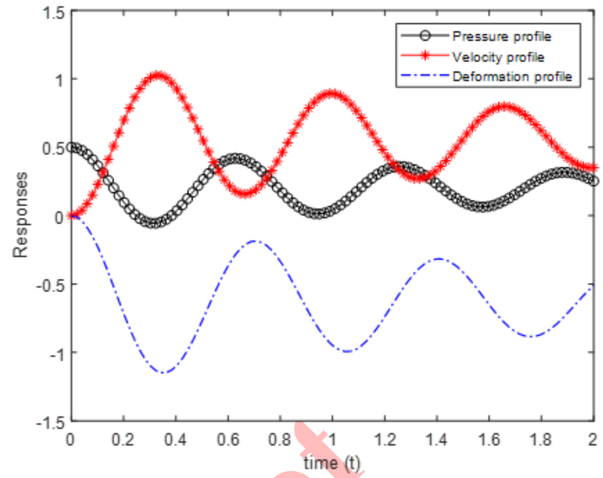

FIGURE 52. Pressure, Velocity and Deformation Profile with magnetic term.

4.1.12. ***Effect of Magnetic Term on Pressure, Velocity and Deformation Profile***. Figures 51–52 illustrate the impact of the magnetic field on pressure, velocity, and deformation profile. When the channel of admittance takes in nanofluid at high velocity, deformation occurs and the CNT starts to possess expanded and contracted regions. Contracted regions are formed when the flow is at high velocity and low pressure while expanded domains are as a result of low flow velocity and high pressure. The magnetic term may however be used to condition the flow pressure by using the flow velocity. These responses are essential in the design of flow-induced structures and material sizing.

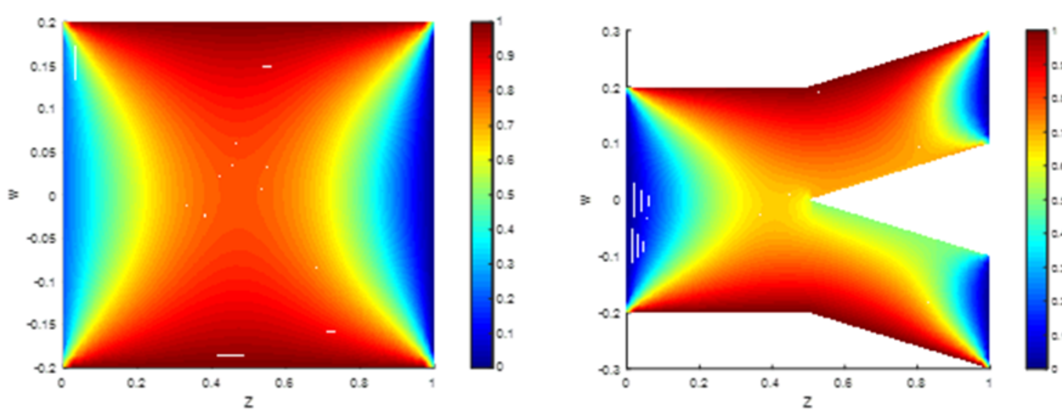

FIGURE 53. (a) CNT Deflection for$\phi = 0^o$, (b) CNT Deflection for $\phi = 30^o$.

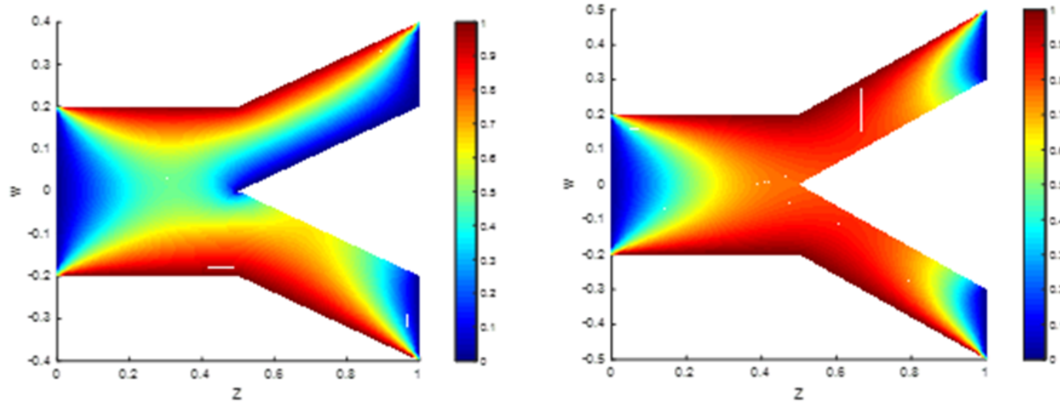

FIGURE 54. (a) CNT Deflection for$\phi = 45^o$, (b) CNT Deflection for $\phi = 60^o$.

4.1.13. ***Visualization of CNT Dynamic Response for Different Downstream Angles without Magnetic Term.***

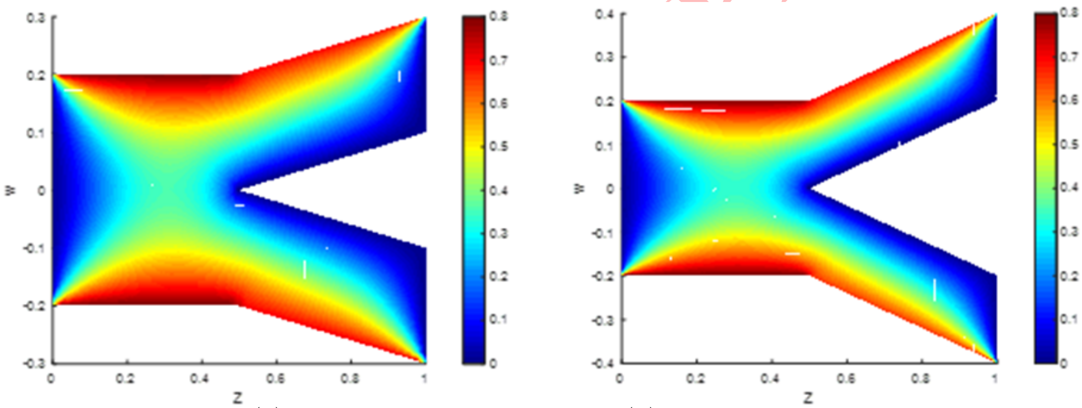

FIGURE 56. (a) CNT Deflection for$\phi = 15^o$, (b) CNT Deflection for $\phi = 30^o$.

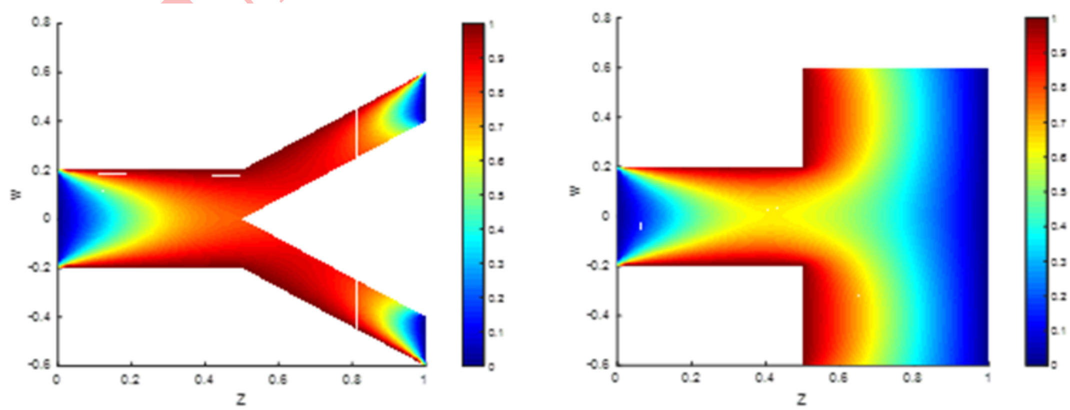

FIGURE 55. (a) CNT Deflection for$\phi = 75^o$, (b) CNT Deflection for $\phi = 90^o$.

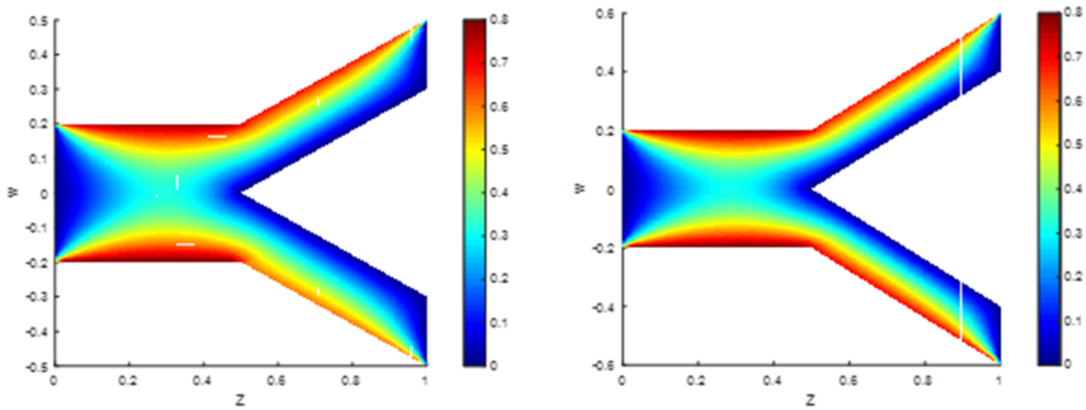

FIGURE 57. (a) CNT Deflection for$\phi = 45^o$, (b) CNT Deflection for $\phi = 60^o$.

4.1.14. ***Visualization of CNT Dynamic Response for Different Downstream Angles with Magnetic Term.***

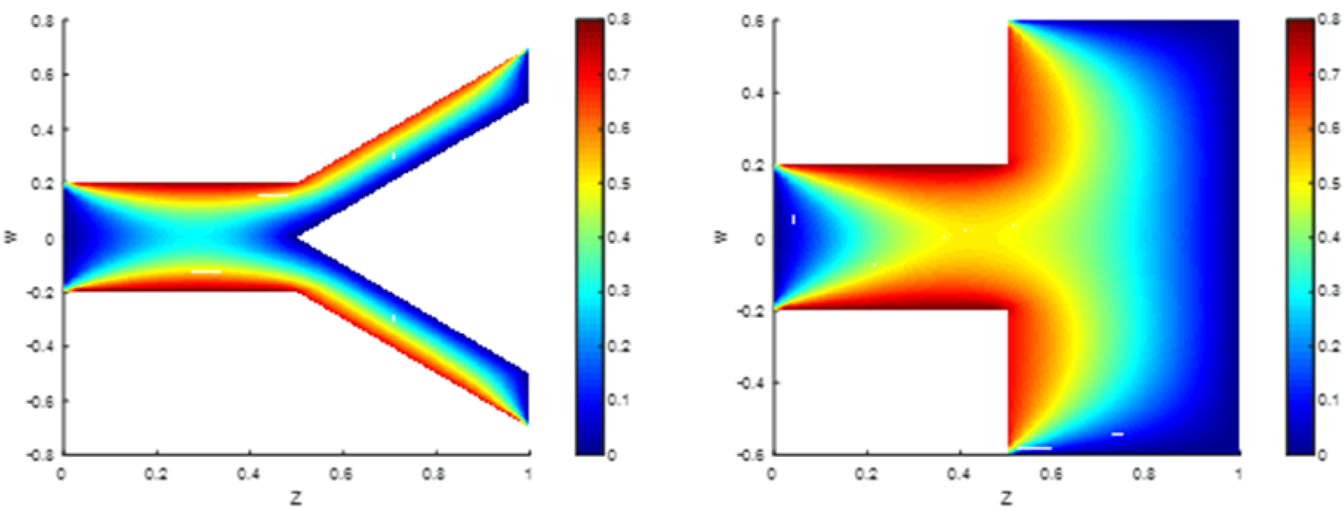

FIGURE 58. (a) CNT Deflection for $\phi = 75°$, (b) CNT Deflection for $\phi = 90°$.

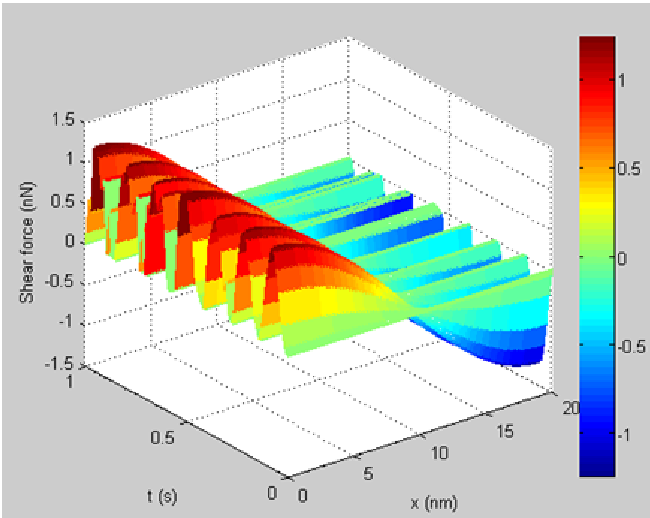

FIGURE 59. Shear force Diagram of the CNT for mode 1.

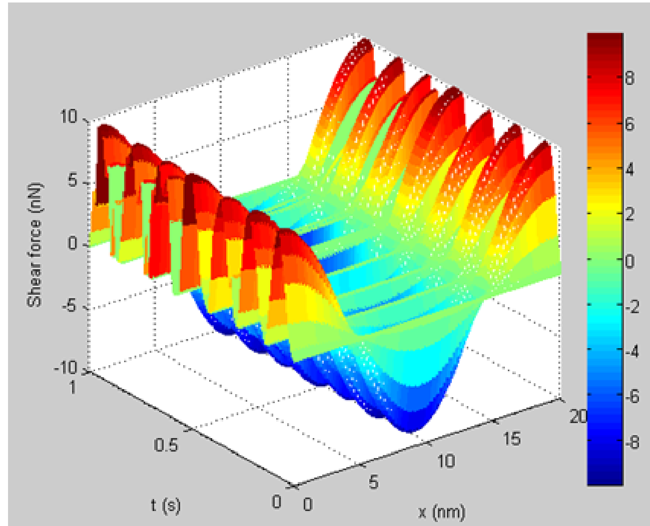

FIGURE 60. Shear force Diagram of the CNT for mode 2.

4.1.15. ***The Shear Force and Bending Moment of the CNT.*** Figures 53–58 and figures 59–62 illustrate three-dimensional visualization plots of the MWCNTs' dynamic responses for different junctions without and with magnetic fields. The absence of a magnetic field generates large deflections at the junctions which is not a desired option in design due to a reduction in the system's stability. Figures 65–68 depict the three-dimensional Shear force and bending moment diagram of the CNT for the first two modes. A critical assessment shows that it is possible to track the positions of maximum shear and maximum moment for the proper design of the CNT device. The dynamic analysis is important as it helps in the quick monitoring and adjustment of the CNT during application. Additionally, the checklists for validation and verification are presented in Table IX. From Table IX, the novelties in the present study are the consideration of branched MWCNT, the coupling of Navier stokes with vibration as well as the inclusion of pressure continuity and deformation models.

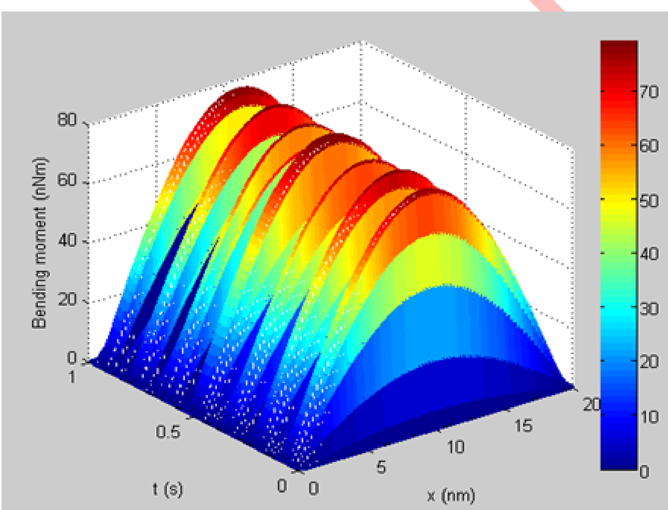

FIGURE 61. Bending moment Diagram of the CNT for mode 1.

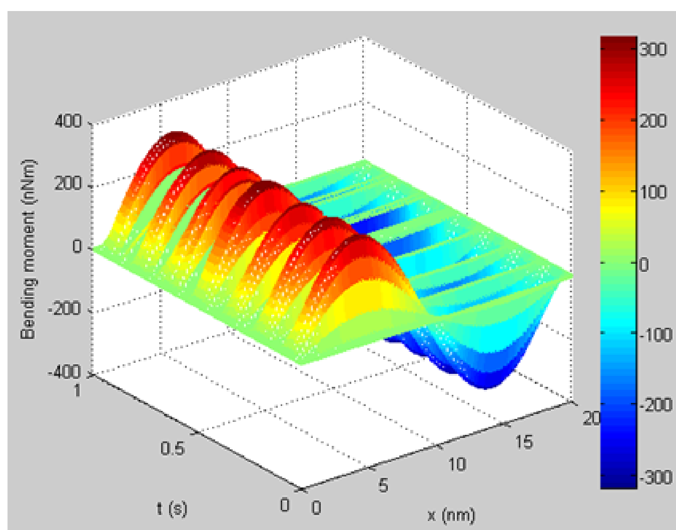

FIGURE 62. Bending moment Diagram of the CNT for mode 2.

Figure 63. Checklist for validations and verifications using previous studies

		Analytical Validation and Numerical Verification using Previous Studies																			
s/n	Research works	Transverse vibration	Longitudinal vibration	Plug-flow induced	NS-flow induced	Nonlinear	SWCNT	DWCNT	MWCNT	Branched	Thermal	Nanofluidic	Cattaneo-Chrisjov	Magnetic	Winkler foundation	Pasternak Foundation	Pressure model	Deformation model	Free vibration	Forced vibration	Nonlocal theory
1	Babic et al. (2003)	√					√				√								√		
2	Li and Chou (2004)	√					√	√											√		
3	Zhang et al. (2005)	√						√												√	
4	Yoon et al. (2005)	√		√			√								√				√		
5	Cao et al. (2006)	√					√				√									√	
6	Wang and Zhang (2008)	√					√														
7	Karaoglu and Aydogdu (2009)	√					√	√							√					√	√
8	Filiz and Aydogdu (2010)	√					√												√		√
9	Ansari et al. (2011)	√					√				√				√	√				√	
10	Şimşek (2011)	√					√	√				√			√					√	√
11	Rafiei et al. (2012)	√		√			√									√				√	√
12	Liang and Su (2013)	√		√			√								√					√	√
13	Askari et al. (2014)	√				√	√				√				√					√	
14	Wang et al. (2015)	√		√		√	√				√			√		√			√		√
15	Sadeghi-Goughari et al. (2016)	√		√		√	√							√	√				√		√
16	Belhadj et al. (2017)	√					√								√				√		√
17	Bijan et al. (2018)	√	√	√		√			√						√	√			√		
18	Oveissia and Hassan (2019)	√		√					√											√	
19	Eltaher and Mohamed (2020)	√					√													√	
20	Sobamowo et al. (2021)	√				√	√	√	√		√			√	√				√		√
21	Present study	√	√	√	√	√	√	√	√	√	√	√	√	√	√	√	√	√	√	√	√

5. CONCLUSION

Generalized and Improved Thermal-Nanofluidic Flow Induced Nonlinear Vibrations of Single and Multi-Walled Branched Nanotubes resting on Elastic Foundations in a Magnetic Environment have been developed. Using the Euler-Bernoulli theory, Hamilton principle, and nonlocal elasticity theory, fully coupled equations of motion governing the transverse and longitudinal vibrations of the nanotube have been developed.

Correspondingly, the deformation equation of the nanotubes as well as the pressure variation in the tubes have also been developed. Furthermore, Navier-Stokes and energy equations for the fluid and nanotube have been successfully coupled with the vibration models to obtain the relationship between the frequency, displacement of the MWCNT and the flow velocity, the pressure as well as the temperature of the nanofluid. Our arguments that the use of nonlocal theories, Navier stoke and energy equations coupled vibration models predict better than the classical approaches and plug flow assumption method of formulation for CNT was significantly noticed during simulation and parametric studies. Closed form solutions of the developed coupled systems of nonlinear partial differential equations have been provided using Galerkin decomposition method, one dimensional and multi-dimensional differential transformation methods. After treatment techniques have also been considered where necessary in the analytical solutions. With the aids of the analytical solutions, effects of nonlocal parameter, branched angles, magnetic field, nanoparticles, slip and jump conditions, fluid velocity, temperature change, foundation and boundary conditions on the dynamic behaviour of the branched flow induced nanotubes have been investigated. The results indicated that:

i. Increasing the downstream angle decreases the stability of the system for pre-bifurcation analysis but increases stability of the system for post bifurcation analysis.
ii. Also, the results obtained from the dynamic behavior of the system indicate that the magnetic effect has an attenuating or damping effect of about 20% on the system's response at any mode and for any boundary condition considered.
iii. Fundamental frequencies of multi-walled carbon nanotubes are about 10% lower than those of single-walled carbon nanotubes of the same outer diameter.
iv. The Navier-Stokes and energy-coupled vibration models have been compared with that of plug flow-induced vibration. In design and practical applications, the plug flow assumption should be discouraged as it deviates from actual working processes by over 11%.

The analytical solutions presented in this study have been found to match with existing analytical, numerical and experimental results, hence the verification and validation of this work. Furthermore, the contributions of the present study include:

i. Generalized and improved thermal-nanofluidic flow-induced nonlinear vibrations of single and multi-walled branched nanotubes resting on elastic foundations in a magnetic environment have been developed. Also, the work developed a visualization platform using MATLAB for monitoring the dynamic and stability responses of CNT when excited.
ii. The present study provides better physical insights into the nonlinear thermal-fluidic flow-induced vibration of both single and multi-walled carbon nanotubes.
iii. The research provided closed-form solutions of the developed coupled systems of nonlinear partial differential equations. This will serve as a platform for comparisons of results for subsequent numerical analysis and experimental investigations.
iv. The work established that the magnetic term has over 20% attenuating or damping effect on the dynamic response of the system.
v. The work established that for optimum design and performance of the flow-induced structure, the use of T-shaped CNT should be avoided or limited if necessary.
vi. Coupled thermal-fluidic induced vibration of multi-walled CNT for laminar flow has now been found to differ from the previously assumed plug flow which shows significant error in the previous studies in the literature.

References

[1] K. Agrawal and K. Keivan, *Longitudinally varying magnetic field influenced transverse vibration of embedded double-walled carbon nanotubes*, Int J Mech Sci, *87* (2014), 179-199.

[2] R. Ansari, M. Hemmatnezhad, and J. Rezapour, *The thermal effect on nonlinear oscillations of carbon nanotubes with arbitrary boundary conditions*, Current App Phys, *11*(3) (2011), 692–697.

[3] J. Ardali, R. Ghadami, and F. Rafii-Tabar, *Effect of microbeam geometry on the nanomass sensor performance*, Mechanics & Industry, *10*(3) (2019), 304.

[4] B. Babic, J. Furer, and S. Sahoo, *Intrinsic thermal vibrations of suspended doubly clamped single-wall carbon nanotubes*, Nano Lett, *10*(3) (2003), 1577–1580.

[5] A. Bedford, *Hamilton's Principle in Continuum Mechanics*, University of Texas at Austin, Pitman Publishing, Ltd, *10* (1985).

[6] A. Belhadj, A. Boukhalfa, and S. Belalia, *Carbon nanotube Structure vibration based on nonlocal elasticity*, J Mod Mater, *10*(1) (2017), 9-13.

[7] L. Biro, Z.Horvath, G.Mark, Z. Osvath, A. Koos, A. Benito, W. Maser, and P. Lambin, *Carbon nanotube Y junctions: growth and properties*, Diam Relat Mater, *10*(3) (2004), 241–249.

[8] A. Bouchaala, H. Ali, and I. Mohammad, *Frequency shifts of micro and nano cantilever beam resonators due to added masses*, J Dyn Sys, Meas and Control, *10*(9) (2016), 1-20.

[9] G. Cao, X. Chen, and J. Kysar, *Thermal vibration and apparent thermal contraction of single-walled carbon nanotubes*, J Mech Phys Sol, *10*(6) (2006), 1206–1236.

[10] R. Chowdhury, S. Adhikari, and J. Mitchell, *Vibrating carbon nanotube based biosensors*, Physica E: Low dimensional Systems and Nanostructures, *10*(2) (2009), 104-109.

[11] H. Dodds and H. Runyan, *Effects of high-velocity fluid flow in the bending vibrations and static divergence of a simply supported pipe*, National Aeronautical and Space Administration Report, NASA TN, D-2870, *10* (1965).

[12] M. Eltaher and N. Mohamed, *Nonlinear stability and vibration of imperfect CNTs by Doublet mechanics*, Applied Mathematics and Computation, *10* (2020), 125311.

[13] C. Fay, *Calculus of Variations*, *10* (2022).

[14] S. Filiz and M. Aydogdu, *Axial vibration of carbon nanotube heterojunctions using nonlocal elasticity*, Comput Mat Sci, *10*(3) (2010), 619–627.

[15] A.A. Ghorbanpour and S. Amir, *Electro-thermal vibration of visco-elastically coupled BNNT systems conveying fluid embedded on elastic foundation via strain gradient theory*, Physica B, *10* (2013), 1-6.

[16] A. Ghorbanpour and M. Zarei, *Nonlocal vibration of Y-shaped CNT conveying nano-magnetic viscous fluid under magnetic field*, Ain Shams Eng Jl, *10*(2) (2015), 565–575.

[17] A. Ghorbanpour, M. Roudbari, and S. Amir, *Nonlocal vibration of SWBNNT embedded in bundle of CNTs under a moving nanoparticle*, Physica B, *10* (2012), 3646–3653.

[18] S. Graham-Kelly, *Mechanical Vibrations: Theory and Applications*, Global Engineering Publisher, *10* (2011), ISBN-13: 978-1-4390-6214-2, ISBN-10: 1-4390-6214-5.

[19] P. Gu and J. Zhao, *Synthesis of Y-branching multiwalled carbon nanotubes with a bamboolike structure*, J. Mater. Res, *10*(11) (2002), 2768–2770.

[20] S. Habibi and M. Nematollahi, *Position and mass identification in nanotube mass sensor using neural networks*, Proceedings of the Institution of Mechanical Engineers, Part C: J Mech Eng Sci, *10*(15) (2019), 5377-5387.

[21] M. Hosseini and M. Sadeghi-Goughari, *Vibration and instability analysis of nanotubes conveying fluid subjected to a longitudinal magnetic field*, Appl Math Mod, *10*(4) (2016), 2560–2576.

[22] S. Iijima, *Helical micro tubes of graphitic carbon*, Nature, *10* (1991), 56–58.

[23] S. Iijima, *Discovery of single-wall carbon nanotube*, Nature, *10* (1993), 603.

[24] N. Kam and H. Dai, *Carbon Nanotubes as Intracellular Protein Transporters: Generality and Biological Functionality*, Journal of the American Chemical Society, *10*(16) (2005), 6021-6026.

[25] P. Karaoglu and M. Aydogdu, *On the forced vibration of carbon nanotubes via a non-local Euler-Bernoulli beam model*, Proc Inst Mech Eng C J Mech Eng Sci, *224*(2) (2009), 497-503.

[26] M. Khater, E. Eihab, and H. Ali, *A mass sensing technique for electrostatically actuated MEMS*, Int Des Eng Tech Conf, *10*(1) (2009), 655-661.

[27] A. Khosrozadeh and M. Hajabasi, *Free vibration of embedded double-walled carbon nanotubes considering nonlinear interlayer van der Waals forces*, Appl Math Model, *36*(3) (2012), 997-1007.

[28] C. Li and T. Chou, *Vibrational behaviors of multiwalled-carbon-nanotube-based nanomechanical resonators*, Appl Phys Lett, *84*(1) (2004), 121-123.

[29] N. Mostafa, A. Ahmad, and K. Ali, *Efficient multi-step differential transform method: Theory and its application to nonlinear oscillators*, Commun Nonlinear Sci Numer Simul, *53* (2017), 54-183.

[30] T. Murmu, A. Michael, and M. McCarthy, *Nonlocal elasticity based magnetic field affected vibration response of double single-walled carbon nanotube systems*, J Appl Phys, *111*(11) (2012), 113511.

[31] T. Murmu, M. McCarthy, and S. Adhikari, *Vibration response of double-walled carbon nanotubes subjected to an externally applied longitudinal magnetic field: A nonlocal elasticity approach*, J Sound Vib, *331*(23) (2012), 5069-5086.

[32] P. Nagy, R. Ehlich, and L. Biro, *Y-branching of single walled carbon nanotubes*, Appl Phys A Mater, *70* (2000), 481-483.

[33] S. Narendar, S. Gupta, and S. Gopalakrishnan, *Wave propagation in single-walled carbon nanotube under longitudinal magnetic field using nonlocal Euler-Bernoulli beam theory*, Appl Math Model, *36*(9) (2012), 4529-4538.

[34] T. Natsuki, T. Hayashi, and M. Endo, *Wave propagation of carbon nanotubes embedded in an elastic medium*, J Appl Phys, *97*(4) (2005), 044307.

[35] T. Natsuki, N. Nobuhiro, S. Jin-Xing, and Q. Qing-Qing, *Vibration analysis of nanomechanical mass sensor using carbon nanotubes under axial tensile loads*, Appl Phys A, *116*(3) (2014), 1001-1007.

[36] S. Oveissia and N. Hassan, *Transverse vibration and instability of fluid conveying triple-walled carbon nanotubes based on strain inertia gradient theory*, Acoust Vib, *10* (2019), 240-253.

[37] A. Patel and Y. Anand, *Detection of biological objects using dynamic characteristics of double-walled carbon nanotubes*, Appl Nanosci, *10*(6) (2015), 681-695.

[38] M. Rafiei, S. Mohebpour, and F. Daneshmand, *Small-scale effect on the vibration of non-uniform carbon nanotubes conveying fluid and embedded in viscoelastic medium*, Physica E, *44*(7) (2012), 1372-1379.

[39] M. Sadeghi-Goughari, J. Soo, and K. Hyock-Ju, *Effects of magnetic-fluid flow on structural instability of a carbon nanotube conveying nanoflow under a longitudinal magnetic field*, Phys Lett A, *381*(35) (2017), 2898-2905.

[40] M. Şimşek, *Nonlocal effects in the forced vibration of an elastically connected double-carbon nanotube system under a moving nanoparticle*, Comput Mater Sci, *50*(7) (2011), 2112-2123.

[41] M. Sobamowo, *Nonlinear thermal and flow induced vibration analysis of fluid-conveying carbon nanotube resting on Winkler and Pasternak foundations*, Therm Sci Eng Prog, *10* (2017), 133-149.

[42] M. Sobamowo and A. Yinusa, *Power Series-After treatment Technique for Nonlinear Cubic Duffing and Double-Well Duffing Oscillators*, J Comput Appl Mech, *10*(24) (2017), 297-306.

[43] M. Sobamowo, J. Akanmu, O. Adeleye, S.Akingbade, and A. Yinusa, *Coupled effects of magnetic field, number of walls, geometric imperfection, temperature change, and boundary conditions on nonlocal nonlinear vibration of carbon nanotubes resting on elastic foundations*, Forces Mech, *10* (2021), 1-41.

[44] P. Soltani, O. Pishkenari, M. Mohammad, and A. Anoushiravan, *Free vibration of a carbon nanotube-based mass sensor*, Adv Mater Res, *10* (2012), 1163-1167.

[45] C. Wang and L. Zhang, *A critical assessment of the elastic properties and effective wall thickness of single-walled carbon nanotubes*, Nanotechnology, *19*(7) (2008), 075705.

[46] B. Wang, Z. Deng, H. Ouyang, and X. Xu, *Free vibration of wavy single-walled fluid-conveying carbon nanotubes in multi-physics fields*, Appl Math Model, *39*(22) (2015), 6780-6792.

[47] L. Wang and Q. Ni, *A reappraisal of the computational modelling of carbon nanotubes conveying viscous fluid*, Mech Res Commun, *36*(7) (2009), 833-837.

[48] A. Yinusa and M. Sobamowo, *Nonlinear Thermal-Magneto-Mechanical Vibration Analysis of Single-Walled Embedded Branched Carbon Nanotubes Conveying Nanofluid*, ASME Open J Eng, *2*(1) (2023).

[49] A. Yinusa, M. Sobamowo, and A. Adelaja, *Thermal analysis of nanofluidic flow through multi-walled carbon nanotubes subjected to perfectly and imperfectly bonded wall conditions*, Chem Thermo Therm Anal, *10* (2022), 100028.

[50] A. Yinusa and M. Sobamowo, *Mechanics of nonlinear internal flow induced vibration and stability analysis of a pre-tensioned SWCNT using classical DTM with CAT and SAT after treatment techniques*, Forces Mech, *10* (2022), 100083.

[51] A. Yinusa, M. Sobamowo, and A. Adelaja, *Flow induced bifurcation and phase-plane stability analysis of branched nanotubes resting on two parameter foundation in a magnetic environment*, Partial Differ Equ Appl Math, *10* (2021), 100234.

[52] A. Yinusa and M. Sobamowo, *Thermal instability and dynamic response analysis of a tensioned carbon nanotube under moving uniformly distributed external pressure*, Nano Mater Sci, *10* (2021), 75-88.

[53] A. Yinusa, M. Sobamowo, and A. Adelaja, *Nonlinear vibration analysis of an embedded branched nanofluid-conveying carbon nanotube: Influences of downstream angle, temperature change and two dimensional external magnetic field*, Nano Mater Sci, *10* (2020), 323-332.

[54] A. Yinusa and M. Sobamowo, *Analysis of Dynamic Behaviour of a Tensioned Carbon Nanotube in Thermal and Pressurized Environments*, Karbala Int J Modern Sci, *10* (2019), 1-11.

[55] A. Yinusa, M. Sobamowo, and A. Adelaja, *Determination of the dynamic shearing force and bending moment of a tension single-walled carbon nanotube subjected to a uniformly distributed external pressure*, Eng Appl Sci Lett, *10* (2019), 40-52.

[56] J. Yoon, C. Ru, and A. Mioduchowski, *Vibration and instability of carbon nanotubes conveying fluid*, Compos Sci Technol, *65*(9) (2005), 1326-1336.

[57] M. Zarepour, S. Hosseini, and M. Ghanbari, *Free vibration investigation of nano mass sensor using differential transformation method*, Appl Phys A, *123*(3) (2014), 1-10.

[58] B. Zhao, H. Hu, S. Mandal, and R. Haddon, *A bone mimic based on the self-assembly of hydroxyapatite on chemically functionalized single-walled carbon nanotubes*, Chem Mater, *17* (2005), 3235-3241.

[59] D. Zhang, Y. Lei, and Z. Shen, *Effect of longitudinal magnetic field on vibration characteristics of single-walled carbon nanotubes in a viscoelastic medium*, Braz J Phys, *47*(6) (2017), 640-656.

[60] D. Zhang, Y. Lei, and Z. Shen, *Vibration analysis of horn-shaped single-walled carbon nanotubes embedded in viscoelastic medium under a longitudinal magnetic field*, Int J Mech Sci, *10* (2016), 219-230.

[61] Y. Zhen, W. Shi-Long, and T. Ye, *Free vibration analysis of viscoelastic nanotubes under longitudinal magnetic field based on nonlocal strain gradient Timoshenko beam model*, Physica E, *10* (2019), 116-124.